THE UNIVERSITY OF CHICAGO

# PAIR THEORY AND OPEN SYSTEMS FROM A REDUCED DENSITY MATRIX PERSPECTIVE

A DISSERTATION SUBMITTED TO
THE FACULTY OF THE DIVISION OF THE PHYSICAL SCIENCES
IN CANDIDACY FOR THE DEGREE OF
DOCTOR OF PHILOSOPHY

DEPARTMENT OF CHEMISTRY

BY
KADE MAYA HEAD-MARSDEN

CHICAGO, ILLINOIS
AUGUST 2019

To Renee, John, and Rowan

# TABLE OF CONTENTS

# LIST OF FIGURES

# LIST OF TABLES

# ACKNOWLEDGMENTS

First, I'd like to thank David Mazziotti for his mentorship and encouragement throughout this degree, none of this work would have been possible without his help and support. I would also like to thank all of the other members of the Mazziotti group that I had the chance to work with: Shrikant, Eric, Andrew, Nick, Chad, Charles, Romit, Erica, Valentine, Manas, Anthony, Ali, Scott, Simon, Nik, LeeAnn, Shiva, Shayan, Claire, Alison, Lexie, and Olivia.

I'd like to thank my other committee members, Prof. Stuart Rice and Prof. David Schuster, for scientific discussions and career advice over the past few years. I would also like to thank the many people in the Chemistry Department and the James Franck Institute who hold this place together and make it such a great place to work, including Vera, Melinda, Maria, Brenda, Elizabeth, and John.

A big thank you to the many wonderful friends I've made here who have been incredibly supportive and have made this whole experience a lot of fun: Memo, Ali, Cat, Elle, Anthony, Maggie, Kelliann, Ziwei, Yining, Jaehyeok, Dan, Darren, Tim, Olivia, Chi-Jui, Donghyuk, Huw, Vera, Jeronimo, and Aixa.

And finally a thank you to my family, Renee, John, and Rowan, whose support and encouragement made this degree possible.

# ABSTRACT

Studying electronic behaviour, whether it's electronic structure or dynamics, is crucial to better understanding many physical and chemical phenomena. While traditional wavefunction methods have been successful for a variety of systems, the computational cost can be prohibitive. A different approach is to use the reduced density matrix (RDM) perspective, which allows for a decrease in computational cost without sacrificing accuracy. Here, the RDM perspective is used to consider two different problems: reducing the computational cost of the variational 2-electron reduced density matrix method and generalizing the treatment of open quantum systems to treat systems of multiple fermions. To approach the first problem, I will outline several approximations to the Schödinger equation, with a particular focus on the variational 2-RDM method constrained to the pair space. I will then present results using this method with orbital localization to recover size extensivity in molecular and polymer chains. Finally, I will use this method in conjunction with the complete active space self-consistent field method to analyze strong correlation in systems up to 80 electrons in 80 orbitals. For the second problem, I derive constraints on the Lindbladian matrices to generalize the Lindblad treatment of Markovian open quantum systems to treat systems of multiple fermions. I then generalize the Lindblad theory to treat non-Markovian open quantum systems, and introduce further constraints to generalize this method to treat systems of multiple fermions. Both of these projects take steps towards more efficient and more accurate use of reduced density matrix mechanics to treat problems in electronic structure and dynamics.

# CHAPTER 1

# INTRODUCTION

## 1.1 Wavefunction Methods

The state of a quantum system can be found through the time-independent, non-relativistic Schrödinger equation,

$$\hat{H}\Psi_n = E_n\Psi_n, \tag{1.1}$$

where $\hat{H}$ is the Hamiltonian, $E_n$ are the stationary-state energies, and $\Psi_n$ are the wave functions[1]. While the $N$-electron wavefunction contains all the elctronic structure information, the electronic Schrödinger equation can only be solved for one-electron systems. For an arbitrary $N$-electron system, approximation methods must be used to obtain energy and state solutions. One common assumption that will be invoked throughout this thesis is the Born-Oppenheimer approximation, which allows us to ignore nuclear motion and just focus on the electronic chemistry[1].

The simplest approximation is the Hartree-Fock method which allows treatment of multiple electrons through use of a mean field approximation. This implies that each electron only feels the repulsion from the mean field of the other electrons. The Hartree-Fock wavefunction can be represented as a single Slater determinant,

$$|\Psi_{HF}\rangle = \frac{1}{\sqrt{N!}}\det\begin{pmatrix} \chi_1(1) & \dots & \chi_N(1) \\ \vdots & & \vdots \\ \chi_1(N) & \dots & \chi_N(N) \end{pmatrix} \tag{1.2}$$

where $N$ is the number of particles and $\{\chi_i\}$ are a set of orthonormal spin molecular orbitals. This wavefunction preserves the desired antisymmetry property and represents the ground state where all electrons are arranged in the lowest energy configuration. Due to the average method of treating electron-electron interactions, Hartree-Fock theory does not capture

electronic correlation and therefore always underestimates the electronic energies. Despite neglecting electron correlation, it does manage to capture roughly 99% of the energy for a wide variety of systems while scaling computationally as $r^3$, where $r$ is the size of the orbital basis.

Another approach for solving the Schödinger equation is the full configuration interaction (FCI) method[1]. This method uses wavefunctions that are sums of all Slater determinants, which implies they consist of contributions from all possible configurations of $N$ electrons. While this method provides accurate results, it scales as $r^N$ where $r$ is the size of the orbital basis and $N$ is the number of electrons. This exponential scaling restricts its use to small molecule applications. Another flavour of configuration interaction calculation is the doubly-occupied configuration interaction, or DOCI, method. While similar to the full configuration interaction, instead of including all possible configurations the doubly-occupied configuration interaction method only includes configurations where sets of two electrons behave as pairs[2]. Electrons can be paired in a variety of ways with the most common choice being by spin. In this framework, only Slater determinants which represent simultaneous excitations of both the $\alpha$ and $\beta$ electrons are included. While this method still scales exponentially, it does significantly decrease the complexity of the full configuration interaction calculation by reducing the number of basis orbitals from $r$ to $\frac{r}{2}$.

Since these configuration interaction methods are successful for small systems, approximations to make them applicable to larger systems are desirable. One such approximation is to consider only a subset of all the possible electrons and orbitals, referred to as active space methods[3]. The fully occupied molecular orbitals that are not in the valence shell are treated as the core space, while the empty orbitals that are higher in energy are treated as the virtual space. The valence shell and low lying unoccupied orbitals make up the active space, as shown in Fig. 1.1 (a). With this division of orbitals the number of orbitals and electrons considered can be significantly smaller often allowing for a full or doubly-occupied configu-

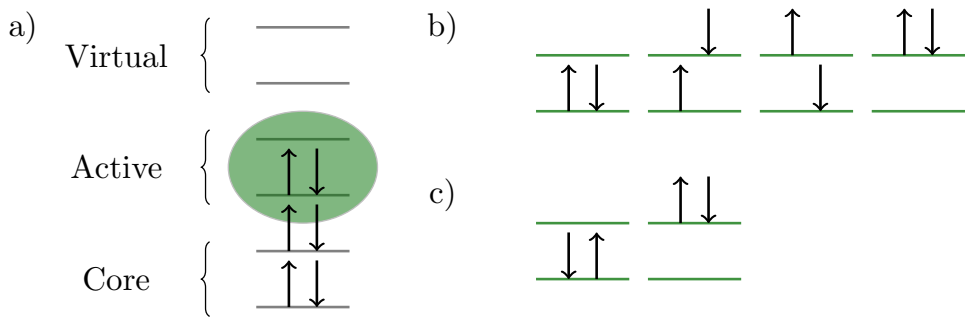


Figure 1.1: a) An example of an active space where the core orbitals are filled, the active space is highlighted in green, and the virtual space is empty, b) a full configuration expansion of the two electrons in four spin orbitals, and c) a doubly-occupied configuration interaction expansion of the two electrons in four spin orbitals.

ration interaction calculation in the active space. This method is referred to as a complete active space configuration interaction, or CASCI, method and is depicted in Fig. 1.1 b) and Fig. 1.1 c) for the full and doubly-occupied configuration interaction expansions respectively.

This type of division of active space can also be applied to self-consistent field methods which generally consist of a full or doubly-occupied configuration interaction calculation in the active space performed iteratively with orbital rotations to help minimize the energy. The combination of the complete active space configuration interaction method with these orbital rotations is referred to as a complete active space self-consistent field, or CASSCF, method.

It should be noted that for a complete active space calculation, the number of variables required is given by,

$$N_{CAS} = \frac{2S+1}{r+1}\binom{r+1}{\frac{N}{2}-S}\binom{r+1}{\frac{N}{2}+S+1}, \tag{1.3}$$

where $S$ is the total spin, $r$ is the number of orbitals, and $N$ is the number of electrons[3]. The equation also holds true for full or doubly-occupied configuration interaction; the number or orbitals and electrons are just considered from the entire space instead of being restricted to the active space.

## 1.2 Reduced Density Matrix Methods

The Schödinger equation in Eq. 1.1 can also be written from a density matrix perspective,

$$\hat{H}^N D_n = E_n {}^N D_n, \tag{1.4}$$

where ${}^N D_n$ is the $N$-particle density matrix given by,

$${}^N D_n = \Psi_n(1, .., N)\Psi_n^*(\overline{1}, .., \overline{N}). \tag{1.5}$$

The full density matrix provides a different framework from the wavefunction approach, however it doesn't provide a computational benefit. Since electrons interact pairwise, integrating out all but two electrons from the $N$-particle density matrix gives the 2-electron reduced density matrix,

$${}^2 D_n(12; \overline{12}) = \int \Psi_n(1, 2, .., N)\Psi_n^*(\overline{1}, \overline{2}, .., N) d3..dN, \tag{1.6}$$

which is a much smaller object than the full wavefunction. This object represents the probability distribution of two electrons interacting in a field of $N-2$ electrons[4–9]. Using the 2-RDM in conjunction with the Schrödinger equation in Eq. 1.4, the energy can be expressed as,

$$E = Tr({}^2 K {}^2 D), \tag{1.7}$$

where ${}^2 K$ is the reduced Hamiltonian.

These two expressions can also be presented in second quantization notation to give the 2-RDM as,

$${}^2 D_{kl}^{ij} = \langle \Psi | \hat{a}_i^\dagger \hat{a}_j^\dagger \hat{a}_l \hat{a}_k | \Psi \rangle, \tag{1.8}$$

where $\hat{a}^\dagger$ and $\hat{a}$ are the creation and annihilation operators respectively and the indices $i$, $j$,

$k$, and $l$ denote the spin orbitals. The energy can then be expressed as,

$$E = \sum_{ijkl} {}^2K_{kl}^{ij} {}^2D_{kl}^{ij}, \tag{1.9}$$

where ${}^2K_{kl}^{ij}$ is the two-electron Hamiltonian given by,

$${}^2K_{kl}^{ij} = \frac{4}{N-1} {}^1K_k^i \wedge \delta_l^j + {}^2V_{kl}^{ij}, \tag{1.10}$$

in which, ${}^1K_k^i$ and ${}^2V_{kl}^{ij}$ are one- and two-electron matrices and $\wedge$ is the Grassmann wedge product [4–13].

Using reduced density matrices compared to wavefunctions saves computational cost; however, care must be taken that the RDMs always represent physical $N$-electron wavefunctions. To ensure that this is the case, $N$-representability conditions must be invoked[4, 6, 14–16]. For the case of the 2-RDM, some approximate $N$-representability conditions are[14, 17–19]:

$$\begin{aligned} {}^2D_{k,l}^{i,j} &\succeq 0 && (1.11)\\ {}^2Q_{k,l}^{i,j} &\succeq 0 && (1.12)\\ {}^2G_{k,l}^{i,j} &\succeq 0, && (1.13) \end{aligned}$$

where ${}^2D$, ${}^2Q$, and ${}^2G$ are the two-particle, two-hole, and particle-hole density matrices respectively,

$$\begin{aligned} {}^2D_{k,l}^{i,j} &= \langle\Psi|a_i^\dagger a_j^\dagger a_l a_k|\Psi\rangle && (1.14)\\ {}^2Q_{k,l}^{i,j} &= \langle\Psi|a_i a_j a_l^\dagger a_k^\dagger|\Psi\rangle && (1.15)\\ {}^2G_{k,l}^{i,j} &= \langle\Psi|a_i^\dagger a_j a_l^\dagger a_k|\Psi\rangle. && (1.16) \end{aligned}$$

Restrictions such as symmetry can produce blocking of the elements which is useful for minimizing computational cost[20].

## 1.3 Variational 2-RDM

The energy in Eq. 1.7 can be variationally minimized as a functional of the 2-RDM constrained by the matrix inequalities in Eq. 1.13 through use of a boundary-point semidefinite programming algorithm[5, 21–23]. With use of the approximate $N$-representability conditions, the computational scaling is $r^6$ which has allowed for its use in many electronic calculations[24–30].

## 1.4 Variational Pair 2-RDM

Active space calculations with the variational 2-RDM method have shown to be effective at calculating strong correlation in a variety of large molecules[27]. Generally as the active space is increased, electronic behaviour emerges that is more in agreement with experimental results. Due to this trend, it is desirable to try to minimize the cost of the variational 2-RDM method in hopes of being able to consider the electronic structure of larger molecules or in larger active spaces. One method of reducing this cost is to invoke the variational 2-RDM method in the DOCI space, which will be referred to as the pair 2-RDM method. In the pair space ${}^2D$, ${}^2Q$, and ${}^2G$ take on a special blocked form depicted in Fig. 1.2. This blocking decreases the computational cost since ${}^2D$, ${}^2Q$, and ${}^2G$ all go from 4 indices to 2 indices. Due to this simplification of the $N$-representability constraints in the pair space, the computational cost of the variational 2-RDM method is decreased from $r^6$ to $r^3$.

The major drawback of restricting the variational 2-RDM method, or many other computational methods, to the pair space is that the approximation is not invariant to unitary orbital transformations. This implies that great care needs to be taken while selecting or-

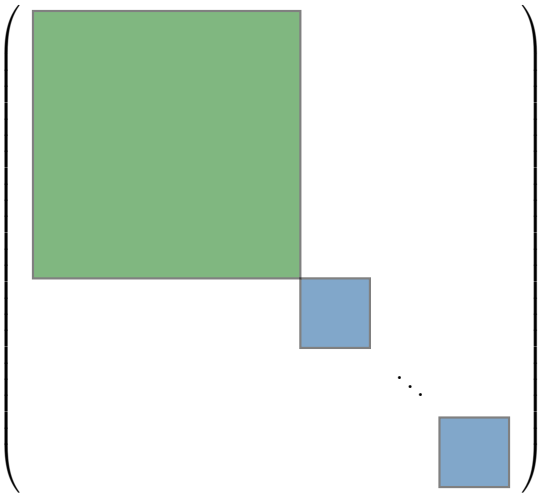

Figure 1.2: Block structure in the pair space for ${}^2D$, ${}^2Q$, and ${}^2G$. For all three RDMs, the large green block represents an $r$ by $r$ block where $r$ is the size of the orbital basis. For ${}^2D$ and ${}^2D$, there are $\binom{r}{2}$ small blue blocks of size 1 by 1. For ${}^2G$, there are $\binom{r}{2}$ small blue block of size 2 by 2.

bitals to obtain accurate results. One approach that we consider in Chapter 2 of this thesis is the use of localized orbitals in the variational pair 2-RDM method. While this method has its benefits, including recovery of approximate size extensivity, it proved to be challenging to implement for larger systems.

A second approach outlined in Chapter 3 was the use of complete active space self-consistent field with the variational pair 2-RDM method. This method shows promise as it can capture strong correlation in a variety of larger systems, including the nitrogenase cofactor, FeMoco in an [80,80] active space. This [80,80] active space calculation would require $10^{44}$ variables using a traditional wavefunction method but was calculated using roughly $10^7$ variables with the complete active space self-consistent field variational pair 2-RDM method.

These two different variational pair 2-RDM methods show promise for capturing strong correlation in larger molecular systems at a reduced cost. Future work will need to be dedicated towards testing the scope of these two approaches as well as applying these methods

to a variety of chemical systems.


(1) Szabo, A.; Ostlund, N. S., *Modern Quantum Chemistry: Introduction to Advanced Electronic Structure Theory*; Dover: New York, 1996.

(2) Weinhold, F.; Wilson Jr., E. B. Reduced Density Matrics of Atoms and Molecules. I. The 2 Matrix of Double-Occupancy, Configuration-Interaction Wavefunctions for Singlet States. *Journal of Chemical Physics* **1967**, *46*, 2752.

(3) Roos, B. O. In *Ab Initio Methods in Quantum Chemistry II*, Lawly, K. P., Ed.; Wiley: New York, 1987, pp 399–446.

(4) Coleman, A. J.; Yukalov, V. I., *Reduced Density Matrices: Coulson's Challenge, Chapter 4*; Springer: 2000.

(5) *Reduced-Density-Matrix Mechanics: With Application to Many-Electron Atoms and Molecules*; Mazziotti, D. A., Ed.; Advances in Chemical Physics 134; Wiley: New York, 2007.

(6) Mazziotti, D. A. Two-Electron Reduced Density Matrix as the Basic Variable in Many-Electron Quantum Chemistry and Physics. *Chemical Reviews* **2012**, *112*, 244–262.

(7) Davidson, E. R., *Reduced Density Matrices in Quantum Chemistry*; Academic: New York, 1976.

(8) Valdemoro, C Approximation the 2nd-Order Reduced Density-Matrix in Terms of the 1st-Order One. *Physical Review A* **1992**, *45*, 4462–4467.

(9) Nakatsuji, H; Yasuda, K Direct Determination of the Quantum-Mechanical Density Matrix Using the Density Equation. *Physical Review Letters* **1996**, *76*, 1039–1042.

(10) Löwdin, P. O. Quantum Theory of Many-Particle Systems .1. Physical Interpretations by Means of Density Matrices, Natural Spin-Orbitals, and Convergence Problems in the Method of Configuration Interaction. *Physical Review* **1955**, *97*, 1474–1489.

(11) Mayer, J. E. Electron Correlation. *Physical Review* **1955**, *100*, 1579–1586.

(12) Mazziotti, D. A. Contracted Schrodinger equation: Determining quantum energies and two-particle density matrices without wave functions. *Physical Review A* **1998**, *57*, 4219–4234.

(13) Slebodziski, W., *Exterior Forms and their Applications*; Polish Scientific Publishers: Warsaw, 1970.

(14) Coleman, A. J. Structure of Fermion Density Matrices. *Reviews of Modern Physics* **1963**, *35*, 668.

(15) Erdahl, R. M. Representability. *International Journal of Quantum Chemistry* **1978**, *13*, 697–718.

(16) Kummer, H $N$-Representability Problem for Reduced Density Matrices. *Journal of Mathematical Physics* **1967**, *8*, 2063.

(17) Mazziotti, D. A.; Erdahl, R. M. Uncertainty Relations and Reduced Density Matrices: Mapping Many-Body Quantum Mechanics onto Four Particles. *Physical Review A* **2001**, *63*, 042113.

(18) Nakata, M; Nakatsuji, H; Ehara, M; Fukuda, M; Nakata, K; Fujisawa, K Variational Calculations of Fermion Second-Order Reduced Density Matrices by Semidefinite Programming Algorithm. *Journal of Chemical Physics* **2001**, *114*, 8282–8292.

(19) Mazziotti, D. A. Variational Minimization of Atomic and Molecular Ground-State Energies via the Two-Particle Reduced Density Matrix. *Physical Review A* **2002**, *65*, 062511.

(20) Gidofalvi, G.; Mazziotti, D. A. Spin and Symmetry Adaptation of the Variational Two-Electron Reduced-Density-Matrix Method. *Physical Review A* **2005**, *72*, 052505.

(21) Mazziotti, D. A. Realization of Quantum Chemistry Without Wave Functions through First-Order Semidefinite Programming. *Physical Review Letters* **2004**, *93*, 213001.

(22) Mazziotti, D. A. First-Order Semidefinite Programming for the Two-Electron Treatment of Many-Electron Atoms and Molecules. *ESAIM: Mathematical Modelling and Numerical Analysis* **2007**, *41*, 249–259.

(23) Mazziotti, D. A. Large-Scale Semidefinite Programming for Many-Electron Quantum Mechanics. *Physical Review Letters* **2011**, *106*, 083001.

(24) Sinitskiy, A.; Greenman, L.; Mazziotti, D. A. Strong Correlation in Hydrogen Chains and Lattices Using the Variational Two-Electron Reduced Density Matrix Method. *Journal of Chemical Physics* **2010**, *133*, 014104.

(25) Pelzer, K.; Greenman, L.; Gidofalvi, G.; Mazziotti, D. A. Strong Correlation in Acene Sheets from the Active-Space Variational Two-Electron Reduced Density Matrix Method Effects of Symmetry and Size. *Journal of Physical Chemistry A* **2011**, *114*, 583–588.

(26) Rubin, N. C.; Mazziotti, D. A. Comparison of one-dimensional and quasi-one-dimensional Hubbard models from the variational two-electron reduced-density-matrix method. *Theoretical Chemistry Accounts* **2014**, *133*, 1492.

(27) Schlimgen, A. W.; Heaps, C. W.; Mazziotti, D. A. Entangled Electrons Foil Synthesis of Elusive Low-Valent Vanadium Oxo Complex. *Journal of Physical Chemistry Letters* **2016**, *7*, 627–631.

(28) Schlimgen, A. W.; Mazziotti, D. A. Static and Dynamic Electron Correlation in the Ligan Noninnocent Oxidation of Nickel Dithiolates. *Journal of Physical Chemistry A* **2017**, *122 (48)*, 9377–9384.

(29) McIsaac, A. R.; Mazziotti, D. A. Ligand Non-innocence and Strong Correlation in Manganese Superoxide Dismutase Mimics. *Physical Chemistry Chemical Physics* **2017**, *19*, 4656–4660.

(30) Montgomery, J. M.; Mazziotti, D. A. Strong Electron Correlation in Nitrogenase Cofactor, FeMoco. *Journal of Physical Chemistry A* **2018**, *122 (22)*, 4988–4996.

# CHAPTER 2

# PAIR 2-ELECTRON REDUCED DENSITY MATRIX THEORY USING LOCALIZED ORBITALS



## 2.1 Introduction

Full configuration interaction (FCI) is an exact method to calculate energies in a finite orbital basis set; however, it is computationally expensive and therefore only applicable to very small molecules[1]. Over the years, many approximations have been placed on the FCI calculation to reduce the computational cost to treat larger systems. One approximation is the doubly occupied configuration interaction (DOCI) method, where the FCI calculation is restricted to doubly occupied determinants[2]. Despite this restriction, however, the DOCI method still scales exponentially with system size. Further restriction of the wavefunction can be pursued to achieve non-exponential scaling; examples of methods include antisymmetrized geminal power (AGP) wavefunctions[3–11], antisymmetrized strongly orthogonal geminal product (ASGP) wavefunctions[12–16], and perfect pairing valence bond theory (ppVB) [17–19]. While all of these methods are less general than the DOCI method, they have polynomial scaling and can therefore be used to treat larger systems. Recent methods, such as antisymmetric product of one-reference-orbital geminals (AP1roG) of Ayers, Van Neck, and their collaborators and pair coupled cluster doubles (pCCD) of Scuseria and his collaborators, have used a product ansatz to reproduce the DOCI wavefunction accurately for repulsive Coulombic systems with $\mathcal{O}(N^3)$ computational cost for its solution where $r$ is the number of orbitals[20–30].

A different approach to reducing the scaling of FCI to polynomial is to apply variational

two-electron reduced-density-matrix (2-RDM) theory[31–52] in the pairing space[53, 54]. In the variational 2-RDM method, the energy is expressed as a linear function of the 2-RDM. To ensure that the 2-RDM represents an $N$-electron density matrix, however, we impose $N$-representability conditions[3, 46–48]. While the complete set of $N$-representability conditions has non-polynomial scaling, an approximate set of $N$-representability conditions such as the 2-positivity (DQG) constraints[34, 35, 37, 46] or the 2-positivity and $T_2$ constraints (DQGT)[36, 38, 44] can be applied at polynomial cost. In the pairing space the variational calculation of the 2-RDM subject to the 2-positivity conditions yields a lower bound to the pair FCI (DOCI) energy at a mean-field-like computational scaling of $\mathcal{O}(r^2)$ and $\mathcal{O}(r^3)$ in memory and floating-point operations, respectively, using the DQG constraints[53] and a scaling of $\mathcal{O}(r^3)$ and $\mathcal{O}(r^4)$ in memory and floating-point operations, respectively, using DQG and $T_2$ constraints. The variational 2-RDM method in the pairing space has connections to parametrization of the 2-RDM, based on $N$-representability conditions, to approximate pairing wavefunctions like AGP, ASGP, and DOCI in the context of geminal and natural-orbital functional theories[10–13, 15, 55, 56].

One of the major drawbacks of the pairing approximation is that it is not invariant to unitary transformations of the orbitals, which makes orbital choice important for accurate results. Iterative optimization of the orbitals, however, is computationally expensive, significantly limiting the advantage of using the pair 2-RDM method in contrast to the full variational 2-RDM method without the pairing approximation. Here we develop and implement a pair 2-RDM method in which the optimized orbitals are approximated by localized molecular orbitals (LMOs)[57–60]. The localized molecular orbitals allow for a non-iterative variational solution of the pair 2-RDM by semidefinite programming[31, 49–52]. Like the variational 2-RDM method, the pair 2-RDM method with LMOs has the ability to treat quantum molecular systems with significant multi-reference electron correlation. The pair 2-RDM has the flexibility to describe the spectrum of one-electron RDM occupation numbers

from a quantum state that is invariant to time-reversal symmetry.

In molecular systems the optimal orbitals in the pairing approximation tend to be highly localized in position space. Canonical molecular orbitals (CMOs) from Hartree-Fock theory are often highly delocalized making them a poor approximation to the optimal orbitals. Furthermore, a pair 2-RDM calculation with CMOs is not a size-extensive method; a method is *size-extensive* if its energy scales linearly with system size. However, localizing these orbitals to produce LMOs numerically recovers the size-extensive property at a much lower computational cost than computing the optimal pair orbitals iteratively. While size extensivity is observed numerically in all of the calculations performed, the property may be theoretically approximate because of the approximate nature of the orbital localization and the $N$-representability conditions[61]. Calculations with pCCD have also shown good results with localized orbitals[26]. The use of localized orbitals is applicable to any pair theory including the parametrization of the wavefunction like pCC and AP1roG[20–30] as well as parametrizations of the 2-RDM to approximate pair wavefunctions in geminal and natural-orbital functional theories[10–12, 55, 56, 62, 63].

The pair 2-RDM theory combined with LMOs gives us a low-cost, approximately size-extensive method that allows for the study of many physical and chemical systems including systems with significant multi-reference correlation. In Section 2.2 we present the framework for the pair 2-RDM theory with the LMOs, and in section 2.3 we explore applications to hydrogen chains, acene chains and cadmium telluride polymer chains.

## 2.2 Theory

The variational 2-RDM theory, the pairing approximation and the issue of orbital non-invariance are discussed in Secs. 2.2.1, 2.2.2, and 2.2.3 respectively.

### 2.2.1 Variational 2-RDM Theory

The 2-RDM represents the probability distribution of two electrons in the field of $(N-2)$ electrons, and in a finite orbital basis set its matrix elements can be expressed as [3, 31, 64–68],

$$^2D^{ij}_{kl} = \langle\Psi|\hat{a}^\dagger_i\hat{a}^\dagger_j\hat{a}_l\hat{a}_k|\Psi\rangle, \tag{2.1}$$

where the indices $i$, $j$, $k$, and $l$ denote the spin orbitals and $\hat{a}^\dagger$ and $\hat{a}$ are the creation and annihilation operators respectively. The energy of an $N$-electron system can be written as[3, 31, 64–70],

$$E = \sum_{ijkl} {}^2K^{ij}_{kl}\,{}^2D^{ij}_{kl}, \tag{2.2}$$

where $^2K^{ij}_{kl}$ is the two-electron Hamiltonian given by,

$$^2K^{ij}_{kl} = \frac{4}{N-1}\,{}^1K^i_k \wedge \delta^j_l + {}^2V^{ij}_{kl}, \tag{2.3}$$

in which, $^1K^i_k$ and $^2V^{ij}_{kl}$ are one- and two-electron matrices containing the one- and two-electron integrals and $\wedge$ is the Grassmann wedge product [68, 71]. Because not every two-electron density matrix represents an $N$-electron quantum system, the ground-state energy of a many-electron atom or molecule cannot be variationally optimized with respect to the 2-RDM without explicit constraints on the 2-RDM. The conditions that ensure that the 2-RDM corresponds to a physical $N$-electron wavefunction are known as $N$-representability conditions[3, 31, 34, 45–48, 64–70, 72, 73].

A necessary, albeit not sufficient, set of $N$-representability conditions on the 2-RDM are

the 2-positivity conditions, also known as the DQG conditions [45, 46, 72]:

$$^2D \succeq 0 \tag{2.4}$$

$$^2Q \succeq 0 \tag{2.5}$$

$$^2G \succeq 0, \tag{2.6}$$

where $^2D$, $^2Q$, and $^2G$ are the two-particle, two-hole, and particle-hole density matrices respectively whose matrix elements are defined by Eq. (2.1) and

$$^2Q^{ij}_{kl} = \langle\Psi|\hat{a}_i\hat{a}_j\hat{a}^\dagger_l\hat{a}^\dagger_k|\Psi\rangle \tag{2.7}$$

$$^2G^{ij}_{kl} = \langle\Psi|\hat{a}^\dagger_i\hat{a}_j\hat{a}^\dagger_l\hat{a}_k|\Psi\rangle. \tag{2.8}$$

Additional $N$-representability conditions can be added, such as the $T_2$ constraint[36, 45, 47, 74],

$$T_2 =^3 E +^3 F \succeq 0, \tag{2.9}$$

where

$$^3E^{qrs}_{ijk} = \langle\Psi|\hat{a}^\dagger_q\hat{a}_r\hat{a}^\dagger_s\hat{a}_k\hat{a}^\dagger_j\hat{a}_i|\Psi\rangle \tag{2.10}$$

$$^3F^{qrs}_{ijk} = \langle\Psi|\hat{a}_q\hat{a}^\dagger_r\hat{a}_s\hat{a}^\dagger_k\hat{a}_j\hat{a}^\dagger_i|\Psi\rangle. \tag{2.11}$$

The general constraint of $M \succeq 0$ means that the matrix $M$ is constrained to be positive semidefinite. A matrix is *positive semidefinite* if and only if its eigenvalues are nonnegative. Rearranging the creation and annihilation operators generates linear mappings between the D, Q, and G metric matrices. The ground-state energy can be minimized with respect to the 2-RDM subject to these conditions[43, 44] by a family of optimization known as semidefinite

programming[31, 49–52].

### *2.2.2 Pairing Approximation*

We invoke pairing of the orbitals such that instead of considering $r$ independent orbitals, we consider $r/2$ pairs of orbitals. Both orbitals in the pair are occupied or unoccupied for all determinants contributing to the wavefunction. We pair the orbitals by spin $\langle \hat{S}_z \rangle$, which is the most common choice[30, 53]. Pairing the orbitals in configuration interaction still scales exponentially with system size; however, pairing in the variational 2-RDM theory[31–44, 46–52] generates calculations with polynomial scaling.

To understand the scaling of the method, consider the reduced density matrices in the natural-orbital basis set[3, 53, 54]. Because the natural orbitals are the eigenfunctions of the 1-RDM, contraction of the ${}^2D$ to the ${}^1D$ produces a diagonal matrix whose elements are

$$\langle \hat{a}^\dagger_{i\alpha} \hat{a}_{i\alpha} \rangle. \tag{2.12}$$

The $\beta$ spin block of the 1-RDM, which is identical to the $\alpha$ spin block by the pairing approximation, need not be stored.

The structure of the 2-RDM is a block diagonal matrix with one $r \times r$ block with $r$-choose-two $1\times1$ blocks given by

$$\begin{pmatrix} \langle \hat{a}^\dagger_{i\alpha} \hat{a}^\dagger_{i\beta} \hat{a}_{i\beta} \hat{a}_{i\alpha} \rangle & \dots & \langle \hat{a}^\dagger_{i\alpha} \hat{a}^\dagger_{i\beta} \hat{a}_{k\beta} \hat{a}_{k\alpha} \rangle \\ \vdots & \ddots & \vdots \\ \langle \hat{a}^\dagger_{k\alpha} \hat{a}^\dagger_{k\beta} \hat{a}_{i\beta} \hat{a}_{i\alpha} \rangle & \dots & \langle \hat{a}^\dagger_{k\alpha} \hat{a}^\dagger_{k\beta} \hat{a}_{k\beta} \hat{a}_{k\alpha} \rangle \end{pmatrix}, \tag{2.13}$$

and

$$\left( \langle \hat{a}^\dagger_{i\alpha} \hat{a}^\dagger_{j\beta} \hat{a}_{j\beta} \hat{a}_{i\alpha} \rangle \right), \tag{2.14}$$

respectively[3]. By particle-hole symmetry, the structure of the ${}^2Q$ and ${}^1Q$ matrices can be

defined analogously. The structure of the ${}^2G$ matrix is a block diagonal matrix with one $r \times r$ block and $r$-choose-two 2×2 blocks given by

$$\begin{pmatrix} \langle \hat{a}^\dagger_{i\alpha} \hat{a}_{i\alpha} \hat{a}^\dagger_{i\alpha} \hat{a}_{i\alpha} \rangle & \dots & \langle \hat{a}^\dagger_{i\alpha} \hat{a}_{i\alpha} \hat{a}^\dagger_{k\alpha} \hat{a}_{k\alpha} \rangle \\ \vdots & \ddots & \vdots \\ \langle \hat{a}^\dagger_{k\alpha} \hat{a}_{k\alpha} \hat{a}^\dagger_{i\alpha} \hat{a}_{i\alpha} \rangle & \dots & \langle \hat{a}^\dagger_{k\alpha} \hat{a}_{k\alpha} \hat{a}^\dagger_{k\alpha} \hat{a}_{k\alpha} \rangle \end{pmatrix}, \tag{2.15}$$

and

$$\begin{pmatrix} \langle \hat{a}^\dagger_{i\alpha} \hat{a}_{j\beta} \hat{a}^\dagger_{j\beta} \hat{a}_{i\alpha} \rangle & \langle \hat{a}^\dagger_{i\alpha} \hat{a}_{j\beta} \hat{a}^\dagger_{i\beta} \hat{a}_{j\alpha} \rangle \\ \langle \hat{a}^\dagger_{j\alpha} \hat{a}_{i\beta} \hat{a}^\dagger_{j\beta} \hat{a}_{i\alpha} \rangle & \langle \hat{a}^\dagger_{j\alpha} \hat{a}_{i\beta} \hat{a}^\dagger_{i\beta} \hat{a}_{j\alpha} \rangle \end{pmatrix}, \tag{2.16}$$

respectively.

The structure of the $T_2$ matrix is a block diagonal matrix consisting of $r$ $r \times r$ blocks and $r$ 2×2 blocks which are obtainable from the sum of corresponding blocks of the ${}^3E$ and ${}^3F$ matrices. The $r$ $r \times r$ blocks and the $r$ 2×2 blocks of the ${}^3E$ matrix are given by

$$\begin{pmatrix} \langle \hat{a}^\dagger_{i\alpha} \hat{a}_{i\alpha} \hat{a}^\dagger_{m\beta} \hat{a}_{m\beta} \hat{a}^\dagger_{i\alpha} \hat{a}_{i\alpha} \rangle & \dots & \langle \hat{a}^\dagger_{i\alpha} \hat{a}_{i\alpha} \hat{a}^\dagger_{m\beta} \hat{a}_{m\beta} \hat{a}^\dagger_{k\alpha} \hat{a}_{k\alpha} \rangle \\ \vdots & \ddots & \vdots \\ \langle \hat{a}^\dagger_{k\alpha} \hat{a}_{k\alpha} \hat{a}^\dagger_{m\beta} \hat{a}_{m\beta} \hat{a}^\dagger_{i\alpha} \hat{a}_{i\alpha} \rangle & \dots & \langle \hat{a}^\dagger_{k\alpha} \hat{a}_{k\alpha} \hat{a}^\dagger_{m\beta} \hat{a}_{m\beta} \hat{a}^\dagger_{k\alpha} \hat{a}_{k\alpha} \rangle \end{pmatrix}, \tag{2.17}$$

and

$$\begin{pmatrix} \langle \hat{a}^\dagger_{i\alpha} \hat{a}_{j\beta} \hat{a}^\dagger_{m\alpha} \hat{a}_{m\alpha} \hat{a}^\dagger_{j\beta} \hat{a}_{i\alpha} \rangle & \langle \hat{a}^\dagger_{i\alpha} \hat{a}_{j\beta} \hat{a}^\dagger_{m\alpha} \hat{a}_{m\alpha} \hat{a}^\dagger_{i\beta} \hat{a}_{j\alpha} \rangle \\ \langle \hat{a}^\dagger_{j\alpha} \hat{a}_{i\beta} \hat{a}^\dagger_{m\alpha} \hat{a}_{m\alpha} \hat{a}^\dagger_{j\beta} \hat{a}_{i\alpha} \rangle & \langle \hat{a}^\dagger_{j\alpha} \hat{a}_{i\beta} \hat{a}^\dagger_{m\alpha} \hat{a}_{m\alpha} \hat{a}^\dagger_{i\beta} \hat{a}_{j\alpha} \rangle \end{pmatrix}, \tag{2.18}$$

respectively, where $m$ ranges from 1 to $r$. Analogous blocks from pairing are definable for the ${}^3F$ matrix.

The pairing subspace has a significant effect on the structure of the 2-RDM, making it a sparse block diagonal matrix[3, 53]. With just the DQG constraints, each $r \times r$ block has a storage scaling of $r^2$ with a computational (floating-point) scaling of $r^3$ while the set of 1×1 blocks has a scaling in storage and floating-point operations of $r^2$. In the full CI space,

the scaling of the variational 2-RDM method with the D, Q, and G conditions[31–44] is $r^6$ in terms of floating-point operations, and hence, the pairing space reduces this cost to $r^3$. Using DQG conditions as well as the $T_2$ constraints increases the computational cost to $r^4$ and $r^3$ in floating-point operations and storage, respectively.

Despite the reduction in computational cost, the pair 2-RDM has the flexibility to describe the spectra of one-electron RDM occupation numbers from all quantum states that are invariant to time-reversal symmetry. The pair 2-RDM is more general than the 2-RDM from the antisymmetrized geminal power (AGP) approximation, which Coleman [3, 10, 11] showed to be sufficiently flexible to parameterize any 1-RDM whose eigenvalues (natural occupations) are pairwise degenerate. Smith [10, 11, 75] showed that any quantum state that is invariant to time-reversal symmetry has a 1-RDM with pairwise degenerate eigenvalues. Consequently, the pair 2-RDM method has the potential to describe quantum states with highly fractional occupation numbers, representing significant multi-reference electron correlation.

### *2.2.3 Orbital Non-Invariance*

The pairing method is not invariant to orbital transformation, which means the choice of orbitals is important. In the pair 2-RDM method, because the 1-RDM is diagonal, the orbitals chosen for the basis set become the natural orbitals. One simple choice is the canonical molecular orbitals (CMOs) from Hartree-Fock theory which are delocalized in space. Although this is an accurate model for some molecular systems, it is insufficient for many others. Because the natural orbitals are generally highly localized, a delocalized basis is not the best approximation. One strategy previously used is to optimize the orbitals with respect to the ground-state energy [53]. This process improves the accuracy of the computation, producing localized orbitals, but it comes with the additional costs of orbital optimizations and electron repulsion integral transformations.

A second strategy that we adopt is to localize the CMOs to obtain localized molecular orbitals (LMOs). There are many different schemes for such localization including fourth moment, Edmiston-Ruedenberg, Foster-Boys, and Pipek-Mezey [57–60]. The Foster-Boys method localizes orbitals by minimizing an objective function,

$$\mathcal{L}^{FB} = \sum_i \langle \phi_i | [\mathbf{r} - \langle \phi_i | \mathbf{r} | \phi_i \rangle]^2 | \phi_i \rangle \tag{2.19}$$

which measures the spatial dispersion of the orbitals[57, 58, 76]. In this work, we use primarily the Pipek-Mezey method which localizes the orbitals by maximizing the Mulliken charge of each orbital,

$$\mathcal{L}^{PM} = \sum_i \sum_A [\langle \phi_i | P_A | \phi_i \rangle]^2, \tag{2.20}$$

where the indices $i$ and $A$ represent orbitals and atoms, respectively[60, 77].

## 2.3 Applications

In this section we will discuss our computational methodology followed by applications to hydrogen chains, acene chains and cadmium telluride polymer chains in Secs. 2.3.1, 2.3.2, 2.3.3, and 2.3.4 respectively.

### *2.3.1 Computational Methodology*

Localized orbitals were generated by NWCHEM[78], while canonical orbitals and electron integrals were generated by GAMESS[79] for all molecules. Semidefinite programming (SDP) was used to minimize the energy as a function of the 2-RDM constrained by linear matrix inequalities [49, 80] by employing a boundary-point algorithm developed by Mazziotti for 2-RDM methods. [50, 52] The STO-6G basis set was used for the acene and hydrogen chains[81], unless otherwise specified, while the 3-21G basis set was used for the cadmium

Table 2.1: The FCI correlation energy along with the pair 2-RDM calculated correlation energies and % recovery for hydrogen chains of lengths four to twelve using both CMOs and LMOs.

| Chain Length | FCI Correlation Energy (a.u.) | CMOs | | LMOs | |
|---|---|---|---|---|---|
| | | Cor. Energy (a.u) | % Recovery | Cor. Energy (a.u) | % Recovery |
| 4 | -0.16788561 | -0.06641161 | 39.56 | -0.14662668 | 87.34 |
| 6 | -0.24680914 | -0.06146402 | 24.90 | -0.20296733 | 82.24 |
| 8 | -0.32536318 | -0.05551949 | 17.06 | -0.25555734 | 78.55 |
| 10 | -0.40380709 | -0.05275382 | 13.06 | -0.31176026 | 77.21 |
| 12 | -0.48222454 | -0.04997869 | 10.36 | -0.36517032 | 75.73 |

telluride polymer chains[82].

### *2.3.2 Hydrogen Chains*

The pair 2-RDM method was used to calculate the correlation energy of hydrogen chains of varying lengths. The calculation was performed using the Hartree-Fock CMOs as well as using the Pipek-Mezey LMOs and the results are presented in comparison to the correlation energy from FCI in Fig. 2.1. It should be noted that the comparison between using DQG and DQGT conditions for both CMOs and LMOs is also presented in Fig. 2.1. As observed with the FCI, the correlation energy from the pair 2-RDM method with LMOs increases linearly with chain length; in contrast, the pair 2-RDM method with CMOs captures much less correlation energy and the amount correlation energy slightly decreases with increasing chain length. The Foster-Boys LMOs and the Pipek-Mezey LMOs give identical results for the hydrogen chains. The calculations with DQG constraints produce very similar results to the calculations with DQGT conditions and will therefore be used for the rest of this paper. Similar trends are observed for hydrogen chains through $H_{50}$ in Fig. 2.2.

Table 2.1 shows the results for hydrogen chains of twelve units or shorter compared to the FCI correlation energy and the percentage of FCI correlation energy recovered. The energy of $H_8$, with an H-H bond distance of 1.5Å was calculated using the cc-pVDZ basis set[83] and

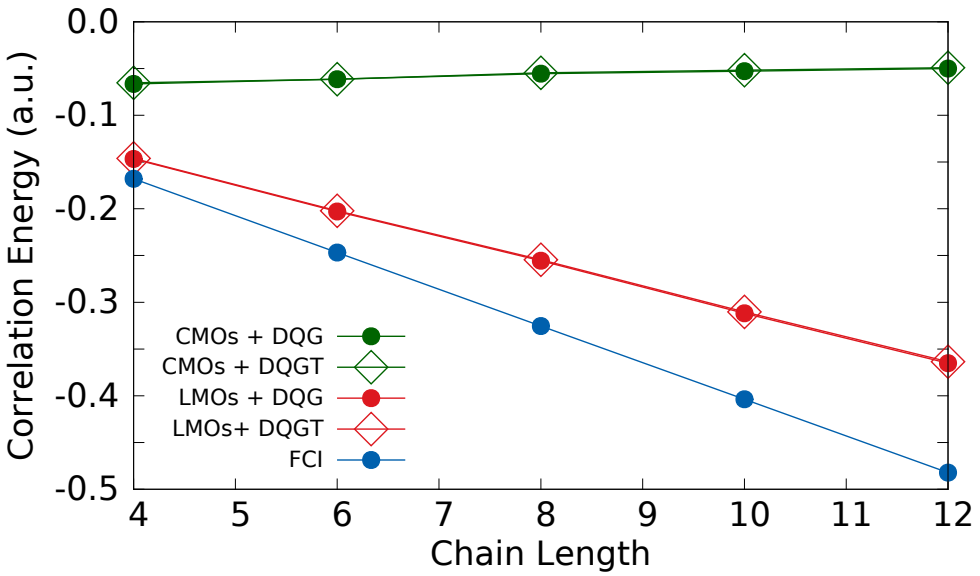


Figure 2.1: Calculated correlation energy of hydrogen chains using pair 2-RDM with CMOs and DQG conditions (green circles), pair 2-RDM with CMOs and DQGT conditions (green diamonds), pair 2-RDM with LMOs and DQG conditions (red circles), pair 2-RDM with LMOs and DQGT conditions (red diamonds), and FCI (blue circles).

Pipek-Mezey localization. The localized results show roughly a 97% recovery of the energy from optimized orbitals[53]. Lastly, a dissociation curve was created for $H_6$ using the 6-31G basis set[84]. The dissociation curve compares the Hartree-Fock energy to the energies from pair 2-RDM theory, using CMOs and LMOs, to the FCI energy, as shown in Fig. 2.3. It should be noted that in the limit of greater separation, the pair 2-RDM theory with CMOs follows the trend of the Hartree-Fock energy while the pair 2-RDM theory with LMOs follows the FCI energy. The *non-parallelity error* of a dissociation curve is the difference between the largest and the smallest deviations of the calculated curve from the exact curve. In these results, the errors of the Hartree-Fock method, pair 2-RDM theory with CMOs, and pair 2-RDM theory with LMOs relative to the FCI curve are 0.3756 a.u., 0.2765 a.u., and 0.0691 a.u. respectively.

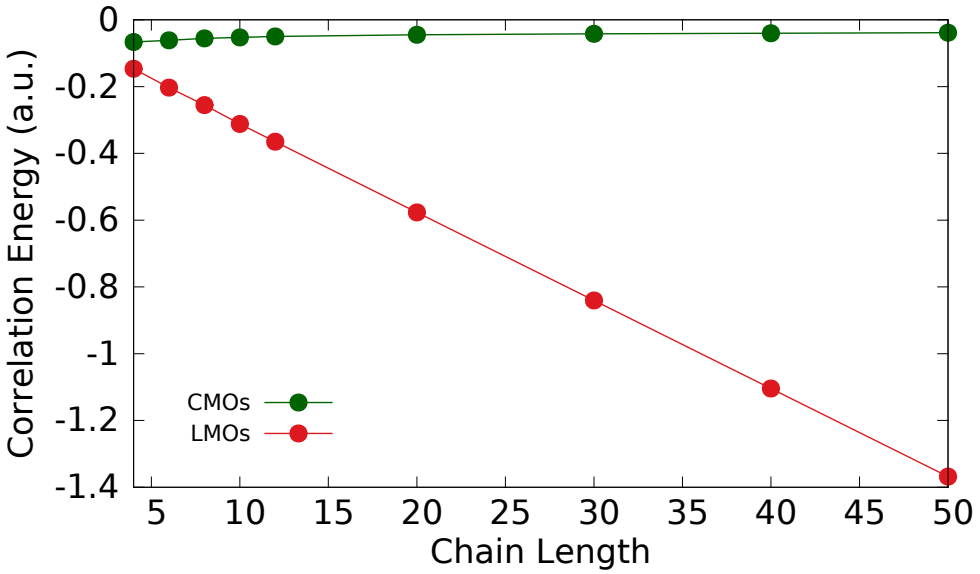


Figure 2.2: Calculated correlation energy of hydrogen chains using pair 2-RDM with CMOs (green) and pair 2-RDM with LMOs (red).

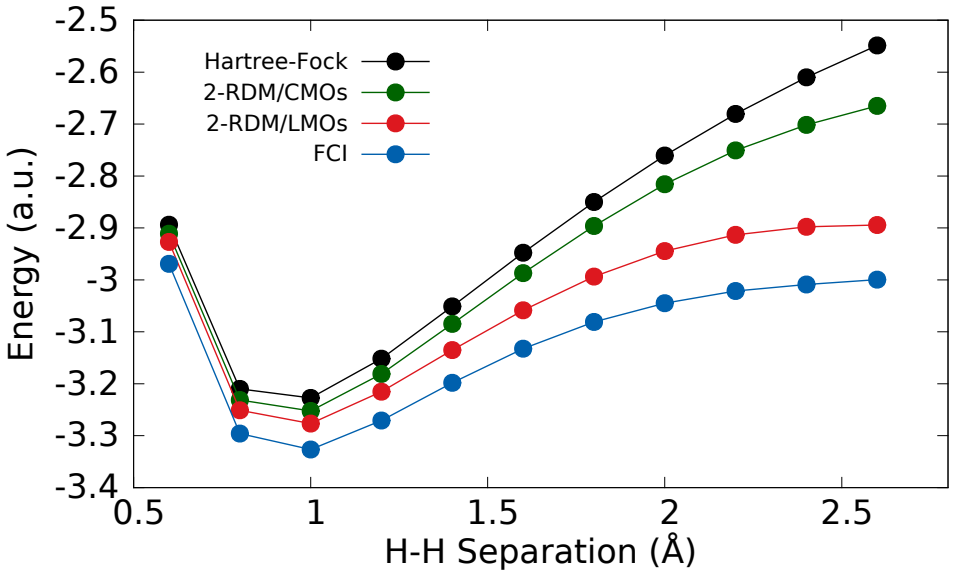


Figure 2.3: Dissociation curve of $H_6$ using Hartree-Fock (black), pair 2-RDM with CMOs (green), pair 2-RDM with LMOs (red), and FCI (blue).

### *2.3.3 Acene Chains*

The pair 2-RDM method with CMOs and Pipek-Mezey LMOs was also applied to a series of acene chains, the longest being octacene as shown in Fig. 2.4. Acene chains have many

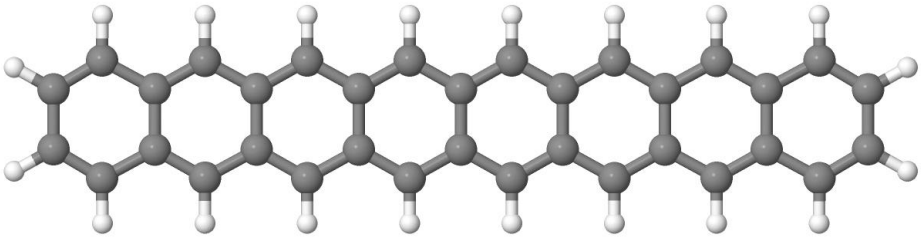

Figure 2.4: Octacene where carbon atoms are grey and hydrogen are white, image produced with Jmol[85].

different useful applications, including tetracene and pentacene in light-emitting diodes and field-effect transistors[86, 87] For napthalene to octacene, the comparison between the correlation energies using CMOs and LMOs is presented in Fig. 2.5. It should be noted that in

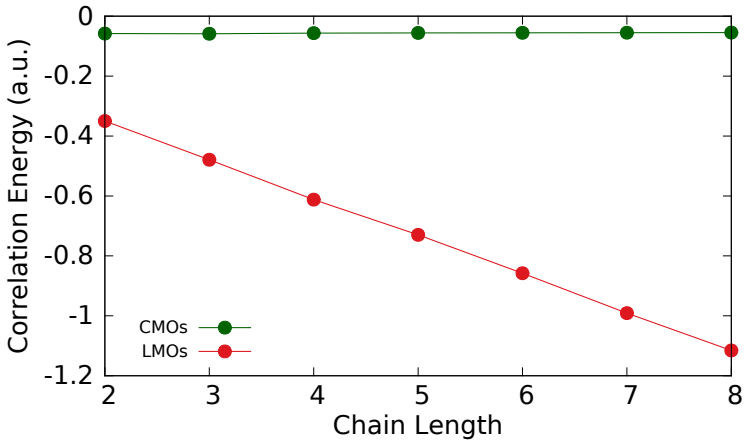


Figure 2.5: Pair 2-RDM method calculations of correlation energy in acene chains using CMOs (green) and LMOs (red).

the case of the CMOs, the correlation energy is actually tending towards zero as the chain length increases.

### *2.3.4 Cadmium Telluride Polymers*

Cadmium telluride polymers were first synthesized by Talapin and co-workers to serve as inorganic linkers which enhance the conductivity between nanoparticles in nanocrystalline arrays[88]. Using the geometry of the base unit obtained from crystal structures, [88] we applied the pair 2-RDM method to cadmium telluride polymer chains ranging from one unit to four units, where the longest chain is shown in Fig. 2.6. The correlation energy was calculated using both CMOs and LMOs and the results are shown in Table 2.2. The pair 2-RDM theory with LMOs recovers one-and-a-half orders of magnitude more correlation energy than the pair theory with CMOs.

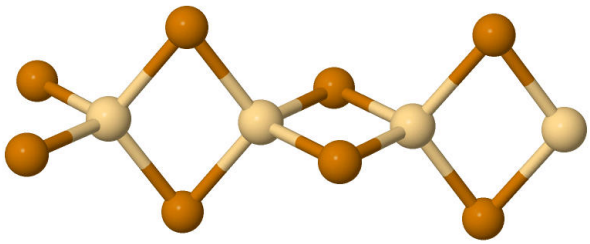


Figure 2.6: $Cd_4Te_8$ where cadmium atoms are beige and telluride are brown, image produced with Jmol[85].

Table 2.2: The calculated correlation energy using the pair 2-RDM method with both CMOs and LMOs for cadmium telluride polymer chains of varying lengths.

| Chain Length | CMOs Corr. Energy (a.u.) | LMOs Corr. Energy (a.u.) |
|---|---|---|
| 1 | -0.02834903 | -0.03173513 |
| 2 | -0.04965044 | -0.06020495 |
| 3 | -0.07781730 | -0.09026143 |
| 4 | -0.07158556 | -0.12465561 |

## 2.4 Discussion and Conclusions

In this paper we introduce a pair 2-RDM method using localized molecular orbitals. Localized orbitals were chosen over both optimized orbitals and canonical orbitals due to their decreased cost and increased accuracy respectively. Optimized orbitals are calculated through an iterative process and are therefore computationally expensive. By using localized orbitals as an approximation to the optimized orbitals, we can perform a single variational 2-RDM calculation which significantly lowers computational cost. Moreover, the result from the calculation of $H_8$ shows that localized orbitals yield energies similar to those from the more expensive full orbital optimization. While canonical orbitals have the same computational cost as localized orbitals, they sacrifice both (i) accuracy and (ii) size-extensivity. Applications of the pair 2-RDM theory with localized molecular orbitals were also made to hydrogen chains, acenes, and cadmium telluride polymers. Each of these calculations showed that the pair 2-RDM theory with localized orbitals recovers non-trivial electron correlation in an approximately size-extensive fashion.

FCI in the pairing subspace is an accurate method, but its computations scale exponentially. There are many other methods which further approximate the pair FCI wavefunction including AGP[3–9, 89], ASGP[12–16], and ppVB[17–19], but they do not approach the accuracy of FCI in the pairing space (DOCI). More recently developed methods, including AP1roG and pCCD, scale polynomially and are in good agreement with the DOCI results. [20–28, 30, 90] The pair 2-RDM method is distinct from the wavefunction methods in that its basic variable is the 2-RDM constrained by $N$-representability conditions.

The pair 2-RDM theory also has significant connections to parameterizations of the 2-RDM to approximate AGP, ASGP,and DOCI wavefunctions in geminal and natural-orbital functional theories[10–13, 15, 55, 56]. In the context of geminal functional theory, Mazziotti formulated the 1-electron RDM (or natural-orbital) functional theory as a parameterization of the2-RDM[10] rather than a parameterization of the wavefunction or $N$-electron

density matrix as in earlier theories based on Levy[91] or Valone[92] constrained search. The advantage of this formulation is that the parameterization can incorporate the ensemble[3, 45, 46] or pure[44] $N$-representability conditions of the 2-RDM. Mazziotti developed a 1-RDM (geminal) functional that recovers the AGP energy and 1-RDM[11]. Piris and collaborators developed a 1-RDM (natural-orbital) functional that recovers the ASGP energy and 1-RDM[55], and recently, Piris[63] as well as Gebauer, Cohen, and Car[56] presented natural-orbital parameterizations of the 2-RDM whose energies approach the accuracy of DOCI. While the natural-orbital (geminal) functional theories and the pair 2-RDM both employ $N$-representability conditions, they differ in that the functional theories parameterize the 2-RDM in terms of the natural orbitals and their occupations (as well as phase factors in the case of geminal functional theory), whereas pair 2-RDM directly employs the 2-RDM restricted to the pairing space.

The accurate $\mathcal{O}(r^3)$ approximation of FCI in the pairing space by the pair 2-RDM methods with localized molecular orbitals presents new possibilities for the description of strong correlation phenomena. Potential applications include the description of both the structure and the dynamics of large molecular systems. The use of localized molecular orbitals is applicable to any pair-type theory whether based on the wavefunction or the 2-RDM.


(1) Szabo, A.; Ostlund, N. S., *Modern Quantum Chemistry: Introduction to Advanced Electronic Structure Theory*; Dover: New York, 1996.

(2) Weinhold, F.; Wilson Jr., E. B. Reduced Density Matrics of Atoms and Molecules. I. The 2 Matrix of Double-Occupancy, Configuration-Interaction Wavefunctions for Singlet States. *Journal of Chemical Physics* **1967**, *46*, 2752.

(3) Coleman, A. J.; Yukalov, V. I., *Reduced Density Matrices: Coulson's Challenge, Chapter 4*; Springer: 2000.

(4) Richardson, R. W. A restricted class of exact eigenstates of the pairing-force Hamiltonian. *Physics Letters* **1963**, *3*, 277.

(5) Richardson, R. W.; Sherman, N. Exact eigenstates of the pairing-force Hamiltonian. *Nuclear Physics* **1964**, *52*, 221.

(6) Parr, R. G.; Ellison, F. O.; Lykos, P. G. Hamiltonian antisymmetrized product wave functions for atoms and molecules. *Journal of Chemical Physics* **1956**, *24*, 1106.

(7) Silver, D. M. Electron pair correlation - pproduct of N(N-1)/2 geminals for N electrons. *Journal of Chemical Physics* **1971**, *55*, 1461.

(8) Coleman, A. J. Structure of Fermion Density Matrices. II. Antisymmetrized Geminal Powers. *Journal of Mathematical Physics* **1965**, *6*, 1425.

(9) Coleman, A. J. The AGP model for fermion systems. *International Journal of Quantum Chemistry* **1997**, *63*, 23.

(10) Mazziotti, D. A. Geminal functional theory: A synthesis of density and density matrix methods. *Journal of Chemical Physics* **2000**, *112*, 10125.

(11) Mazziotti, D. A. Energy Functional of the One-Particle Reduced Density Matrix: A Geminal Approach. *Chemical Physics Letters* **2001**, *338*, 323–328.

(12) Pernal, K. The equivalence of the Piris Natural Orbital Functional 5 (PNOF5) and the antisymmetrized product of strongly orthogonal geminal theory. *Compututational and Theoretical Chemistry* **2013**, *1003*, 127–129.

(13) Piris, M. Bounds on the PNOF5 natural geminal occupation numbers. *Compututational and Theoretical Chemistry* **2013**, *1003*, 123–126.

(14) Johnson, P. A.; Ayers, P. W.; Limacher, P. A.; De Baerdemacker, S.; Van Neck, D.; Bultinck, P. A size-consistent approach to strongly correlated systems using a generalized antisymmetrized product of nonorthogonal geminals. *Computational and Theoretical Chemistry* **2013**, *1003*, 101–113.

(15) Piris, M.; Matxain, J. M.; Lopez, X.; Ugalde, J. M., *8th Congress on Electronic Structure: Principles and Applications*; Novoa, J. J., Ruiz Lopez, M. F., Eds.; Springer: Verlag Berlin Heidelberg, 2014.

(16) Rassolov, V. A. A geminal model chemistry. *Journal of Chemical Physics* **2002**, *117*, 5978–5987.

(17) Dykstra, C. E. Perfect Pairing Valence Bond Generalization of Self-Consistent Electron Pair Theory. *Journal of Chemical Physics* **1980**, *72*, 2928–2935.

(18) Goddard, W. A.; Dunning, T. H.; Hunt, W. J.; Hay, P. J. Generalized Valence Bond Description of Bonding in Low-Lying States of Molecules. *Accounts of Chemical Research* **1973**, *6*, 368–376.

(19) Hunt, W. J.; Hay, P. J.; Goddard, W. A. Self-Consistent Procedures for Generalized Valence Bond Wavefunctions - Applications H-3, BH, H2O, C2H6, and O2. *Journal of Chemical Physics* **1972**, *57*, 738.

(20) Limacher, P. A.; Ayers, P. W.; Johnson, P. A.; De Baerdemacker, S.; Van Neck, D.; Bultinck, P. A New Mean-Field Method Suitable for Strongly Correlated Electrons: Computationally Facile Antisymmetric Products of Nonorthogonal Geminals. *Journal of Chemical Theory and Computation* **2013**, *9*, 1394–1401.

(21) Boguslawski, K.; Tecmer, P.; Limacher, P. A.; Johnson, P. A.; Ayers, P. W.; Bultinck, P.; Baerdemacker, S. D.; Van Neck, D. Projected seniority-two orbital optimization of the antisymmetric product of one-reference orbital geminal. *Journal of Chemical Physics* **2014**, *140*, 214114.

(22) Boguslawski, K.; Tecmer, P.; Ayers, P. W.; Bultinck, P.; De Baerdemacker, S.; Van Neck, D. Efficient description of strongly correlated electrons with mean-field cost. *Physical Review B* **2014**, *89*, 201106.

(23) Tecmer, P.; Boguslawski, K.; Johnson, P. A.; Limacher, P. A.; Chan, M.; Verstraelen, T.; Ayers, P. W. Assessing the Accuracy of New Geminal-Based Approaches. *Journal of Physical Chemistry A* **2014**, *118*, 9058–9068.

(24) Boguslawski, K.; Ayers, P. W. Linearized Coupled Cluster Correction on the Antisymmetric Product of 1-Reference Orbital Geminals. *Journal of Chemical Theory and Computation* **2015**, *11*, 5252–5261.

(25) Bytautas, L.; Henderson, T. M.; Jimnez-Hoyos, C. A.; Ellis, J. K.; Scuseria, G. E. Seniority and orbital symmetry as tools for establishing a full configuration interaction hierarchy. *Journal of Chemical Physics* **2011**, *135*, 044119.

(26) Stein, T.; Henderson, T. M.; Scuseria, G. E. Seniority zero pair coupled cluster doubles theory. *Journal of Chemical Physics* **2014**, *140*, 214113.

(27) Henderson, T. M.; Bulik, I. W.; Stein, T.; Scuseria, G. E. Seniority-based coupled cluster theory. *Journal of Chemical Physics* **2014**, *141*, 244104.

(28) Henderson, T. M.; Bulik, I. W.; Scuseria, G. E. Pair extended coupled cluster doubles. *Journal of Chemical Physics* **2015**, *142*, 214116.

(29) Bulik, I. W.; Henderson, T. M.; Scuseria, G. E. Can Single-Reference Coupled Cluster Theory Describe Static Correlation? *Journal of Chemical Theory and Computation* **2015**, *11*, 7, 3171–3179.

(30) Shepherd, J. J.; Henderson, T. M.; Scuseria, G. E. Using full configuration interaction quantum Monte Carlo in a seniority zero space to investigate the correlation energy equivalence of pair coupled cluster doubles and doubly occupied configuration interaction. *Journal of Chemical Physics* **2016**, *144*, 094112.

(31) *Reduced-Density-Matrix Mechanics: With Application to Many-Electron Atoms and Molecules*; Mazziotti, D. A., Ed.; Advances in Chemical Physics 134; Wiley: New York, 2007.

(32) Garrod, C; Mihailovic, M.; Rosina, M Variational Approach to 2-Body Density Matrix. *Journal of Mathematical Physics* **1975**, *16*, 868–874.

(33) Erdahl, R. M. Two algorithms for the lower bound method of reduced density matrix theory. *Reports on Mathematical Physics* **1979**, *15*, 147–162.

(34) Mazziotti, D. A.; Erdahl, R. M. Uncertainty Relations and Reduced Density Matrices: Mapping Many-Body Quantum Mechanics onto Four Particles. *Physical Review A* **2001**, *63*, 042113.

(35) Nakata, M; Nakatsuji, H; Ehara, M; Fukuda, M; Nakata, K; Fujisawa, K Variational Calculations of Fermion Second-Order Reduced Density Matrices by Semidefinite Programming Algorithm. *Journal of Chemical Physics* **2001**, *114*, 8282–8292.

(36) Zhao, Z.; Braams, B.; Fukuda, M; Overton, M.; Percus, J. The reduced density matrix method for electronic structure calculations and the role of three-index representability conditions. *Journal of Chemical Physics* **2004**, *120*, 2095–2104.

(37) Mazziotti, D. A. Variational Minimization of Atomic and Molecular Ground-State Energies via the Two-Particle Reduced Density Matrix. *Physical Review A* **2002**, *65*, 062511.

(38) Mazziotti, D. A. Variational reduced-density-matrix method using three-particle N-representability conditions with application to many-electron molecules. *Physical Review A* **2006**, *74*, 032501.

(39) Gidofalvi, G.; Mazziotti, D. A. Active-Space Two-Electron Reduced-Density-Matrix Method: Complete Active-Space Calculations Without Diagonalization of the N-electron Hamiltonian. *Journal of Chemical Physics* **2008**, *129*, 134108.

(40) Pelzer, K.; Greenman, L.; Gidofalvi, G.; Mazziotti, D. A. Strong Correlation in Acene Sheets from the Active-Space Variational Two-Electron Reduced Density Matrix Method Effects of Symmetry and Size. *Journal of Physical Chemistry A* **2011**, *114*, 583–588.

(41) Verstichel, B.; van Aggelen, H.; Poelmans, W.; Van Neck, D. Variational Two-Particle Density Matrix Calculation for the Hubbard Model Below Half Filling Using Spin-Adapted Lifting Conditions. *Physical Review Letters* **2012**, *108*, 213001.

(42) Fosso-Tande, J.; Nguyen, T. S.; Gidofalvi, G.; DePrince III, A. E. Large-Scale Variational Two-Electron Reduced-Density-Matrix-Driven Complete Active Space Self-Consistent Field Methods. *Journal of Chemical Theory and Computation* **2016**, *12*, 2260–2271.

(43) Schlimgen, A. W.; Heaps, C. W.; Mazziotti, D. A. Entangled Electrons Foil Synthesis of Elusive Low-Valent Vanadium Oxo Complex. *Journal of Physical Chemistry Letters* **2016**, *7*, 627–631.

(44) Mazziotti, D. A. Enhanced Constraints for Accurate Lower Bounds on Many-Electron Quantum Energies from Variational Two-Electron Reduced Density Matrix Theory. *Physical Review Letters* **2016**, *117*, 153001.

(45) Mazziotti, D. A. Structure of Fermionic Density Matrices: Complete N-Representability Conditions. *Physical Review Letters* **2012**, *108*, 263002.

(46) Coleman, A. J. Structure of Fermion Density Matrices. *Reviews of Modern Physics* **1963**, *35*, 668.

(47) Erdahl, R. M. Representability. *International Journal of Quantum Chemistry* **1978**, *13*, 697–718.

(48) Kummer, H $N$-Representability Problem for Reduced Density Matrices. *Journal of Mathematical Physics* **1967**, *8*, 2063.

(49) Vandenberghe, L; Boyd, S Semidefinite programming. *SIAM Reviews* **1996**, *38*, 49–95.

(50) Mazziotti, D. A. Realization of Quantum Chemistry Without Wave Functions through First-Order Semidefinite Programming. *Physical Review Letters* **2004**, *93*, 213001.

(51) Mazziotti, D. A. First-Order Semidefinite Programming for the Two-Electron Treatment of Many-Electron Atoms and Molecules. *ESAIM: Mathematical Modelling and Numerical Analysis* **2007**, *41*, 249–259.

(52) Mazziotti, D. A. Large-Scale Semidefinite Programming for Many-Electron Quantum Mechanics. *Physical Review Letters* **2011**, *106*, 083001.

(53) Poelmans, W.; Van Raemdonck, M.; Verstichel, B.; De Baerdemacker, S.; Torre, A.; Lain, L.; Massaccesi, G. E.; Alcoba, D. R.; Bultinck, P.; Van Neck, D. Variational Optimization of the Second-Order Density Matrix Corresponding to a Seniority-Zero Configuration Interaction Wave Function. *Journal of Chemical Theory and Computation* **2015**, *11*, 4064–4076.

(54) Naftchi-Ardebili, K.; Hau, N. W.; Mazziotti, D. A. Rank restriction for the variational calculation of two-electron reduced density matrices of many-electron atoms and molecules. *Physical Review A* **2011**, *84*, 052506.

(55) Lopez, X.; Ruiperez, F.; Piris, M.; Matxain, J. M.; Ugalde, J. M. Diradicals and Diradicaloids in Natural Orbital Functional Theory. *Journal of Chemical Physics* **2011**, *134*, 164102.

(56) Gebauer, G.; Cohen, M. H.; Car, R. A well-scaling natural orbital theory. *Procedings of the National Academy of Sciences of the United States of America* **2016**, *113 (46)*, 12913–12918.

(57) Lehtola, S.; Jónsson, H. Unitary Optimization of Localized Molecular Orbitals. *Journal of Chemical Theory and Computation* **2013**, *9*, 5365–5372.

(58) Foster, J. M.; Boys, S. F. Canonical Configuration Interaction Procedure. *Reviews of Modern Physics* **1960**, *32*, 300–302.

(59) Edmiston, C.; Ruedenberg, K. Localized Atomic and Molecular Orbitals. *Reviews of Modern Physics* **1963**, *35*, 457–464.

(60) Pipek, J.; Mezey, P. G. A Fast Intrinsic Localization Procedure Applicable for Abinitio and Semiempirical Linear Combination of Atomic Orbital Wave-Functions. *Journal of Chemical Physics* **1989**, *90*, 4916–4926.

(61) Nakata, M.; Yasuda, K. Size extensivity of the variational reduced-density-matrix method. *Physical Review A* **2009**, *80*, 042109.

(62) Piris, M. A natural orbital functional based on an explicit approach of the two-electron cumulant. *International Journal of Quantum Chemistry* **2013**, *113 (5)*, 620.

(63) Piris, M. Interacting pairs in natrual orbital functional theory. *Journal of Chemical Physics* **2014**, *141*, 044107.

(64) Mazziotti, D. A. Two-Electron Reduced Density Matrix as the Basic Variable in Many-Electron Quantum Chemistry and Physics. *Chemical Reviews* **2012**, *112*, 244–262.

(65) Davidson, E. R., *Reduced Density Matrices in Quantum Chemistry*; Academic: New York, 1976.

(66) Valdemoro, C Approximation the 2nd-Order Reduced Density-Matrix in Terms of the 1st-Order One. *Physical Review A* **1992**, *45*, 4462–4467.

(67) Nakatsuji, H; Yasuda, K Direct Determination of the Quantum-Mechanical Density Matrix Using the Density Equation. *Physical Review Letters* **1996**, *76*, 1039–1042.

(68) Mazziotti, D. A. Contracted Schrodinger equation: Determining quantum energies and two-particle density matrices without wave functions. *Physical Review A* **1998**, *57*, 4219–4234.

(69) Löwdin, P. O. Quantum Theory of Many-Particle Systems .1. Physical Interpretations by Means of Density Matrices, Natural Spin-Orbitals, and Convergence Problems in the Method of Configuration Interaction. *Physical Review* **1955**, *97*, 1474–1489.

(70) Mayer, J. E. Electron Correlation. *Physical Review* **1955**, *100*, 1579–1586.

(71) Slebodziski, W., *Exterior Forms and their Applications*; Polish Scientific Publishers: Warsaw, 1970.

(72) Garrod, C.; Percus, J. K. Reduction of the N-Particle Varational Problem. *Journal of Mathematical Physics* **1964**, *5*, 1756.

(73) Fukuda, M.; Braams, B. J.; Nakata, M.; Overton, M. L.; Percus, J. K.; Yamashita, M.; Zhao, Z. Large-scale semidefinite programs in electronic structure calculation. *Mathematical Programming* **2007**, *109*, 553–580.

(74) Mazziotti, D. A. Variational two-electron reduced density matrix theory for many-electron atoms and molecules: Implementation of the spin- and symmetry-adapted T-2 condition through first-order semidefinite programming. *Physical Review A* **2005**, *72*.

(75) Smith, D. W. N-Representability Problem for Fermion Density Matrices. II. The First-Order Density Matrix with N Even. *Physical Review* **1966**, *147*, 896–898.

(76) Høyvik, I.-M.; Jansik, B.; Jørgensen, P. Orbital localization using fourth central moment minimization. *Journal of Chemical Physics* **2012**, *137*, 224114.

(77) Lehtola, S.; Jónsson, H. Pipek-Mezey Orbital Localization Using Various Partial Charge Estimates. *Journal of Chemical Theory and Computation* **2014**, *10*, 642–649.

(78) Valiev, M.; Bylaska, E. J.; Govind, N.; Kowalski, K.; Straatsma, T. P.; Van Dam, H. J. J.; Wang, D.; Nieplocha, J.; Apra, E.; Windus, T. L.; de Jong, W. NWChem: A comprehensive and scalable open-source solution for large scale molecular simulations. *Computer Physics Communications* **2010**, *181*, 1477–1489.

(79) Schmidt, M. W.; Baldridge, K. K.; Boatz, J. A.; Elbert, S. T.; Gordon, M. S.; Jensen, J. H.; Koseki, S.; Matsunaga, N.; Nguyen, K. A.; Su, S. J; Windus, T. L.; Dupuis, M; Montgomery, J. A. General Atomic and Molecular Electronic-Structure System. *Journal of Computational Chemistry* **1993**, *14*, 1347–1363.

(80) Erdahl, R. M. In *Reduced-Density-Matrix Mechanics - with Applications to Many-Electron Atoms and Molecules*, Mazziotti, D. A., Ed.; Advances in Chemical Physics, Vol. 134; Wiley: New York, 2007, pp 61–91.

(81) Hehre, W. J.; Stewart, R. F.; Pople, J. A. Self-Consistent Molecular-Orbital Methods .I. Use of Gaussian Expansions of Slate-Type Atomic Orbitals. *Journal of Chemical Physics* **1969**, *51*, 2657.

(82) Dobbs, K. D.; Hehre, W. J. Molecular-Orbital Theory of the Properties of Inorganic and Organometallic Compounds .6. Extended Basis-Sets for 2nd-Row Transition-Metals. *Journal of Computational Chemistry* **1987**, *8*, 880–893.

(83) Dunning Jr., T. H. Gaussian-Basis Sets for Use in Correlated Molecular Calculations .1. The Atoms Boron through Neon and Hydrogen. *Journal of Chemical Physics* **1989**, *90*, 1007–1023.

(84) Hehre, W. J.; Ditchfield, R; Pople, J. A. Self-Consistent Molecular-Orbital Methods .12. Further Extensions of Gaussian-Type Basis Sets for Use in Molecular-Orbital Studies of Organic-Molecules. *Journal of Chemical Physics* **1972**, *56*, 2257.

(85) Jmol: an open-source Java viewer for chemical structures in 3D.

(86) Hepp, A; Heil, H; Weise, W; Ahles, M; Schmechel, R; von Seggern, H Light-emitting field-effect transistor based on a tetracene thin film. *Physical Review Letters* **2003**, *91*, 157406.

(87) Geerts, Y.; Klärner, G.; Müllen, K., *Electronic Materials: The Oligomer Approach*; Wiley: Weinhein, Germany, 1998.

(88) Dolzhnikov, D. S.; Zhang, H.; Jang, J.; Son, J. S.; Panthani, M. G.; Shibata, T.; Chattopadhyay, S.; Talapin, D. V. Composition-matched molecular "solders" for semiconductors. *Science* **2015**, *347*, 425–428.

(89) Neuscamman, E. Size Consistency Error in the Antisymmetric Geminal Power Wave Function can be Completely Removed. *Physical Review Letters* **2012**, *109*, 203001.

(90) Zhao, L.; Neuscamman, E. Amplitude Determinant Coupled Cluster with Pairwise Doubles. *Journal of Chemical Theory and Computation* **2016**, *12*, 5841–5850.

(91) Levy, M. Universal variational functionals of electron densities, first-order density matrices, and natural spin-orbitals and solution of the v-representability problem. *Proceedings of the National Academy of Sciences of the United States of America* **1979**, *76 (12)*, 6062–6065.

(92) Valone, S. M. Consequences of extending 1matrix energy functionals from purestate representable to all ensemble representable 1 matrices. *Journal of Chemical Physics* **1980**, *73*, 1344.

# CHAPTER 3

# ACTIVE SPACE PAIR 2-ELECTRON REDUCED DENSITY MATRIX THEORY FOR STRONG CORRELATION

This chapter is reprinted from a paper submitted for publication by K. Head-Marsden and D. A. Mazziotti (2019).

## 3.1 Introduction

Recent work uses active space selection in conjunction with the variational 2-RDM method to capture strong electron correlation in a variety of molecules of chemical interest[1–3]. An active space is a set of orbitals within the molecule that are correlated. Increasing the size of the active space alters the amount of electron correlation that can be captured with larger active spaces producing more accurate results. Because the variational 2-RDM method with the 2-positive $N$-representability conditions[1, 4–24] scales as $\mathcal{O}(r_a^6)$ where $r_a$ is the number of active orbitals, it can treat much larger active spaces than conventional configuration interaction, which scales exponentially with $r_a$. Here we combine the recently developed pair variational 2-RDM method[25–30] with active space methods, both complete active space configuration interaction (CASCI) and complete active space self consistent field (CASSCF), to generate an $O(r_a^3)$ method that can efficiently treat strong correlation in molecules with potentially very large active spaces.

The pair space restricts the wavefunction to include only doubly-occupied determinants; however, in traditional wavefunction methods this approximation alone still scales exponentially with system size[31, 32]. While the variational 2-RDM method reduces the computational scaling to polynomial, there are also several wavefunction approximations for decreasing the doubly occupied configuration interaction scaling to polynomial such as antisymmetric product of one-reference-orbital geminals (AP1roG) and pair coupled cluster

doubles (pCCD)[33–43]. Moreover, some work has examined active space calculations in spaces of different seniority for small molecules[44].

In this paper the variational 2-RDM theory with a complete active space self-consistent field (CASSCF) method is utilized where the active and inactive orbitals are iteratively rotated to decrease the energy. We benchmark this method using the dissociation of a nitrogen dimer and a p-benzyne diradical. We then apply it to two larger systems: a recently synthesized bis-cobalt complex and a recently studied iron complex, FeMoco[2].

## 3.2 Variational Pair 2-RDM Theory

The energy of an $N$-electron system can be expressed as[4, 45–52],

$$E = \sum_{ijkl} {}^2K_{kl}^{ij} {}^2D_{kl}^{ij}, \tag{3.1}$$

where ${}^2K_{kl}^{ij}$ is the two-electron Hamiltonian given by,

$${}^2K_{kl}^{ij} = \frac{4}{N-1} {}^1K_k^i \wedge \delta_l^j + {}^2V_{kl}^{ij}, \tag{3.2}$$

in which, ${}^1K_k^i$ and ${}^2V_{kl}^{ij}$ are one- and two-electron matrices containing the one- and two-electron integrals and $\wedge$ is the Grassmann wedge product[50, 53]. The 2-RDM can be expressed as[4, 45–50],

$${}^2D_{kl}^{ij} = \langle \Psi | \hat{a}_i^\dagger \hat{a}_j^\dagger \hat{a}_l \hat{a}_k | \Psi \rangle, \tag{3.3}$$

where $\hat{a}^\dagger$ and $\hat{a}$ are the creation and annihilation operators respectively and the indices $i$, $j$, $k$, and $l$ denote the spin orbitals.

Variational calculation of the 2-RDM in the pair space requires approximate $N$-representability

constraints on the 2-RDM[4, 7, 17–19, 45–52, 54–56]:

$$^2D \succeq 0 \tag{3.4}$$

$$^2Q \succeq 0 \tag{3.5}$$

$$^2G \succeq 0, \tag{3.6}$$

where $^2D$, $^2Q$, and $^2G$ are the two-particle, two-hole, and particle-hole density matrices respectively whose matrix elements are defined by Eq. (3.3) and

$$^2Q^{ij}_{kl} = \langle\Psi|\hat{a}_i\hat{a}_j\hat{a}^\dagger_l\hat{a}^\dagger_k|\Psi\rangle \tag{3.7}$$

$$^2G^{ij}_{kl} = \langle\Psi|\hat{a}^\dagger_i\hat{a}_j\hat{a}^\dagger_l\hat{a}_k|\Psi\rangle. \tag{3.8}$$

In the pair approximation, these matrices factorize into a series of smaller blocks. For the 2-particle and 2-hole RDMs, these blocks consist of one $r \times r$ block and $r$-choose-two $1\times1$ blocks; for example, for $^2D$ they are given by [27, 46]:

$$\begin{pmatrix} \langle\hat{a}^\dagger_{i\alpha}\hat{a}^\dagger_{i\beta}\hat{a}_{i\beta}\hat{a}_{i\alpha}\rangle & \dots & \langle\hat{a}^\dagger_{i\alpha}\hat{a}^\dagger_{i\beta}\hat{a}_{k\beta}\hat{a}_{k\alpha}\rangle \\ \vdots & \ddots & \vdots \\ \langle\hat{a}^\dagger_{k\alpha}\hat{a}^\dagger_{k\beta}\hat{a}_{i\beta}\hat{a}_{i\alpha}\rangle & \dots & \langle\hat{a}^\dagger_{k\alpha}\hat{a}^\dagger_{k\beta}\hat{a}_{k\beta}\hat{a}_{k\alpha}\rangle \end{pmatrix}, \tag{3.9}$$

and

$$\left(\langle\hat{a}^\dagger_{i\alpha}\hat{a}^\dagger_{j\beta}\hat{a}_{j\beta}\hat{a}_{i\alpha}\rangle\right). \tag{3.10}$$

The blocked structure of the particle-hole RDM is similar but slightly more complex in

structure with one $r \times r$ block and $r$-choose-two 2×2 blocks given by[27]

$$\begin{pmatrix} \langle \hat{a}^\dagger_{i\alpha} \hat{a}_{i\alpha} \hat{a}^\dagger_{i\alpha} \hat{a}_{i\alpha} \rangle & \dots & \langle \hat{a}^\dagger_{i\alpha} \hat{a}_{i\alpha} \hat{a}^\dagger_{k\alpha} \hat{a}_{k\alpha} \rangle \\ \vdots & \ddots & \vdots \\ \langle \hat{a}^\dagger_{k\alpha} \hat{a}_{k\alpha} \hat{a}^\dagger_{i\alpha} \hat{a}_{i\alpha} \rangle & \dots & \langle \hat{a}^\dagger_{k\alpha} \hat{a}_{k\alpha} \hat{a}^\dagger_{k\alpha} \hat{a}_{k\alpha} \rangle \end{pmatrix}, \tag{3.11}$$

and

$$\begin{pmatrix} \langle \hat{a}^\dagger_{i\alpha} \hat{a}_{j\beta} \hat{a}^\dagger_{j\beta} \hat{a}_{i\alpha} \rangle & \langle \hat{a}^\dagger_{i\alpha} \hat{a}_{j\beta} \hat{a}^\dagger_{i\beta} \hat{a}_{j\alpha} \rangle \\ \langle \hat{a}^\dagger_{j\alpha} \hat{a}_{i\beta} \hat{a}^\dagger_{j\beta} \hat{a}_{i\alpha} \rangle & \langle \hat{a}^\dagger_{j\alpha} \hat{a}_{i\beta} \hat{a}^\dagger_{i\beta} \hat{a}_{j\alpha} \rangle \end{pmatrix}. \tag{3.12}$$

The ground-state energy can be minimized with respect to the 2-RDM subject to these $N$-representability constraints by semidefinite programming[1, 4, 16, 20–23]. With the block diagonal forms of ${}^2D$, ${}^2Q$, and ${}^2G$, the scaling of the variational pair 2-RDM method is $\mathcal{O}(r^3)$.

Here, we use the pair theory within the context of an active space calculation. Performing a calculation in an active space consists of choosing $N$ electrons in $r$ orbitals to correlate while treating the remainder of the electrons and orbitals at a mean-field level of theory[57]. We consider two primary active space methods within the variational pair 2-RDM framework. First, we consider a method equivalent to both complete active space configuration interaction (CASCI), where the active space is computed with respect to the Hartree-Fock canonical molecular orbitals. Second, we explore a method equivalent to the complete active space self consistent field (CASSCF) method[58], where active and inactive orbitals are iteratively rotated through a self-consistent field method. We use the second-order orbital optimization method described in Ref. [59].

## 3.3 Applications

In this section we will discuss our computational methodology followed by applications to the dissociation of a nitrogen dimer, a p-benzyne diradical, a newly synthesized Bis-Cobalt

complex and FeMoco in Secs. 3.3.1,3.3.2, 3.3.3, 3.3.4, and 3.3.5 respectively.

### *3.3.1 Computational Methodology*

We have implemented the active-space pair variational 2-RDM method in the Maple Quantum Chemistry Toolbox, an add-on package for electronic structure in the computer algebra system Maple[60, 61]. A cc-pvdz basis set is used for nitrogen and the p-benzyne diradical calculations with [10,8] and [6,6] active spaces respectively[62]. A 6-31g basis set is used for the Bis-Cobalt complex calculations in a [12,10] active space[63]. Finally, a sto-3g basis set is employed for the FeMoco calculations in both [30,30] and [80,80] active spaces[64–66].

### *3.3.2 Nitrogen Dissociation*

The nitrogen dimer is a known example of fractional occupations as it dissociates. In Fig. 3.1 we compare the Hartree-Fock method, the variational 2-RDM CASCI and CASSCF methods, the CASCI and CASSCF methods, and the pair 2-RDM CASCI and CASSCF methods. For the same methods, the occupation numbers of the $N_2$ dimer at 1.2 Å and 2.0 Å are shown in Table 3.1.

Figure 3.1 shows that the energy recovered by the pair methods is less than that recovered by the variational method, but that the trends are similar. Orbital rotations in the pair CASSCF slightly decrease the energy as compared to the pair CASCI. As the two nitrogen atoms are separated, Table 3.1 shows an increase in partial occupations for all methods.

### *3.3.3 p-Benzyne Diradical*

The variational 2-RDM CASCI and CASSCF methods and the pair variational 2-RDM CASCI and CASSCF methods are used to calculate the energies for the p-benzyne diradical as shown in Table 3.2. The occupation numbers using the same four methods are also presented in Table 3.3 and in the plots of Fig. 3.2.

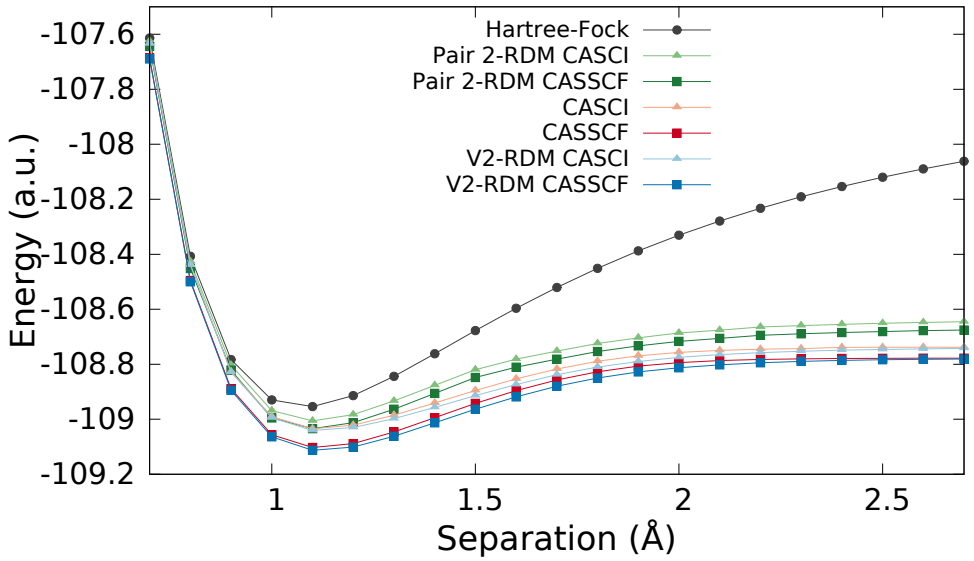


Figure 3.1: The dissociation of $N_2$ using Hartee-Fock (grey circles), pair 2-RDM CASCI (light green triangles), pair 2-RDM CASSCF (green squares), CASCI (orange triangles), CASSCF (red squares), variational 2-RDM CASCI (light blue triangles), and variational 2-RDM CASSCF (blue squares).

Table 3.1: The occupation numbers of $N_2$ at 1.2 Å and 2.0 Å separation using variational 2-RDM CASCI and CASSCF, CASCI and CASSCF, and pair 2-RDM CASCI and CASSCF.

| Sep. | Variational 2-RDM | | Active Space | | Pair 2-RDM | |
|---|---|---|---|---|---|---|
| (Å ) | CASCI | CASSCF | CASCI | CASSCF | CASCI | CASSCF |
| 1.2 | 1.9937 | 1.9852 | 1.9952 | 1.9953 | 1.9997 | 1.9975 |
| | 1.9828 | 1.9835 | 1.9927 | 1.9886 | 1.9894 | 1.9890 |
| | 1.9876 | 1.9760 | 1.9882 | 1.9743 | 1.9970 | 1.9928 |
| | 1.9183 | 1.9104 | 1.9269 | 1.9215 | 1.9361 | 1.9195 |
| | 1.9183 | 1.9104 | 1.9269 | 1.9215 | 1.9361 | 1.9195 |
| | 0.0942 | 0.1015 | 0.0810 | 0.0855 | 0.0700 | 0.0867 |
| | 0.0942 | 0.1015 | 0.0810 | 0.0855 | 0.0700 | 0.0867 |
| | 0.0111 | 0.0315 | 0.0080 | 0.0278 | 0.0017 | 0.0082 |
| 2.0 | 1.9887 | 1.9875 | 1.9982 | 1.9985 | 1.9989 | 1.9988 |
| | 1.9850 | 1.9860 | 1.9953 | 1.9953 | 1.9970 | 1.9966 |
| | 1.7140 | 1.7042 | 1.6740 | 1.6585 | 1.7796 | 1.7834 |
| | 1.3573 | 1.3480 | 1.3303 | 1.3158 | 1.3466 | 1.3343 |
| | 1.3573 | 1.3480 | 1.3303 | 1.3158 | 1.3466 | 1.3343 |
| | 0.6513 | 0.6605 | 0.6713 | 0.6857 | 0.6546 | 0.6672 |
| | 0.6513 | 0.6605 | 0.6713 | 0.6857 | 0.6546 | 0.6672 |
| | 0.2951 | 0.3055 | 0.3293 | 0.3448 | 0.2221 | 0.2182 |

Table 3.2: The energies of p-benzyne using the variational 2-RDM method and the pair 2-RDM method both with CASCI and CASSCF.

| | Variational 2-RDM | | Pair 2-RDM | |
|---|---|---|---|---|
| | CASCI | CASSCF | CASCI | CASSCF |
| Total Energy | -229.3952 | -229.4357 | -229.3737 | -229.4116 |
| Correlation Energy | -0.1242 | -0.1647 | -0.1027 | -0.1406 |

Table 3.3: The occupation numbers of p-benzyne using the variational 2-RDM method and the pair 2-RDM method both with CASCI and CASSCF.

| Variational 2-RDM | | Pair 2-RDM | |
|---|---|---|---|
| CASCI | CASSCF | CASCI | CASSCF |
| 1.9380 | 1.9287 | 1.9652 | 1.9602 |
| 1.9264 | 1.9172 | 1.9439 | 1.9418 |
| 1.5641 | 1.4179 | 1.4258 | 1.2553 |
| 0.4365 | 0.5827 | 0.5745 | 0.7452 |
| 0.0747 | 0.0841 | 0.0633 | 0.0680 |
| 0.0603 | 0.0693 | 0.0273 | 0.0295 |

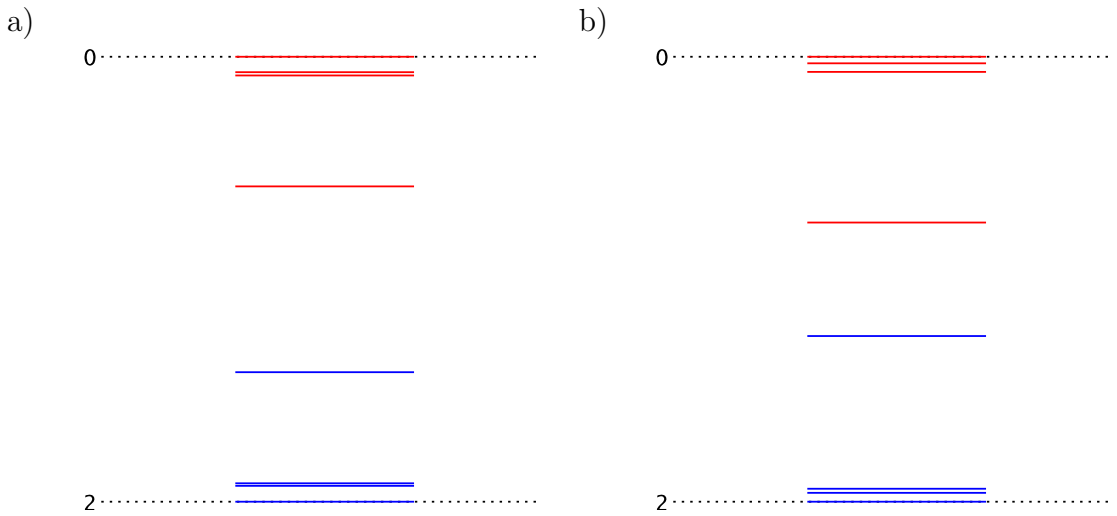


Figure 3.2: Molecular orbital occupations line plot for the p-benzyne diradical using a) the variational 2-RDM CASSCF method and b) the pair 2-RDM CASSCF method.

Table 3.2 shows that while more energy is recovered using the full variational method, a significant portion is recovered by the pair approximation with CASCI and CASSCF. Both Table 3.3 and Fig. 3.2 show fractional occupations, and therefore strong electron correlation, of the molecular orbitals of the p-benzyne diradical both in the full and pair spaces.

### *3.3.4 Cobalt Complex*

Next, we consider a Bis-Cobalt complex, shown in Fig. 3.3, that has recently been synthesized and studied[67]. Recent work has considered the effects of different linker molecules between the Cobalt centers for tuning the amount of electron correlation for a variety of potential applications[67].

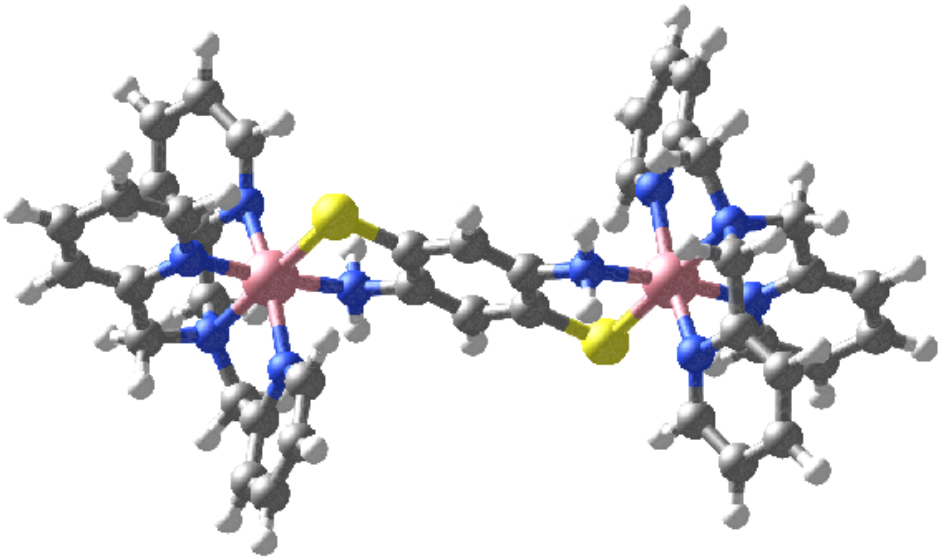

Figure 3.3: Bis-Cobalt complex where Carbon atoms are shown in grey, Hydrogen in white, Cobalt in pink, Sulfur in yellow, and Nitrogren in blue[60].

The occupation numbers using pair 2-RDM CASCI and pair 2-RDM CASSCF are shown in Table 3.4 The two half-occupied molecular orbitals, which as the highest occupied natural orbital (HONO) and lowest unoccupied natural orbital (LUNO) in the closed-shell description of the ground state, are shown using pair 2-RDM CASCI and pair 2-RDM CASSCF in Fig. 3.4. The correlation energy recovered is -0.2081 a.u. and -0.3839 a.u. for the pair 2-RDM CASCI and CASSCF calculations respectively. The energy recovered by the pair theory with SCF rotations is 6 mHartrees less than that recovered by the full variational method with similar rotations.

Table 3.4: The occupation numbers of Bis-Cobalt complex using pair 2-RDM CASCI and CASSCF.

| | Pair 2-RDM | |
|---|---|---|
| Molecular Orbital | CASCI | CASSCF |
| 219 | 2.0000 | 2.0000 |
| 220 | 2.0000 | 2.0000 |
| 221 | 2.0000 | 1.9991 |
| 222 | 2.0000 | 1.9543 |
| 223 | 1.9999 | 1.9534 |
| 224 | 1.0634 | 1.0000 |
| 225 | 0.9366 | 0.9999 |
| 226 | 0.0000 | 0.0457 |
| 227 | 0.0000 | 0.0369 |
| 228 | 0.0000 | 0.0108 |

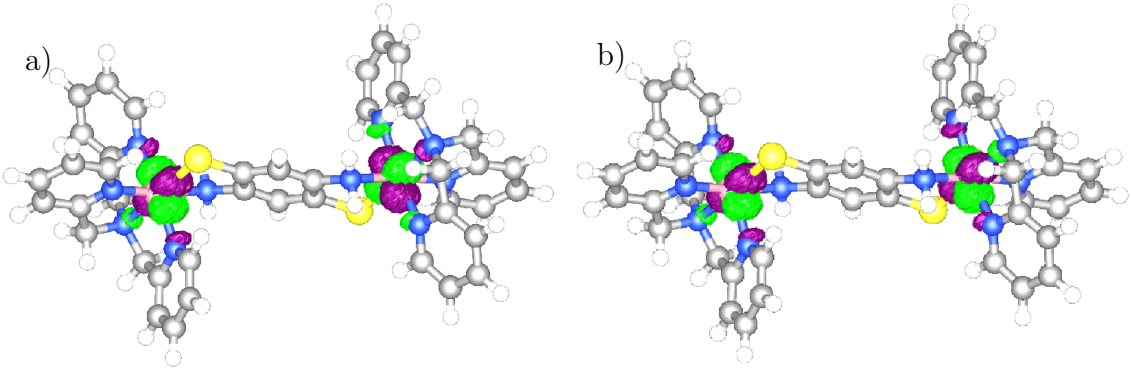


Figure 3.4: Bis-cobalt complex molecular orbital densities using pair 2-RDM CASSCF for molecular orbital a) HONO and b) LUNO.

### *3.3.5 FeMoco*

Finally, we consider the modified FeMoco molecule, where the base chemical formula is $MoFe_7S_9C$, as shown in Fig. 3.5[2]. FeMoco is the active catalytic site in the reduction of nitrogen gas to ammonia during the process of nitrogen fixation[2].

The occupation numbers using the pair 2-RDM CASCI and CASSCF methods in both [30,30] and [80,80] active spaces are shown in Table 3.5; for the pair 2-RDM CASSCF calculations we also show the occupations in the plots in Fig. 3.6. While the [30,30] calculations capture fractional occupation, they predict numerous half-filled orbitals. When the active

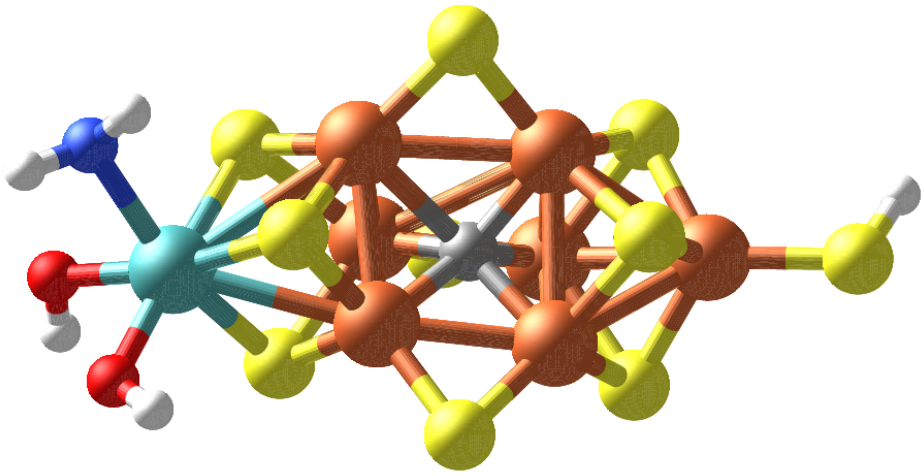

Figure 3.5: Modified FeMoco molecule where Molybdenum is shown in cyan, Sulfur in yellow, Iron in brown, Oxygen in red, Nitrogen in blue, Carbon in grey, and Hydrogen in white[60].

space is increased to [80,80], there is a much greater spread of fractional occupations. It should be noted that the [80,80] calculation is using approximately $10^7$ variables, while a traditional wavefunction calculation in the same space would take $10^{44}$ variables.

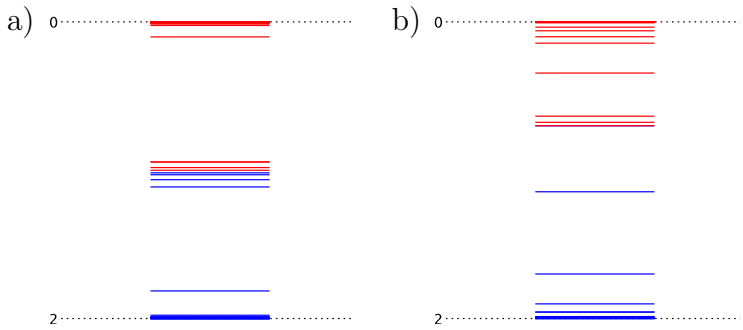


Figure 3.6: Molecular orbital occupations line plot for FeMoco using the pair 2-RDM method with CASSCF in a a) [30,30] active space and b) [80,80] active space.

Table 3.5: The occupation numbers of FeMOCO using pair 2-RDM CASCI and CASSCF in [30,30] and [80,80] active spaces.

| | Variational 2-RDM [30,30] | | Pair 2-RDM [80,80] | |
|---|---|---|---|---|
| Molecular Orbital | CASCI | CASSCF | CASCI | CASSCF |
| 203 | 1.9992 | 1.9811 | 1.9892 | 1.9813 |
| 204 | 1.9939 | 1.7353 | 1.9778 | 1.9592 |
| 205 | 1.9837 | 1.0650 | 1.8134 | 1.9450 |
| 206 | 1.9727 | 1.0120 | 1.1128 | 1.9097 |
| 207 | 1.9675 | 1.0120 | 1.0657 | 1.7841 |
| 208 | 1.8081 | 1.0109 | 1.0306 | 1.1594 |
| 209 | 1.0225 | 0.9880 | 1.0176 | 0.8104 |
| 210 | 0.9708 | 0.9880 | 0.9999 | 0.7698 |
| 211 | 0.1561 | 0.9756 | 0.9824 | 0.5806 |
| 212 | 0.0608 | 0.9056 | 0.9452 | 0.4562 |
| 213 | 0.0308 | 0.7526 | 0.9441 | 0.2597 |
| 214 | 0.0256 | 0.7468 | 0.1014 | 0.1895 |
| 215 | 0.0048 | 0.4162 | 0.0244 | 0.1289 |
| 216 | 0.0041 | 0.2356 | 0.0123 | 0.0720 |
| 217 | 0.0004 | 0.1613 | 0.0123 | 0.0402 |
| 218 | 0.0001 | 0.0316 | 0.0116 | 0.0068 |

## 3.4 Discussion and Conclusions

Active space variational calculations of the 2-RDM are performed where the active orbitals are correlated within the pair approximation. The pair approximation, which consists of only considering $r/2$ pairs of orbitals in the wavefunction, greatly simplifies the structure of the 2-RDM. By invoking this approximation, the computational cost of the variational calculation of the 2-RDM constrained to the 2-positive (DQG) approximate $N$-representability conditions is reduced to $\mathcal{O}(r^3)$. Both CASCI and CASSCF calculations are considered in the treatment of $N_2$, a p-benzyne diradical, a Bis-Cobalt complex, and the nitrogenase cofactor, FeMoco. In each of these four systems, fractional occupation is observered, indicating the detection of strong electronic correlation. Due to the reduced computational cost and ability to capture strong correlation, the active-space pair 2-RDM methods show promise for studying a wide variety of large molecular systems of chemical and biological interest.

(1) Schlimgen, A. W.; Heaps, C. W.; Mazziotti, D. A. Entangled Electrons Foil Synthesis of Elusive Low-Valent Vanadium Oxo Complex. *Journal of Physical Chemistry Letters* **2016**, *7*, 627–631.

(2) Montgomery, J. M.; Mazziotti, D. A. Strong Electron Correlation in Nitrogenase Cofactor, FeMoco. *Journal of Physical Chemistry A* **2018**, *122 (22)*, 4988–4996.

(3) McIsaac, A. R.; Mazziotti, D. A. Ligand Non-innocence and Strong Correlation in Manganese Superoxide Dismutase Mimics. *Physical Chemistry Chemical Physics* **2017**, *19*, 4656–4660.

(4) *Reduced-Density-Matrix Mechanics: With Application to Many-Electron Atoms and Molecules*; Mazziotti, D. A., Ed.; Advances in Chemical Physics 134; Wiley: New York, 2007.

(5) Garrod, C.; Mihailovic, M. V.; Rosina, M. Variational Approach to 2-Body Density Matrix. *Journal of Mathematical Physics* **1975**, *16*, 868–874.

(6) Erdahl, R. M. Two algorithms for the lower bound method of reduced density matrix theory. *Reports on Mathematical Physics* **1979**, *15*, 147–162.

(7) Mazziotti, D. A.; Erdahl, R. M. Uncertainty Relations and Reduced Density Matrices: Mapping Many-Body Quantum Mechanics onto Four Particles. *Physical Review A* **2001**, *63*, 042113.

(8) Nakata, M; Nakatsuji, H; Ehara, M; Fukuda, M; Nakata, K; Fujisawa, K Variational Calculations of Fermion Second-Order Reduced Density Matrices by Semidefinite Programming Algorithm. *Journal of Chemical Physics* **2001**, *114*, 8282–8292.

(9) Zhao, Z.; Braams, B.; Fukuda, M; Overton, M.; Percus, J. The reduced density matrix method for electronic structure calculations and the role of three-index representability conditions. *Journal of Chemical Physics* **2004**, *120*, 2095–2104.

(10) Mazziotti, D. A. Variational Minimization of Atomic and Molecular Ground-State Energies via the Two-Particle Reduced Density Matrix. *Physical Review A* **2002**, *65*, 062511.

(11) Mazziotti, D. A. Variational reduced-density-matrix method using three-particle N-representability conditions with application to many-electron molecules. *Physical Review A* **2006**, *74*, 032501.

(12) Gidofalvi, G.; Mazziotti, D. A. Active-Space Two-Electron Reduced-Density-Matrix Method: Complete Active-Space Calculations Without Diagonalization of the N-electron Hamiltonian. *Journal of Chemical Physics* **2008**, *129*, 134108.

(13) Pelzer, K.; Greenman, L.; Gidofalvi, G.; Mazziotti, D. A. Strong Correlation in Acene Sheets from the Active-Space Variational Two-Electron Reduced Density Matrix Method Effects of Symmetry and Size. *Journal of Physical Chemistry A* **2011**, *114*, 583–588.

(14) Verstichel, B.; van Aggelen, H.; Poelmans, W.; Van Neck, D. Variational Two-Particle Density Matrix Calculation for the Hubbard Model Below Half Filling Using Spin-Adapted Lifting Conditions. *Physical Review Letters* **2012**, *108*, 213001.

(15) Fosso-Tande, J.; Nguyen, T. S.; Gidofalvi, G.; DePrince III, A. E. Large-Scale Variational Two-Electron Reduced-Density-Matrix-Driven Complete Active Space Self-Consistent Field Methods. *Journal of Chemical Theory and Computation* **2016**, *12*, 2260–2271.

(16) Mazziotti, D. A. Enhanced Constraints for Accurate Lower Bounds on Many-Electron Quantum Energies from Variational Two-Electron Reduced Density Matrix Theory. *Physical Review Letters* **2016**, *117*, 153001.

(17) Coleman, A. J. Structure of Fermion Density Matrices. *Reviews of Modern Physics* **1963**, *35*, 668.

(18) Erdahl, R. M. Representability. *International Journal of Quantum Chemistry* **1978**, *13*, 697–718.

(19) Kummer, H $N$-Representability Problem for Reduced Density Matrices. *Journal of Mathematical Physics* **1967**, *8*, 2063.

(20) Vandenberghe, L.; Boyd, S. Semidefinite programming. *SIAM Reviews* **1996**, *38*, 49–95.

(21) Mazziotti, D. A. Realization of Quantum Chemistry Without Wave Functions through First-Order Semidefinite Programming. *Physical Review Letters* **2004**, *93*, 213001.

(22) Mazziotti, D. A. First-Order Semidefinite Programming for the Two-Electron Treatment of Many-Electron Atoms and Molecules. *ESAIM: Mathematical Modelling and Numerical Analysis* **2007**, *41*, 249–259.

(23) Mazziotti, D. A. Large-Scale Semidefinite Programming for Many-Electron Quantum Mechanics. *Physical Review Letters* **2011**, *106*, 083001.

(24) Piris, M. Bounds on the PNOF5 natural geminal occupation numbers. *Compututational and Theoretical Chemistry* **2013**, *1003*, 123–126.

(25) Poelmans, W.; Van Raemdonck, M.; Verstichel, B.; De Baerdemacker, S.; Torre, A.; Lain, L.; Massaccesi, G. E.; Alcoba, D. R.; Bultinck, P.; Van Neck, D. Variational Optimization of the Second-Order Density Matrix Corresponding to a Seniority-Zero Configuration Interaction Wave Function. *Journal of Chemical Theory and Computation* **2015**, *11*, 4064–4076.

(26) Naftchi-Ardebili, K.; Hau, N. W.; Mazziotti, D. A. Rank restriction for the variational calculation of two-electron reduced density matrices of many-electron atoms and molecules. *Physical Review A* **2011**, *84*, 052506.

(27) Head-Marsden, K.; Mazziotti, D. A. Pair 2-electron Reduced Density Matrix Theory Using Localized Orbitals. *Journal of Chemical Physics* **2017**, *147*, 084101.

(28) Alcoba, D. R.; Torre, A.; Lain, L.; Massaccesi, G. E.; Ona, O. B.; Honoré, E. M.; Poelmans, W.; Van Neck, D.; Bultinck, P.; De Baerdemacher, S. Direct variational determination of the two-electron reduced density matrix for doubly occupied-configuration interaction wave functions: The influence of three-index $N$-representability conditions. *Journal of Chemical Physics* **2018**, *148*, 024105.

(29) Alcoba, D. R.; Capuzzi, P.; Rubio-Garcia, A.; Dukelsky, J.; Massaccesi, G. E.; Ona; Torre, A.; Lain, L. Variational reduced density matrix method in the doubly occupied configuration interaction space using three-particle $N$-representability conditions. *Journal of Chemical Physics* **2018**, *149*, 194105.

(30) Alcoba, D. R.; Torre, A.; Lain, L.; Massaccesi, G. E.; Ona; Rìos, E. Unrestricted treatment for the direct variational determination of the two-electron reduced density matrix for doubly occupied-configuration-interaction wave functions. *Journal of Chemical Physics* **2019**, *150*, 164106.

(31) Weinhold, F.; Wilson Jr., E. B. Reduced Density Matrics of Atoms and Molecules. I. The 2 Matrix of Double-Occupancy, Configuration-Interaction Wavefunctions for Singlet States. *Journal of Chemical Physics* **1967**, *46*, 2752.

(32) Szabo, A.; Ostlund, N. S., *Modern Quantum Chemistry: Introduction to Advanced Electronic Structure Theory*; Dover: New York, 1996.

(33) Limacher, P. A.; Ayers, P. W.; Johnson, P. A.; De Baerdemacker, S.; Van Neck, D.; Bultinck, P. A New Mean-Field Method Suitable for Strongly Correlated Electrons: Computationally Facile Antisymmetric Products of Nonorthogonal Geminals. *Journal of Chemical Theory and Computation* **2013**, *9*, 1394–1401.

(34) Boguslawski, K.; Tecmer, P.; Limacher, P. A.; Johnson, P. A.; Ayers, P. W.; Bultinck, P.; Baerdemacker, S. D.; Van Neck, D. Projected seniority-two orbital optimization

of the antisymmetric product of one-reference orbital geminal. *Journal of Chemical Physics* **2014**, *140*, 214114.

(35) Boguslawski, K.; Tecmer, P.; Ayers, P. W.; Bultinck, P.; De Baerdemacker, S.; Van Neck, D. Efficient description of strongly correlated electrons with mean-field cost. *Physical Review B* **2014**, *89*, 201106.

(36) Tecmer, P.; Boguslawski, K.; Johnson, P. A.; Limacher, P. A.; Chan, M.; Verstraelen, T.; Ayers, P. W. Assessing the Accuracy of New Geminal-Based Approaches. *Journal of Physical Chemistry A* **2014**, *118*, 9058–9068.

(37) Boguslawski, K.; Ayers, P. W. Linearized Coupled Cluster Correction on the Antisymmetric Product of 1-Reference Orbital Geminals. *Journal of Chemical Theory and Computation* **2015**, *11*, 5252–5261.

(38) Bytautas, L.; Henderson, T. M.; Jimnez-Hoyos, C. A.; Ellis, J. K.; Scuseria, G. E. Seniority and orbital symmetry as tools for establishing a full configuration interaction hierarchy. *Journal of Chemical Physics* **2011**, *135*, 044119.

(39) Stein, T.; Henderson, T. M.; Scuseria, G. E. Seniority zero pair coupled cluster doubles theory. *Journal of Chemical Physics* **2014**, *140*, 214113.

(40) Henderson, T. M.; Bulik, I. W.; Stein, T.; Scuseria, G. E. Seniority-based coupled cluster theory. *Journal of Chemical Physics* **2014**, *141*, 244104.

(41) Henderson, T. M.; Bulik, I. W.; Scuseria, G. E. Pair extended coupled cluster doubles. *Journal of Chemical Physics* **2015**, *142*, 214116.

(42) Bulik, I. W.; Henderson, T. M.; Scuseria, G. E. Can Single-Reference Coupled Cluster Theory Describe Static Correlation? *Journal of Chemical Theory and Computation* **2015**, *11*, 7, 3171–3179.

(43) Shepherd, J. J.; Henderson, T. M.; Scuseria, G. E. Using full configuration interaction quantum Monte Carlo in a seniority zero space to investigate the correlation energy equivalence of pair coupled cluster doubles and doubly occupied configuration interaction. *Journal of Chemical Physics* **2016**, *144*, 094112.

(44) Bytautas, L.; Henderson, T. M.; Jiménez-Hoyos, C. A.; Ellis, J. K.; Scuseria, G. E. Seniority and orbital symmetry as tools for establishing a full configuration interaction hierarchy. *Journal of Chemical Physics* **2011**, *135*, 044119.

(45) Mazziotti, D. A. Two-Electron Reduced Density Matrix as the Basic Variable in Many-Electron Quantum Chemistry and Physics. *Chemical Reviews* **2012**, *112*, 244–262.

(46) Coleman, A. J.; Yukalov, V. I., *Reduced Density Matrices: Coulson's Challenge, Chapter 4*; Springer: 2000.

(47) Davidson, E. R., *Reduced Density Matrices in Quantum Chemistry*; Academic: New York, 1976.

(48) Valdemoro, C Approximation the 2nd-Order Reduced Density-Matrix in Terms of the 1st-Order One. *Physical Review A* **1992**, *45*, 4462–4467.

(49) Nakatsuji, H; Yasuda, K Direct Determination of the Quantum-Mechanical Density Matrix Using the Density Equation. *Physical Review Letters* **1996**, *76*, 1039–1042.

(50) Mazziotti, D. A. Contracted Schrodinger equation: Determining quantum energies and two-particle density matrices without wave functions. *Physical Review A* **1998**, *57*, 4219–4234.

(51) Löwdin, P. O. Quantum Theory of Many-Particle Systems .1. Physical Interpretations by Means of Density Matrices, Natural Spin-Orbitals, and Convergence Problems in the Method of Configuration Interaction. *Physical Review* **1955**, *97*, 1474–1489.

(52) Mayer, J. E. Electron Correlation. *Physical Review* **1955**, *100*, 1579–1586.

(53) Slebodziski, W., *Exterior Forms and their Applications*; Polish Scientific Publishers: Warsaw, 1970.

(54) Mazziotti, D. A. Structure of Fermionic Density Matrices: Complete N-Representability Conditions. *Physical Review Letters* **2012**, *108*, 263002.

(55) Garrod, C.; Percus, J. K. Reduction of the N-Particle Varational Problem. *Journal of Mathematical Physics* **1964**, *5*, 1756.

(56) Fukuda, M.; Braams, B. J.; Nakata, M.; Overton, M. L.; Percus, J. K.; Yamashita, M.; Zhao, Z. Large-scale semidefinite programs in electronic structure calculation. *Mathematical Programming* **2007**, *109*, 553–580.

(57) Roos, B. O. In *Ab Initio Methods in Quantum Chemistry II*, Lawly, K. P., Ed.; Wiley: New York, 1987, pp 399–446.

(58) Werner, H.-J.; Knowles, P. J. A second order multiconfiguration self-consistent-field procedure with optimum convergence. *Journal of Chemical Physics* **1985**, *82 (11)*, 5053–5063.

(59) Sun, Q.; Yang, J.; Chan, G. K. A general second order complete active space self-consistent-field solver for large-scale systems. *Chemical Physics Letters* **2017**, *683*, 291–299.

(60) *Maple Quantum Chemistry Toolbox*; RDMChem, Chicago: 2019.

(61) *Maple 2019*; Maplesoft, Waterloo: 2019.

(62) Dunning Jr., T. H. Gaussian-Basis Sets for Use in Correlated Molecular Calculations .1. The Atoms Boron through Neon and Hydrogen. *Journal of Chemical Physics* **1989**, *90*, 1007–1023.

(63) Hehre, W. J.; Ditchfield, R; Pople, J. A. Self-Consistent Molecular-Orbital Methods .12. Further Extensions of Gaussian-Type Basis Sets for Use in Molecular-Orbital Studies of Organic-Molecules. *Journal of Chemical Physics* **1972**, *56*, 2257.

(64) Hehre, W. J.; Stewart, R. F.; Pople, J. A. Self-Consistent Molecular-Orbital Methods .I. Use of Gaussian Expansions of Slate-Type Atomic Orbitals. *Journal of Chemical Physics* **1969**, *51*, 2657.

(65) Pietro, W. J.; Hehre, W. J. Molecular orbital theory of the properties of inorganic and organometallic compounds. 3. STO-3G basis sets for first- and second-row transition metals. *Journal of Computational Chemistry* **1983**.

(66) Dobbs, K. D.; Hehre, W. J. Molecular-Orbital Theory of the Properties of Inorganic and Organometallic Compounds .6. Extended Basis-Sets for 2nd-Row Transition-Metals. *Journal of Computational Chemistry* **1987**, *8*, 880–893.

(67) Xie, J.; Boyn, N.-J.; Mazziotti, D. A.; Anderson, J. S. **(In Prep. 2019)**.

# CHAPTER 4

# OPEN QUANTUM SYSTEMS

## 4.1 1-RDM Methods

There are many physical and chemical systems whose behaviour is dominated by the influence of the environment. While the 2-RDM can still be of use, electron-electron interactions are generally less important in these situations and the 1-electron reduced density matrix becomes a powerful tool,

$$^1D_n = \int \Psi_n(1,..,N)\Psi_n^*(1,..,N)d2..dN. \tag{4.1}$$

The 1-RDM represents the probability distribution of 1-electron in the field of $N$-1 electrons. The $N$-representability conditions are implied from the 2-positivity conditions discussed in Chapter 1[1–3]. They are Hermiticity, normalization to $N$ particles, and the two matrix inequalities:

$$^1D_k^i \succeq 0 \tag{4.2}$$

$$^1Q_k^i \succeq 0. \tag{4.3}$$

For systems of fermions, the above two inequalities also imply that the sum of the one-particle and one-hole RDMs must always satisfy,

$$\mathbf{1} = {}^1D + {}^1Q, \tag{4.4}$$

where $\mathbf{1}$ is the identity matrix. This is equivalent to the Pauli exclusion principle which means that for systems of fermions, fermionic statistics are implied by the $N$-representability conditions.

The 1-RDM will be the primary object used in future chapters for studying the dynamics of open quantum systems, where the environment has a greater influence over the electronic behaviour than the electron-electron interactions.

## 4.2 Open Quantum Systems

Treating molecules as isolated is a common assumption when calculating electronic behaviour; however, in reality most systems do not exist in a vacuum but in some sort of environment. Systems which are interacting with their surroundings are referred to as open quantum systems, as shown in Fig. 4.1 where energy, heat, or information can be exchanged between the system and the bath. Mathematically, the system is defined as $\mathcal{H}_s \otimes \mathcal{I}_b$ and the bath $\mathcal{H}_b \otimes \mathcal{I}_s$[4, 5], where $\mathcal{H}_s$ is the system Hamiltonian and $\mathcal{H}_b$ is the bath Hamiltonian and $\mathcal{I}_s$ and $\mathcal{I}_b$ are the identity operators for the system and bath respectively.

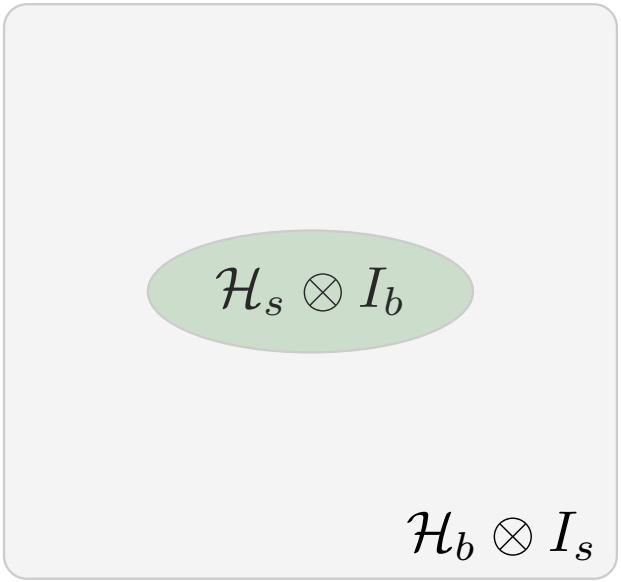


Figure 4.1: Open quantum system interacting with its surroundings.

The interaction between the system and the bath can vary in complexity depending on a number of factors, including relative relaxation times and coupling strength. If the system is weakly coupled to the bath and has a much slower relaxation time then it can be assumed

that the system is Markovian as depicted in Fig. 4.2.

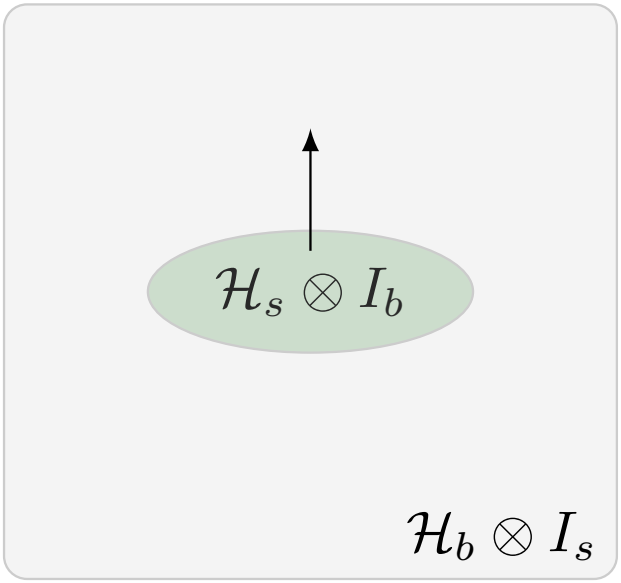


Figure 4.2: Markovian open quantum system interacting with its surroundings.

In Markovian open quantum systems, the bath behaves as a sink for the system. Energy or information that is lost from the system to the bath is not recovered; once lost it will never play a roll in future dynamics. Markovian processes are often referred to as memoryless processes[4, 5]. Extensive work has been done on these systems as the Markovian approximation holds true in a vast number of physical and chemical systems of interest[4, 6–9].

## 4.3 Lindblad's Equation

One of the most widely used methods of treating open system dynamics in the Markovian regime is the Lindblad equation[4, 10, 11],

$$\frac{dD_s(t)}{dt} = -i[H, D_s(t)] + \sum_k C_k D_s(t) C_k^\dagger - \frac{1}{2}\{C_k C_k^\dagger, D_s(t)\}, \tag{4.5}$$

where $D_s$ is the system density matrix, $H$ is the system Hamiltonian, and $\{C_k\}$ are the set of Lindbladian operators for $k$ channels[10]. The choice of $C_k$ generally come from physical arguments in the weak coupling limit.

One of the major benefits of the Lindblad equation is that due to its derivation from Kraus maps, it maintains the positivity of the density matrix for all times[10, 12]. However, it has been shown that care needs to be taken when using the Lindblad equation in conjunction with the 1-electron RDM for systems of multiple fermions[13]. While the positivity is maintained, there is nothing in the Lindblad equation that guarantees fermionic statistics. Depending on the choice of $C_k$, it is possible to observe unphysical results in the form of multiple fermions piling into the lowest energy state, thus violating $N$-representability and the Pauli exclusion principle. Chapter 5 addresses a method of constraining the Lindbladian matrices to generalize the Lindblad equation to treat systems of multiple fermions.

## 4.4 Non-Markovian Open Quantum Systems

If the coupling between the system and bath is strong, the bath is sufficiently complex, or the system relaxation time is much faster than that of the bath, the Markovian approximation breaks down. In this regime, energy or information lost from the system to the bath may return to the system at a later time. This implies that the system has memory of its past and instead of purely dissipative dynamics, a back-flow of energy or information can be observed as depicted in Fig. 4.3. This type of behaviour is a signature of non-Markovian dynamics[4, 5].

The introduction of memory makes the dynamics of these systems much more challenging to treat. There are currently a variety of approaches being developed and used to treat this problem including hierarchical equations of motion methods[14, 15], quantum jump methods[16], quantum trajectory methods[17–19], master equation methods[20–23], and many more[24]. The master equation methods are particularly appealing as they treat the reduced

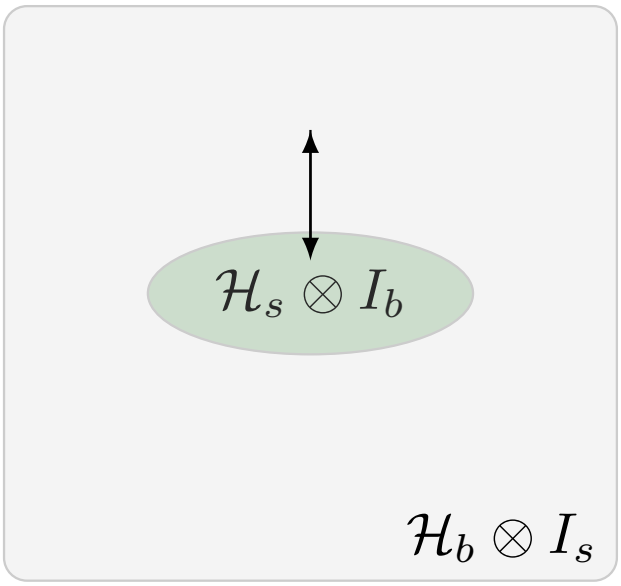


Figure 4.3: Non-Markovian open quantum system interacting with its surroundings.

density matrix directly.

Many of the current methods of treating non-Markovian dynamics do not inherently preserve the positivity of the density matrix. For instance perturbative techniques often violate the positivity of the density matrix in the strong coupling limit of system-bath interactions[4, 25]. The positivity is crucial for the $N$-representability of the density matrix, and therefore losing this property implies unphysical behaviour. Since Lindblad's equation preserves positivity by construction, Chapter 6 outlines our method of generalizing the Lindblad equation to capture non-Markovian dynamics without sacrificing the guaranteed positivity. This method takes an ensemble average of Lindbladian trajectories from numerous points in the system's history to capture memory effects while maintaining positivity. Chapter 7 outlines a method of generalizing the constraints from the Markovian Lindblad equation to ensure fermionic statistics in the ensemble of Lindbladian trajectories, or ELT, framework.

While the ELT method and constraints have generalized the Lindblad equation to treat systems of multiple fermions in both the Markovian and non-Markovian regime, there is still plenty of work that remains. One major area for improvement is in choosing the statistical

weights in the ELT method. Currently, only small, exactly solvable systems have been studied so numerical optimization is sufficient. However, to consider larger systems, a more general method of choosing weights needs to be developed.


(1) Mazziotti, D. A. Two-Electron Reduced Density Matrix as the Basic Variable in Many-Electron Quantum Chemistry and Physics. *Chemical Reviews* **2012**, *112*, 244–262.

(2) Coleman, A. J. Structure of Fermion Density Matrices. *Reviews of Modern Physics* **1963**, *35*, 668.

(3) Mazziotti, D. A. Structure of Fermionic Density Matrices: Complete N-Representability Conditions. *Physical Review Letters* **2012**, *108*, 263002.

(4) Breuer, H. P.; Petruccione, F., *The Theory of Open Quantum Systems*; Oxford University Press: 2002.

(5) Rivas, A.; Huelga, S. F., *Open Quantum Systems An Introduction*; Springer Briefs in Physics: 2012.

(6) Feynman, R. P.; Vernon Jr., F. L. The theory of a general quantum system interacting with a linear dissipative system. *Annals of Physics* **1963**, *24*, 118–173.

(7) Weiss, U., *Quantum Dissipative Systems, Series in Modern Condensed Matter Physics Volume 10*; World Scientific, Singapore: 2006.

(8) Skolnik, J. T.; Mazziotti, D. A. Cumulant reduced density matrices as measures of statistical dependence and entanglement between electronic quantum domains with application to photosynthetic light harvesting. *Physical Review A* **2013**, *88*, 032517.

(9) Skochdopole, N.; Mazziotti, D. A. Functional subsystems and strong correlation in photosynthetic light harvesting. *Advances in Chemical Physics* **2014**, *154*, 355–370.

(10) Lindblad, G. On the generators of quantum dynamical semigroups. *Communications in Mathematical Physics* **1976**, *48 (2)*, 119–130.

(11) Gorini, V.; Kossakowski, A.; Sudarshan, E. C. G. Complete positive dynamical semigroups of $N$-level systems. *Journal of Mathematical Physics* **1976**, *17 (5)*, 821–825.

(12) Kraus, K., *States, Effects, and Operations: Fundamental Notions of Quantum Theory*; Springer-Verlag Berlin Heidelberg: 1983.

(13) Pershin, Y. V.; Dubi, Y.; Di Ventra, M. Effective single-particle order-N scheme for the dynamics of open noninteracting many-body systems. *Physical Review B* **2008**, *78*, 054302.

(14) Jin, J. S.; Zheng, X.; Yan, Y. J. Exact dynamics of dissipative elctronic systems and quantum transport: Hierarchical equations of motion approach. *Journal of Chemical Physics* **2008**, *128 (23)*, 234703.

(15) Moix, J. M.; Cao, J. A hybrid stochastic hierarchy equations of motion approach to treat the low temperature dynamics of non-Markovian open quantum systems. *Journal of Chemical Physics* **2013**, *139*, 134106.

(16) Piilo, J.; Harkonen, K.; Maniscalco, S.; Suominen, K. A. Open system dynamics with non-Markovian quantum jumps. *Physical Review A* **2009**, *79 (6)*, 062112.

(17) Yu, T.; Diósi, L.; Gisin, N.; Strunz, W. T. Post-Markov master equation for the dynamics of open quantum systems. *Physical Review A* **2004**, *70 (1)*, 012106.

(18) Breuer, H. P. Genuine quantum trajctories for non-Markovian processes. *Physical Review A* **2004**, *70 (1)*, 012106.

(19) Shabani, A.; Lidar, D. A. Completely positive post-Markovian master equation via a measurement approach. *Physical Review A* **2005**, *71*, 020101(R).

(20) Breuer, H. P.; Kappler, B.; Petruccione, F. Stochastic wave-function method for non-Markovian quantum master equations. *Physical Review A* **1999**, *59 (2)*, 1633–1643.

(21) Montoya-Castillo, A.; Berklebach, T. C.; Reichman, D. R. Extending the applicability of Redfield theories into highly non-Markovian regimes. *Journal of Chemical Physics* **2015**, *143*, 194108.

(22) Fetherolf, J. H.; Berkelbach, T. C. Linear and nonlinear spectroscopy from quantum master equations. *Journal of Chemical Physics* **2017**, *147*, 244109.

(23) Ferialdi, L. Exact closed master equation for Gaussian non-Markovian dynamics. *Physical Review Letters* **2016**, *116*, 120402.

(24) Wismann, S.; Karlsson, A.; Laine, E.; Piilo, J.; Breuer, H. P. Optimal state pairs for non-Markovian quantum dynamics. *Physical Review A* **2012**, *86*, 062108.

(25) Chruscinski, D.; Kossakowski, A. Non-Markovian Quantum Dynamics: Local vs. Nonlocal. *Physical Review Letters* **2010**, *104*, 070406.

# CHAPTER 5

# SATISFYING FERMIONIC STATISTICS IN THE MODELING OF OPEN TIME-DEPENDENT QUANTUM SYSTEMS WITH ONE-ELECTRON REDUCED DENSITY MATRICES



## 5.1 Introduction

Open time-dependent quantum systems are important to understanding a range of chemical phenomena from molecules in solvent or protein environments to materials embedded in a larger-scale structure [1–3]. The influence of the environment on a system's energy can be as significant or even more significant than the influence of electron correlation. The evolution of the closed quantum system is governed by the quantum Liouville equation, also known as the von Neumann equation [4, 5]. For an open quantum system Lindblad derived the most general modification of the quantum Liouville equation in the Markovian approximation that models environmental effects while preserving the non-negativity of the probability distribution (or more specifically, the positive semidefiniteness of the system's density matrix) [6–9].

While Lindblad's operator is correct for $N$-electron density matrices, the operator has been observed to cause significant violation of the Pauli exclusion principle in the time evolution of the 1-electron reduced density matrix (1-RDM) [10]. As discussed in Refs. [10–12], the preservation of the fermionic statistics of the 1-RDM in an open, time-dependent system, even with an interaction-free Hamiltonian, is a non-trivial problem. Despite previous difficulties the generalization of the Lindblad operator to preserve fermionic statistics is critical to the accurate treatment of environmental effects in the time evolution of effective one-

electron theories such as the time-dependent Hartree-Fock and density functional theories. Constraining the 1-RDM to obey the Pauli exclusion principle, which requires the eigenvalues of the 1-RDM to lie between 0 and 1, is equivalent to constraining the 1-RDM to be *ensemble $N$-representable*, that is representable by at least one ensemble $N$-electron density matrix [13, 14]. In this Communication we derive the necessary and sufficient constraints on the Lindbladian matrix within the Lindblad operator to ensure that the 1-RDM remains ensemble $N$-representable throughout its time evolution, which is equivalent to its obeying the Pauli exclusion principle for all time. The theory is illustrated by considering the relaxation of an excitation in several molecules, $F_2$, $N_2$, CO, and $BeH_2$, subject to environmental noise.

## 5.2 Theory

### *5.2.1 Fermion Conditions on Lindbladian Matrices*

An open, time-dependent quantum system of $N$-electrons can be described by the time dependent $N$-electron density matrix $D$ governed by the quantum Liouville equation [4]

$$\frac{dD}{dt} = -i[H, D] + L(D, C) \tag{5.1}$$

with a Lindblad terms $L(D, C)$ added to account for the interaction of the $N$-electron system with its environment [6]

$$L(D, C) = CDC^\dagger - \frac{1}{2}\{C^\dagger C, D\}. \tag{5.2}$$

Importantly, the Lindblad term treats the interaction of the system with the environment while keeping the $N$-electron density matrix positive semidefinite at each time, that is

$$D \succeq 0. \tag{5.3}$$

A matrix is *positive semidefinite* if and only if all of its eigenvalues are nonnegative. Collectively, this semidefinite constraint on the matrix and additional constraints that the matrix be (*i*) Hermitian, (*ii*) normalized, and (*iii*) antisymmetric in the exchange of its particles ensure that it is an $N$-particle density matrix with fermion statistics [13].

Although the above formalism is exact, it is often computationally expensive to propagate the $N$-electron density matrix as a function of time with the Liouville equation. One mean-field-like approximation is to replace (*i*) the $N$-electron Hamiltonian with its explicit two body electron-electron interactions by an interaction-free Hamiltonian and (*ii*) the $N$-electron density matrix with its explicit treatment of electron correlation by a 1-RDM. The simplest derivation of this approximation is to generalize the one-electron Liouville equation

$$\frac{d\,{}^1D}{dt} = -i[{}^1H, {}^1D] + L({}^1D, {}^1C), \tag{5.4}$$

where ${}^1D$ is the 1-RDM, ${}^1H$ is the one-body interaction-free Hamiltonian, and ${}^1C$ is the one-body Lindblad matrix. If we set $Tr({}^1D) = N$, then Eq. (5.4) can describe not only a one-electron system with $N = 1$ but also an ensemble of $N$ non-interacting one-electron systems when $N > 1$. As in the $N$-electron case, the structure of the Lindblad term in Eq. (5.2) ensures that the 1-RDM remains positive semidefinite for all time.

Unlike the $N$-electron density matrix, however the 1-RDM has additional constraints to ensure that it represents an ensemble $N$-electron density matrix, known as *$N$-representability conditions* [13, 15]. In addition to the non-negativity of the 1-RDM, it is also necessary for the one-hole RDM ${}^1Q$ to be positive semidefinite. Therefore, in addition to being (*i*) Hermitian and (*ii*) normalized to $N$, the 1-RDM must also satisfy two linear matrix inequalities

$${}^1D \succeq 0 \tag{5.5}$$

$${}^1Q \succeq 0. \tag{5.6}$$

Coleman showed that these conditions on the 1-RDM are necessary and sufficient ensemble $N$-representability conditions [13]. Furthermore, they are equivalent to the well-known Pauli principle that the occupation numbers of the 1-RDM must lie between zero and one.

While the Lindblad term by construction is known to keep the 1-RDM positive semidefinite for all time [6–9], it is necessary to explore the effect of the Lindblad term on the requisite positive semidefiniteness of the one-hole RDM. To address this question, we substitute the expression for the one-particle RDM in terms of the one-hole RDM

$$^1D =^1 I -^1 Q \tag{5.7}$$

into the Liouville equation with the Lindblad term in Eq. (5.4). Because the one-particle identity matrix $^1I$ is time-independent and commutes with the Hamiltonian, the non-dissipative portion of Eq. (5.4) simplifies forthwith, and we obtain

$$\frac{d\,^1Q}{dt} = -i[^1H,^1 Q] + L(^1I -^1 Q, C). \tag{5.8}$$

Now we consider the Lindblad term as a functional of $^1I -^1 Q$,

$$L(^1I -^1 Q,^1 C) = -L(^1Q,^1 C) + [^1C,^1 C^\dagger]. \tag{5.9}$$

From Eq. (5.9) it can be seen that to obtain an equation analogous to Eq. (5.4) for the one-hole RDM, an added restriction must be imposed on the Lindbladian matrix $^1C$. Specifically, for the 1-hole RDM to evolve according to the Liouville equation with a Lindblad operator, it is necessary and sufficient that the second term in Eq. (5.4) vanishes. If $[^1C,^1 C^\dagger] = 0$, then Liouville equation for the one-hole RDM can be expressed as

$$\frac{d\,^1Q}{dt} = -i[^1H,^1 Q] + L(^1Q,^1 C), \tag{5.10}$$

which is the hole analogue of Eq. (5.4). Just as in the case of the 1-electron RDM, this equation keeps the one-hole RDM positive semidefinite for all time. We have proven that the time evolution of the one-particle RDM by Eq. (5.4) keeps both the one-particle RDM and the one-hole RDM positive semidefinite for all time under the condition that the Lindbladian matrix ${}^1C$ commutes with its adjoint. Therefore, *constraining the Lindbladian matrix* ${}^1C$ *such as its commutator with its adjoint vanishes causes the 1-fermion RDM solution of the quantum Liouville equation to satisfy the Pauli exclusion principle for all time* (that is, remain $N$-representable for all time). For the commutator to vanish, the ${}^1C$ matrix can be constraint to be Hermitian $S$, anti-Hermitian $A$, or a sum of Hermitian and anti-Hermitian matrices $S+A$, where $SA = 0$. This restricted class of ${}^1C$ includes the generators of Gaussian semigroups.

### *5.2.2 Fermion Conditions on Multiple Lindbladian Matrices*

Considering the case where there are numerous dissipation channels represented by multiple Lindbladian matrices, we can use Eq. (5.4) as a starting point to generalize the theory of the previous section. Taking the summation of the Lindblad terms over $m$ channels yields

$$\frac{d\,{}^1D}{dt} = -i[{}^1H, {}^1D] + \sum_{i=1}^{m} L({}^1D, {}^1C_i). \tag{5.11}$$

By the same method as previously presented, an analogous equation can be derived for the 1-hole RDM

$$\frac{d\,{}^1Q}{dt} = -i[{}^1H, {}^1Q] + \sum_{i=1}^{m} L({}^1Q, {}^1C_i). \tag{5.12}$$

Once again, to have Eq. (5.12) hold true to preserve the fermionic character of the system, each Lindbladian matrix ${}^1C_i$ must satisfy

$$[{}^1C_i, {}^1C_i^\dagger] = 0. \tag{5.13}$$

Constraining each of the Lindbladian matrices ${}^1C_i$ to be either Hermitian or anti-Hermitian is sufficient for the 1-fermion RDM solution of the quantum Liouville equation to satisfy the Pauli exclusion principle and remain $N$-representable for all time.

A specific, physically important example of Lindbladian matrices that satisfy the above requirement is the case where each Lindbladian matrix ${}^1C_i$ is a rank-one projection operator

$$ {}^1C_i = \gamma_i v_i v_i^\dagger. \tag{5.14}$$

If $m$ is chosen to equal the number $r$ of one-electron orbitals and each $v_i$ is a vectors representing the $i^{\text{th}}$ orbital, then each ${}^1C_i$ represents the interaction of the $i^{\text{th}}$ orbital of the system with the environment with $\gamma_i$ controlling the degree of the interaction. If we further restrict the number $m$ of channels to the $N$ occupied orbitals, then we recover the form of the Lindbladian matrix presented by Pershin et al. [10]. The present work shows that the rank-one Lindbladian matrices in Ref. [10] are a special case of the more general arbitrary-rank Hermitian Lindbladian matrices that preserve the fermionic statistics of the 1-RDM for all time. Even within the rank-one approximation generalizing the number of Lindbladian channels from the $N$ occupied orbitals to the $r$ occupied and unoccupied (virtual) orbitals provides additional flexibility for modeling the interaction of the system with the environment that maintains particle-hole symmetry [16, 17].

## 5.3 Applications

To illustrate, we consider the time evolution of 4 molecules $N_2$, CO, $F_2$, and $BeH_2$ initialized to their first excited states. For each molecule the effective one-electron Hamiltonian is constructed at the Hartree-Fock level of theory. Hartree-Fock calculations were performed in the Dunning-Hay double-zeta basis set [18] with the quantum chemistry package GAMESS [19]. For each molecule the time evolution was performed with both a Hermitian ${}^1C$ matrix and

a non-Hermitian ${}^1C$ matrix. The elements of the ${}^1C$ matrix were generated with the random number generator in the computer algebra system Maple [20]. The time propagation of the 1-RDM was performed by solving the Liouville equation with a fourth-fifth order Runge-Kutta method for solving initial-value differential equations [21].

Table 5.1: The first 8 occupation numbers of $F_2$, $N_2$, and CO are presented at 0.0 fs where they have their time-independent Hartree-Fock values and at 2.0 fs after evolution of the Liouville equation in the presence of environmental noise. When the Lindbladian matrix ${}^1C$ is selected to be Hermitian, the occupation numbers remain between 0 and 1. In contrast, when the Lindbladian matrix ${}^1C$ is selected to be non-Hermitian, the highest occupation numbers increase in value to violate the Pauli exclusion principle dramatically by 2 fs.

| Occupation Number | t = 0 | $F_2$ | | $N_2$ | | CO | |
|---|---|---|---|---|---|---|---|
| | | t=2.0 fs | | | | | |
| | | ${}^1C = {}^1C^\dagger$ | ${}^1C \neq {}^1C^\dagger$ | ${}^1C = {}^1C^\dagger$ | ${}^1C \neq {}^1C^\dagger$ | ${}^1C = {}^1C^\dagger$ | ${}^1C \neq {}^1C^\dagger$ |
| 1 | 1 | 0.993 | 3.636 | 0.865 | 5.428 | 0.866 | 3.168 |
| 2 | 1 | 0.924 | 3.636 | 0.767 | 5.428 | 0.768 | 3.168 |
| 3 | 1 | 0.923 | 2.382 | 0.762 | 0.777 | 0.764 | 1.646 |
| 4 | 1 | 0.921 | 2.382 | 0.758 | 0.777 | 0.760 | 1.646 |
| 5 | 1 | 0.920 | 1.639 | 0.754 | 0.333 | 0.759 | 1.251 |
| 6 | 1 | 0.914 | 1.639 | 0.750 | 0.333 | 0.757 | 1.251 |
| 7 | 1 | 0.911 | 0.548 | 0.747 | 0.178 | 0.752 | 0.483 |
| 8 | 1 | 0.911 | 0.548 | 0.720 | 0.178 | 0.722 | 0.483 |

Table 5.1 presents the first 8 occupation numbers of $F_2$, $N_2$, and CO at 0.0 fs as well as at 2.0 fs. At 0.0 fs the occupation numbers are those from solving the time-independent Hartree-Fock approximation to the Schrödinger equation. When the Lindbladian matrix ${}^1C$ is selected to be Hermitian, the interaction of each electronic system with an environment causes the occupations to change from 1 and 0 for the occupied and unoccupied orbitals, respectively, to values between 0 and 1 at 2 fs. In contrast, when the Lindbladian matrix ${}^1C$ is selected to be non-Hermitian, the highest occupation numbers increase in value to violate the Pauli exclusion principle dramatically by 2 fs.

Figure 5.1 shows the twelve occupation numbers of $BeH_2$ as functions of time using (a) a Hermitian and (b) a non-Hermitian Lindbladian matrix ${}^1C$. With a Hermitian matrix ${}^1C$ the occupation numbers lie between 0 and 1 in accordance with the Pauli exclusion principle,

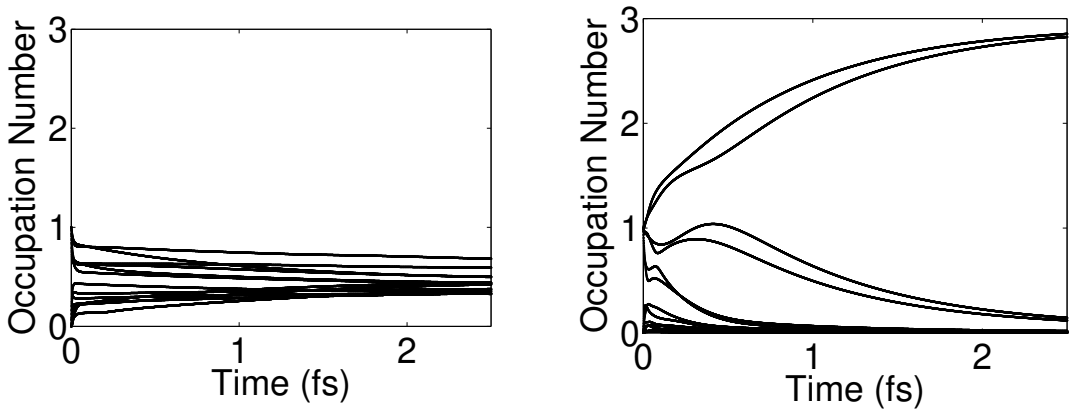


Figure 5.1: The twelve occupation numbers of $BeH_2$ are shown as functions of time using (a) a Hermitian and (b) a non-Hermitian Lindbladian matrix ${}^1C$. With a Hermitian matrix ${}^1C$ the occupation numbers lie between 0 and 1 in accordance with the Pauli exclusion principle, but with a non-Hermitian ${}^1C$ matrix the occupation numbers dramatically exceed 1 as the electrons in $BeH_2$ assume bosonic character.

but with a non-Hermitian ${}^1C$ matrix the occupation numbers dramatically exceed 1 as the electrons in $BeH_2$ assume bosonic character. The anti-Hermitian part of the non-Hermitian matrix ${}^1C$ has the ability to convert a system obeying fermionic statistics to a system obeying only bosonic statistics.

## 5.4 Discussion and Conclusions

Addition of the Lindblad operator to the quantum Liouville equation provides the most general time evolution within the Markovian approximation that preserves the non-negativity of the $N$-electron density matrix [6–8]. The most common use of the quantum Liouville equation in many-electron quantum systems, however, is to evolve a reduced density matrix (RDM) such as the one-electron RDM according to an effective one-electron Hamiltonian. In this case Lindblad's derivation is not complete because additional constraints, known as $N$-representability conditions, are necessary to ensure that an RDM represents at least one ensemble $N$-electron system [13–15]. The breakdown of fermionic statistics (in other words,

the violation of the Pauli exclusion principle) has been observed in Ref. [10] for the time evolution of the 1-RDM subject to the Lindblad operator. A generalization of the Lindblad operator to preserve fermion statistics is necessary for treating environmental effects such as noise and dissipation in the time evolution of effective one-electron theories (i.e. in the time-dependent Hartree-Fock and density functional theories).

In this Communication a general constraint on the Lindblad operator was derived to ensure that 1-RDM generated by the quantum Liouville equation satisfies the Pauli exclusion principle for all time. Specifically, we showed that if the Lindbladian matrix is constrained to commute with its adjoint, then the 1-RDM satisfies the Pauli exclusion principle at all times, meaning that during the time evolution its eigenvalues always lie in the interval $[0, 1]$. We formally derived this result by showing that if the Lindbladian matrix commutes with its adjoint, then the Lindblad operator preserves the non-negativity of both the one-particle RDM ${}^1D$ and the one-hole RDM ${}^1Q$, that is ${}^1D \succeq 0$ and ${}^1Q \succeq 0$, which imply the Pauli exclusion principle. We also generalized the results to the addition of multiple Lindblad operators to the quantum Liouville equation. In that case it is necessary to constrain each Lindbladian matrix to commute with its adjoint. A sufficient condition for the dynamics to obey fermionic statistics is to constrain the Lindbladian matrix to be either Hermitian or anti-Hermitian.

The present generalization of Lindblad operator provides a general framework for incorporating environmental effects, especially dephasing and dissipation, into the time evolution of 1-RDMs within effective one-electron theories. Our generalization reduces to Pershin et al.'s earlier work [10] if we introduce a rank-one Lindbladian matrix for controlling the interaction of each occupied orbital with the environment. Within a rank-one model of the Lindbladian matrices we recommend including bath channels for both the occupied and unoccupied orbitals as a more realistic approximation that obeys particle-hole symmetry [16, 17]. $N$-representable approximations to the Lindblad operator may be especially impor-

tant within the framework of time-dependent density functional theories that incorporates environmental noise.


(1) Feynman, R. P.; Vernon Jr., F. L. The theory of a general quantum system interacting with a linear dissipative system. *Annals of Physics* **1963**, *24*, 118–173.

(2) Weiss, U., *Quantum Dissipative Systems, Series in Modern Condensed Matter Physics Volume 10*; World Scientific, Singapore: 2006.

(3) Breuer, H. P.; Petruccione, F., *The Theory of Open Quantum Systems*; Oxford University Press: 2002.

(4) Von Neumann, J., *Mathematical Foundations of Quantum Mechanics*; Princeton University Press: 1955.

(5) Berman, M.; Kosloff, R. Time-dependent solution of the Liouville-von Neumann equation: non-dissipative evolution. *Computer Physics Communications* **1991**, *63 (1-3)*, 1–20.

(6) Lindblad, G. On the generators of quantum dynamical semigroups. *Communications in Mathetical Physics* **1976**, *48 (2)*, 119–130.

(7) Gorini, V.; Kossakowski, A.; Sudarshan, E. C. G. Complete positive dynamical semigroups of $N$-level systems. *Journal of Mathematical Physics* **1976**, *17 (5)*, 821–825.

(8) Spohn, H. Kinetic equations from Hamiltonian dynamics: Markovian limits. *Reviews of Modern Physics* **1980**, *52*, 569.

(9) Kohen, D.; Marston, C. C.; Tannor, D. J. Phase space approach to theories of quantum dissipation. *Journal of Chemical Physics* **1997**, *107*, 5236.

(10) Pershin, Y. V.; Dubi, Y.; Ventra, M. D. Effective single-particle order-$N$ scheme for the dynamics of open noninteracting many-body systems. *Physical Review B* **2008**, *78*, 054302.

(11) Rothman, A. E.; Mazziotti, D. A. Nonequilibrium steady-state electron transport with $N$-representable density matrices from the anti-Hermitian contracted Schrodinger equation. *Journal of Physical Chemistry* **2010**, *132*, 104112.

(12) Rosati, R.; Iotti, R. C.; Dolcini, F.; Rossi, F. Derivation of nonlinear single-particle equations via many-body Lindblad superoperators: A density-matrix approach. *Physical Review B* **2014**, *90*, 125140.

(13) Coleman, A. J. Structure of Fermion Density Matrices. *Reviews of Modern Physics* **1963**, *35*, 668.

(14) Mazziotti, D. A. Structure of Fermionic Density Matrices: Complete $N$-Representability Conditions. *Physical Review Letters* **2012**, *108*, 263002.

(15) Chakraborty, R.; Mazziotti, D. A. Generalized Pauli conditions on the spectra of one-electron reduced density matrices of atoms and molecules. *Physical Review A* **2014**, *89*, 042505.

(16) Erdahl, E. The convex structure of the set of $N$-representable reduced 2-matrices. *Journal of Mathematical Physics* **1972**, *13*, 1608.

(17) Ruskai, M. $N$ Completeness, $N$ Representability, and Geminal Expansions. *Physical Review A* **1972**, *5*, 1336.

(18) Dunning Jr., T. H. Gaussian basis sets for use in correlated molecular calculations. I. The atoms boron through neon and hydrogen. *Journal of Physical Chemistry* **1989**, *90*, 1007.

(19) Schmidt, M. W.; Baldridge, K. K.; Boatz, J. A.; Elbert, S. T.; Gordon, M. S.; Jensen, J. H.; Koseki, S.; Matsunaga, N.; Nguyen, K. A.; Su, S.; Windus, T. L.; Dupuis, M.; Montgomery, J. A. General atomic and molecular electronic structure system. *Journal of Computational Chemistry* **1993**, *14 (11)*, 1347.

(20) *Maple 2015*; Maplesoft, Waterloo: 2015.

(21) E. Hairer, S. N.; Wanner, G., *Solving Ordinary Differential Equations I: Nonstiff Problems 2nd Ed.* Springer-Verlag, Berlin: 1993.

# CHAPTER 6

# ENSEMBLE OF LINDBLAD'S TRAJECTORIES FOR NON-MARKOVIAN DYNAMICS



## 6.1 Introduction

Non-Markovian effects are important in a variety of physical quantum systems including but not limited to exciton transport in photosynthetic light harvesting complexes[1–8], qubits and quantum control[9–12], and quantum optics[13]. Yet despite their prevalence there remain many unanswered questions in the theoretical treatment of such systems[14, 15]. The most common starting point for treating non-Markovian dynamics is an exact kernel equation, which is challenging to solve in the most general case[14, 15]. Many methods approximate the kernel through perturbative techniques, and while they are effective for small perturbations about the Markovian limit, they can in general limit or destroy the positivity of the density matrix[16]. Other methods have been developed to treat non-Markovian dynamics with built-in positivity in specific systems[17–29], but the development of a general, practical framework for non-Markovian approximations that maintains the positive semidefiniteness of the density matrix remains a significant problem[19]. Recent work has produced an exact, closed form master equation which allows the treatment of non-Markovian dynamics for Gaussian environments[30]. Other related work includes quantum jump methods and trajectory approaches[31–37].

Lindblad developed an elegant, completely general theory for treating Markovian dynamics in an open quantum system while maintaining the positive semidefinite property of the density matrix for all time[38–40]. In this paper we present a general extension of

Lindblad's theory to the case of non-Markovian quantum systems. While Lindblad examines the equation of motion for a single trajectory that generalizes the Liouville equation to the Markovian case, we consider an ensemble of Lindbladian trajectories (ELT) which allows for an accurate calculation of dynamics in the strong coupling, non-Markovian regime while maintaining the positivity of the density matrix. The constraint of the system's density matrix to be consistent with the total density matrix (i.e. positive semidefinte) has connections to the $N$-representability problem in which a $p$-partice density matrix is constrained to represent an $N$-particle density matrix with $N > p$[41–45]. The ELT theory is also related to post-Markovian methods [31, 33, 37] based on Kraus maps with further details given below. The Jaynes-Cummings model is used to demonstrate the accuracy of the ELT method as it is exactly solvable and many perturbative methods fail at capturing the exact dynamics in the strong coupling regime[46, 47].

## 6.2 Theory

### *6.2.1 Ensemble of Lindbladian Trajectories Method*

An ensemble of Lindbladian trajectories is used to calculate the density matrix at a given time $t$. In Fig. 6.1 the blue density matrix at time $t$ is the actual density matrix of the quantum system while the green density matrices are auxiliary variables, each of which represents a trajectory in the ensemble. Each green density matrix $\tilde{D}(t, \tau_i)$ is the endpoint of a Lindblad trajectory originating from an actual (blue) density matrix at time $t - \tau_i$. The ensemble of the green density matrices $\tilde{D}(t, \tau_i)$ originating at different times $t - \tau_i$ defines the actual (blue) density matrix at time $t$. Formally, this is equivalent to,

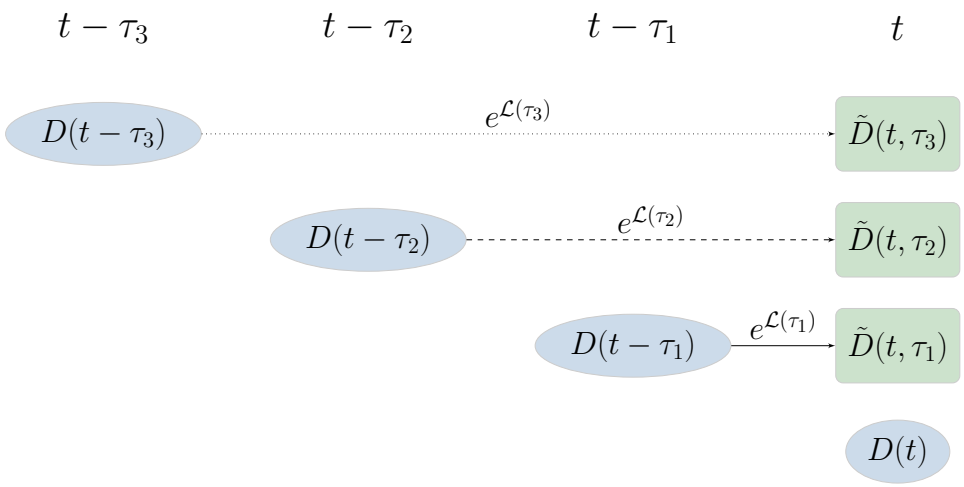


Figure 6.1: An ensemble of Lindbladian trajectories whose weighted ensemble produces the density matrix at time $t$.

$$D(t) = \sum_{i=1}^{N} \omega(\tau_i)\tilde{D}(t,\tau_i) \tag{6.1}$$

$$= \sum_{i=1}^{N} \omega(\tau_i)e^{\mathcal{L}(\tau_i)}D(t-\tau_i) \tag{6.2}$$

where $N$ is an integer controlling the maximum amount of memory, $\omega(\tau_i)$ are the weights of the trajectories, and $e^{\mathcal{L}(\tau_i)}$ are the propagators. Each trajectory is a Kraus map which we can represent by the following Lindbladian trajectory:

$$\frac{dD}{ds} = -i[H,D] + \sum_{j=1}^{N} C_j D C_j^\dagger - \frac{1}{2}\{C_j^\dagger C_j, D\} \tag{6.3}$$

where $s$ represents an effective time within the mapping and the Lindblad terms $C_j$ account for the interaction of the $N$-electron system with its environment through different dissipative channels [39]. From the properties of Kraus maps the trajectories produce positive semidefinite density matrices whose ensemble is also positive semidefinite[48]. If the Hamiltonian and the Lindbladian matrices are all time dependent, that is dependent on the effective time $s$, then the Lindblad trajectory can approach an arbitrary Kraus map. The

proof follows from writing the Lindblad trajectory as a composition of Kraus maps where all but one of the Kraus maps can be chosen to be the identity operation.

This ansatz is an extension of the Lindbladian theory to the general case of non-Markovian dynamics under the mild assumption that each point in history can be mapped to the present using a Kraus map. Because any positive semidefinite density matrix at time $t$ can be generated by a Kraus map from a historical density matrix at $t-\tau$[9–12, 48], the assumption is equivalent to requiring that each trajectory's density matrix be positive semidefinite. Any positive semidefinite density matrix can be generated from an initial density matrix from a Kraus map. By assuming the positivity of each individual map in the ensemble average, we can select the nonnegative weights in the ensemble average without any additional restriction. Although Kraus maps are employed in other open-system theories such as the post-Markovian methods [31, 33, 37], ELT does not rely on measurement theory to generalize the Lindblad equation, which leads to a different set of final equations.

### *6.2.2 Relationship to Kernel Methods*

The general kernel equation is given by,

$$\frac{dD}{dt} = \int_0^t \mathcal{K}(t,\tau)D(t,\tau)d\tau, \tag{6.4}$$

where $D(t,\tau)$ is the reduced density matrix at time $t-\tau$ and $\mathcal{K}(t,\tau)$ is the memory kernel[14, 15]. We can convert Eq. 6.2 into the form of Eq. 6.4 by taking the summation in Eq. 6.2 to the continuous limit, differentiating each side of Eq. 6.2 with respect to $t$, and invoking the Leibnitz rule:

$$\frac{dD(t)}{dt} = \int_0^t \omega(\tau)e^{\mathcal{L}(\tau)}\frac{dD(t,\tau)}{dt}d\tau, \tag{6.5}$$

where $t$ is the current time, $t-\tau$ is the initial time for each trajectory, $e^{\mathcal{L}(\tau)}$ are the Kraus maps, and $\omega(\tau)$ are the weights. The key difference between the Eq. 6.5 and the standard

kernel equation in Eq. 6.4 is that the integral depends on the first derivative of the density matrix with respect to time while the standard method relies on just the density matrix. Eq. 6.5 is the key equation because the time derivative is central to the process of maintaining a positive semidefinite density matrix. It also has the benefit of transforming the integro-differential equation in Eq. 6.4 into a simplified type 2 Volterra equation[49, 50], which has well-developed numerical solutions[51].

## 6.3 Application

### *6.3.1 Jaynes-Cummings Model*

To illustrate this theory, we consider the damped Jaynes-Cummings model on resonance with and without detuning. This model consists of a single excitation in a two-level system coupled to a reservoir of harmonic oscillators[14, 17, 46, 47]. The Hamiltonian for the model is given by

$$\hat{H} = \frac{\omega_0 \hat{\sigma}_z}{2} + \int \omega \hat{a}^\dagger \hat{a} + \lambda\big(\hat{\sigma}_+ \hat{a} + \hat{\sigma}_- \hat{a}^\dagger\big) d\omega, \tag{6.6}$$

where $\omega_0$ is the two-level system's transition frequency and $\lambda$ is inversely proportional to the reservoir correlation time. The $\hat{a}^\dagger_\omega$ and $\hat{a}_\omega$ are the creation and are annihilation operators for frequency modes $\omega$, and $\hat{\sigma}_{x,y,z}$ are the Pauli spin operators with $\hat{\sigma}_\pm = \frac{\hat{\sigma}_x \pm \hat{\sigma}_y}{2}$[17]. The spectral density of the bath is

$$J(\omega) = \frac{1}{2\pi} \frac{\gamma_0 \lambda^2}{(\omega_0 - \Delta - \omega)^2 + \lambda^2}, \tag{6.7}$$

where $\gamma_0$ is inversely proportional to the time scal of the system changes and $\Delta$ is the amount of detuning[14]. Here the decay rates and populations in the excited level from our method are compared to those calculated exactly from the spectral density of the bath[14, 17]. We also compare our results with the Markovian solution, the solution to the generalized master

equation to second order (GME2), and the time convolutionless solution to second (TCL2) and fourth (TCL4) orders[52, 53].

In the weak coupling case without detuning the correlation time of the reservoir is set to one-fifth of the system's time scale, and in the strong coupling case without detuning the correlation time of the reservoir is set to five times the system's time scale. In all calculations we set the Markovian decay rate $\gamma_0$ to 1.091. The trajectory of each density matrix in the ELT method was computed with the computer algebra system Maple[54].

The excited-level population of the Jaynes-Cummings model has the following closed-form solution in the Markovian limit:

$$D_{11}(t) = D_{11}(0)e^{-\gamma_0 t}. \tag{6.8}$$

In the ELT method we consider an ensemble of such Lindbladian trajectories, one trajectory from each historical point in time,

$$D_{11}(t) = \sum_i \omega(\tau_i)\tilde{D}_{11}(t, \tau_i) \tag{6.9}$$

where $\tilde{D}_{11}(t, \tau_i) = D_{11}(t - \tau_i)e^{-\gamma(\tau_i)(t-\tau_i)}$. To match the dynamics from the ELT method with the dynamics from the full quantum system including both system and bath, we optimized both the weights $\omega(\tau_i)$ and the decay parameters $\gamma(\tau_i)$ simultaneously with a least squares fit to the exact solution by a sequential programming algorithm in Maple[55].

### *6.3.2 Results*

Figure 6.2 (a) shows the excited-level populations of the Markovian, ELT, and exact solutions while Fig. 6.2 (b) shows the errors in the excited-state population from all methods relative to the exact solution. The excited-level population of the Markovian solution decays too quickly at short times and too slowly at longer times. While the perturbative methods,

GME2, TCL2, and TCL4, improve upon this behavior, only the ELT method agrees with the exact solution to the precision of the numerical solution.

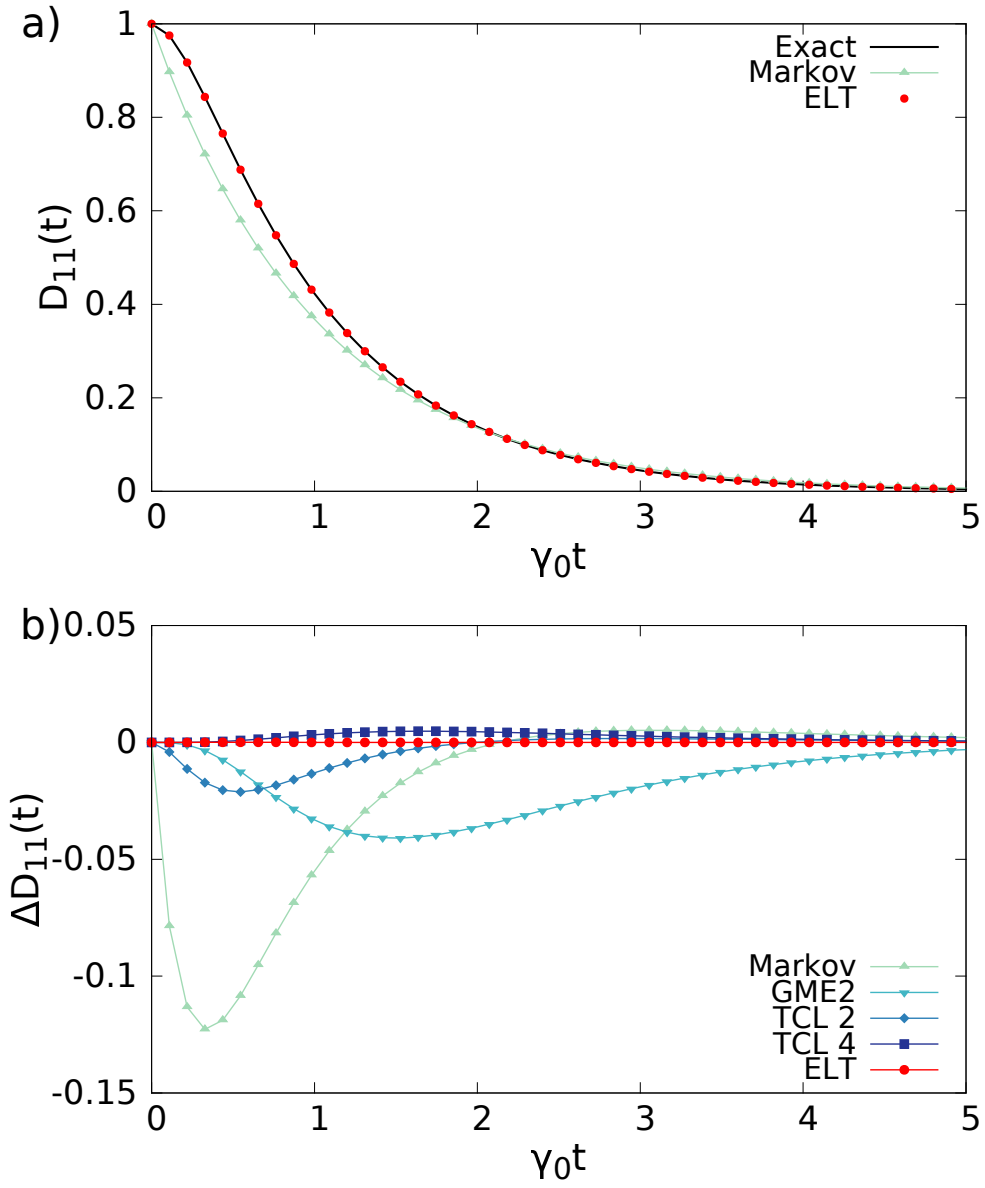


Figure 6.2: The exact (black), Markovian (green), GME2 (green-blue), TCL2 and TCL4 (teal and blue respectively), and ELT (red) (a) populations of the excited level and (b) errors relative to the exact solution are shown for the weak coupling limit ($\lambda = 5\gamma_0$ ,$\gamma_0 = 1.091, \Delta = 0$) in the Jaynes-Cummings model. The ELT method shows closest agreement to the exact solution.

In the strong coupling limit the excited-level population of each method is shown in

Fig. 6.3. The Markovian, TCL2, and TCL4 methods give physical results and the correct long-time behavior, they capture only the decay of the population and not its recovery. The GME2 solution exhibits unphysical behavior in the form of large negative probabilities for finding the model in its excited level. The ELT method correctly predicts the recovery, matching the exact solution to the precision of the numerical methods. Physically, the recovery arises from the energy previously transferred to the surroundings driving the system back into the excited state, which is often referred to as a back-flow of energy or information.

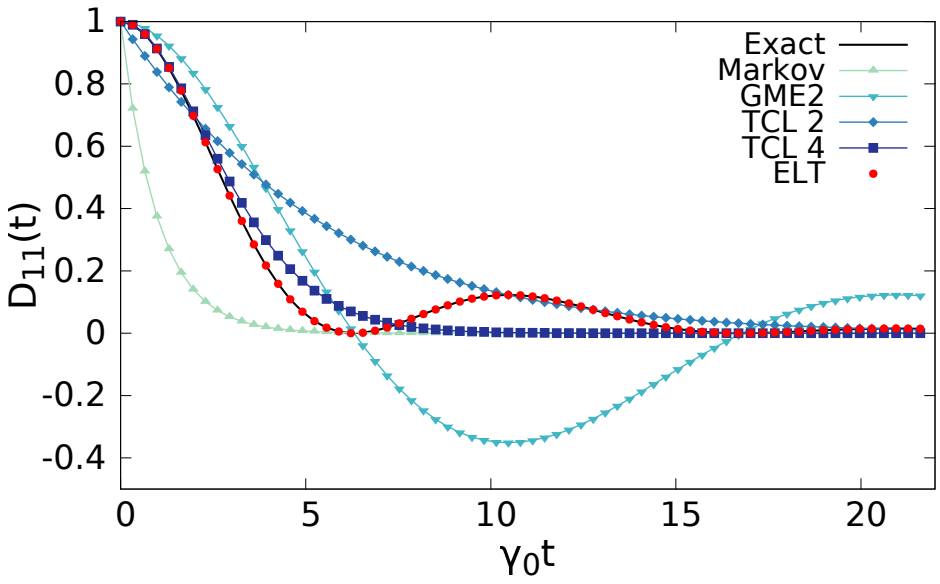


Figure 6.3: The population of the Jaynes-Cummings excited level in the strong coupling limit ($\lambda = 0.2\gamma_0$, $\gamma_0 = 1.091, \Delta = 0$) is shown as a function of time for the exact (black), Markovian (green), GME2 (green-blue), TCL2 and TCL4 (teal and blue respectively) and ELT (red) solutions. The ELT method agrees with the exact solution for all times.

Finally, we consider the Jaynes-Cummings model with detuning, comparing the Markovian, TCL4, and ELT solutions in Fig. 6.4, where $\lambda = 0.3\gamma_0$ and $\Delta = 2.4\gamma_0$. In this case the ensemble of such Lindbladian trajectories is augmented with trajectories of the hole density matrix:

$$D_{11}(t) = \sum_i \left[\omega(\tau_i)\tilde{D}_{11}(t,\tau_i) + \tilde{\omega}(\tau_i)(1 - \tilde{Q}_{11}(t,\tau_i))\right] \tag{6.10}$$

where $\tilde{Q}_{11}(t,\tau_i) = Q_{11}(t-\tau_i)e^{-\gamma(\tau_i)(t-\tau_i)}$ in which $Q_{11}(t) = 1-D_{11}(t)$. Physically, consideration of the hole density matrix is equivalent to including an additional Lindbladian channel corresponding to the decay of a hole from the upper level (or excitation of a particle from the lower level). It is seen that although the detuning case is inherently non-Lindbladian by nature[14], due to the ensemble nature of the ELT method, the exact dynamics are still captured.

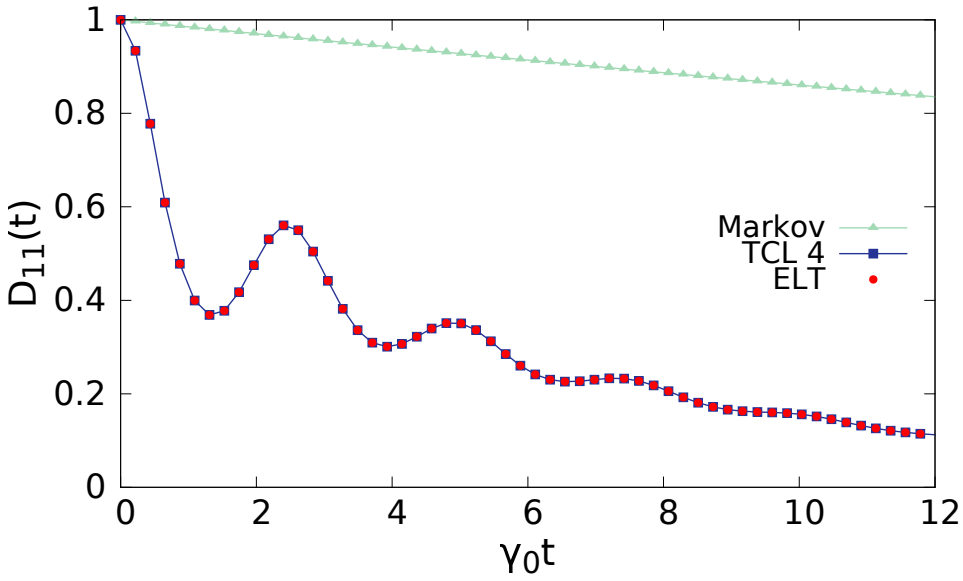


Figure 6.4: The population of the excited level of the Jaynes-Cummings model in the strong coupling, detuning limit ($\lambda = 0.3\gamma_0$, $\gamma_0 = 1.091$, $\Delta = 2.4\gamma_0$) is shown as a function of time for the Markovian (green), TCL4 (blue) and ELT (red) solutions. The ELT agrees with the TCL4 solution.

## 6.4 Conclusion

The most general form of treating non-Markovian dynamics in open quantum systems is with the kernel equation in Eq. (6.4). However, practical use of the kernel equation is computationally challenging in its general form. Approximations to the kernel, especially those that rely upon perturbative arguments, tend to sacrifice the positive semidefiniteness of the density matrix. Here, we have presented a general theory that considers an

ensemble of Lindbladian trajectories originating from different times in the system's history. In this manner the approach provides a complete account of the system's memory in a framework that preserves the positivity of the system's density matrix for all time. The Lindbladian trajectories capture the full range of potential dynamics because of the one-to-one mapping between Lindbladian trajectories and Kraus maps. Application of ELT to the Jaynes-Cummings model demonstrates its ability to capture non-Markovian dynamics in both the weak and strong coupling regimes. As with Lindblad's theory, the present generalization requires physical insight from theory and/or experiments to select the appropriate system-bath parameters. Future work will further explore the application of these results to the more accurate description of non-Markovian quantum systems.


(1) Lee, H.; Cheng, Y. C.; Fleming, G. R. Coherence dynamics in photosynthesis: protein protection of excitonic coherence. *Science* **2007**, *316 (5830)*, 1462–5.

(2) Scholes, G. D.; Fleming, G. R.; Olaya-Castro, A.; van Grondelle, R. Lessons from nature about solar light harvesting. *Nature Chemistry* **2011**, *3 (10)*, 763–74.

(3) Rebentrost, P.; Aspuru-Guzik, A. Comunication: Excition-phonon information flow in the energy transfer process of phtosynthetic complexes. *Journal of Chemical Physics* **2011**, *134*, 101103.

(4) Ritschel, G.; Suess, D.; Mobius, S.; Strunz, W. T.; Eisfeld, A. Non-Markovian quantum state diffusion for temperature-dependent linear spectra of light harvesting aggregates. *Journal of Chemical Physics* **2015**, *142*, 034115.

(5) Ritschel, G.; Roden, J.; Strunz, W. T.; Aspuru-Guzik, A.; Eisfeld, A. Supression of quantum oscillations and the dependence on site energies in electronic excitation transfer in the Fenna-Matthews-Olsen trimer. *Journal of Physical Chemistry Letters* **2011**, *2*, 2912.

(6) Chin, A. W.; Rivas, A.; Huelga, S. F.; Plenio, M. P. Exact mapping between system-reservoir quantum model and semi-infinite discrete chains using orthogonal polynomials. *Journal of Mathematical Physics* **2010**, *51*, 092109.

(7) Skochdopole, N.; Mazziotti, D. A. Functional Subsystems and Quantum Redundancy in Photosynthetic Light Harvesting. *Physical Chemistry Letters* **2011**, *2*, 2989.

(8) Mazziotti, D. A. Effect of strong electron correlation on the efficiency of photosynthetic light harvesting. *Journal of Chemical Physics* **2012**, *137*, 074117.

(9) Oza, A.; Pechen, A.; Dominy, J.; Beltrani, V.; Moore, K.; Rabitz, H. Optimization search effort over the control landscapes for open quantum systems with Kraus-map evolution. *Journal of Physics A: Mathematical and Theoretical* **2009**, *42*, 205305.

(10) Pechen, A.; Prokhorenko, D.; Wu, R.; Rabitz, H. Control landscapes for two-level open quantum systems. *Journal of Physics A: Mathematical and Theoretical* **2008**, *41*, 045205.

(11) Wu, R.; Pechen, A.; Brif, C.; Rabitz, H. Controllability of open quantum systems with Kraus-map dynamics. *Journal of Physics A: Mathematical and Theoretical* **2007**, *40*, 5681–5693.

(12) Wu, R.; Rabitz, H. Control landscapes for open system quantum operations. *Journal of Physics A: Mathematical and Theoretical* **2012**, *45*, 485303.

(13) Weiss, U., *Quantum Dissipative Systems, 4th Edition*; World Scientific, Singapore: 2012.

(14) Breuer, H. P.; Petruccione, F., *The Theory of Open Quantum Systems*; Oxford University Press: 2002.

(15) Rivas, A.; Huelga, S. F., *Open Quantum Systems An Introduction*; Springer Briefs in Physics: 2012.

(16) Breuer, H. P.; Burgarth, D.; Petruccione, F. Non-Markovian dynamics in a spin star system: Exact solution and approximation techniques. *Physical Review B* **2004**, *70 (4)*, 045323.

(17) Breuer, H. P.; Kappler, B.; Petruccione, F. Stochastic wave-function method for non-Markovian quantum master equations. *Physical Review A* **1999**, *59 (2)*, 1633–1643.

(18) Semin, V.; Petruccione, F. Nonequilibrium-thermodynamics approach to open quantum systems. *Physical Review A* **2014**, *90*, 052112.

(19) Chruscinski, D.; Kossakowski, A. Non-Markovian Quantum Dynamics: Local vs. Non-local. *Physical Review Letters* **2010**, *104*, 070406.

(20) Berklebach, T. C.; Reichman, D. R.; Markland, T. E. Reduced density matrix hybrid approach: An efficient and accurate method for adiabatic and non-adiabatic quantum dynamics. *Journal of Chemical Physics* **2012**, *136*, 034113.

(21) Berklebach, T. C.; Markland, T. E.; Reichman, D. R. Reduced density matrix hybrid approach: Application to electronic energy transfer. *Journal of Chemical Physics* **2012**, *136*, 084104.

(22) Chruscinski, D.; Kossakowski, A. Feshback Projection Formalism for Open Quantum Systems. *Physical Review Letters* **2013**, *111*, 050402.

(23) Montoya-Castillo, A.; Berklebach, T. C.; Reichman, D. R. Extending the applicability of Redfield theories into highly non-Markovian regimes. *Journal of Chemical Physics* **2015**, *143*, 194108.

(24) Fetherolf, J. H.; Berkelbach, T. C. Linear and nonlinear spectroscopy from quantum master equations. *Journal of Chemical Physics* **2017**, *147*, 244109.

(25) Li, A. C. Y.; Petruccione, F.; Koch, J. Perturbative approach to Markovian open quantum systems. *Scientific Reports* **2014**, *4*, 4887.

(26) Moix, J. M.; Cao, J. A hybrid stochastic hierarchy equations of motion approach to treat the low temperature dynamics of non-Markovian open quantum systems. *Journal of Chemical Physics* **2013**, *139*, 134106.

(27) Wismann, S.; Karlsson, A.; Laine, E.; Piilo, J.; Breuer, H. P. Optimal state pairs for non-Markovian quantum dynamics. *Physical Review A* **2012**, *86*, 062108.

(28) Semina, I.; Petruccione, F. The simulation of the non-Markovian behaviour of a two-level system. *Physica A* **2016**, *450*, 395.

(29) Barchielli, A.; Pellegrini, C.; Petruccione, F. Quantum Trajectories: Memory and continuous observation. *Physical Review A* **2012**, *86 (6)*, 063814.

(30) Ferialdi, L. Exact closed master equation for Gaussian non-Markovian dynamics. *Physical Review Letters* **2016**, *116*, 120402.

(31) Yu, T.; Diósi, L.; Gisin, N.; Strunz, W. T. Post-Markov master equation for the dynamics of open quantum systems. *Physical Review A* **2004**, *70 (1)*, 012106.

(32) Breuer, H. P. Genuine quantum trajctories for non-Markovian processes. *Physical Review A* **2004**, *70 (1)*, 012106.

(33) Shabani, A.; Lidar, D. A. Completely positive post-Markovian master equation via a measurement approach. *Physical Review A* **2005**, *71*, 020101(R).

(34) Mazzola, L.; Laine, E. M.; Breuer, H. P.; Maniscalco, S.; Piilo, J. Phenomenological memory-kernel master equations and time-dependent Markovian processes. *Physical Review A* **2010**, *81 (6)*, 062120.

(35) Campbell, S.; Smirne, A.; Mazzola, L.; Lo Gullo, N.; Vacchini, B.; Busch, T.; Paternostro, M. Critical assessment of two-qubit post-Markovian master equations. *Physical Review A* **2012**, *85*, 032120.

(36) Budini, A. A. Post-Markovian quantum master equations from classical environment fluctuations. *Physical Review E* **2014**, *89 (1)*, 012147.

(37) Sutherland, C.; Brun, T. A.; Lidar, D. A. Non-Markovianity of the post-Markovian Master Equation. *Physical Review A* **2018**, *98*, 042119.

(38) Kossakowski, A. On quantum statistical mechanics of non-Hamiltonian systems. *Reports in Mathematical Physics* **1972**, *3*, 247.

(39) Lindblad, G. On the generators of quantum dynamical semigroups. *Communications in Mathematical Physics* **1976**, *48 (2)*, 119–130.

(40) Gorini, V.; Kossakowski, A.; Sudarshan, E. C. G. Complete positive dynamical semigroups of $N$-level systems. *Journal of Mathematical Physics* **1976**, *17 (5)*, 821–825.

(41) Coleman, A. J. Structure of Fermion Density Matrices. *Reviews of Modern Physics* **1963**, *35*, 668.

(42) Mazziotti, D. A. Structure of Fermionic Density Matrices: Complete N-Representability Conditions. *Physical Review Letters* **2012**, *108*, 263002.

(43) Foley IV, J. J.; Mazziotti, D. A. Measurement-driven reconstruction of many-particle quantum processes by semidefinite programming with application to photosynthetic light harvesting. *Physical Review A* **2012**, *86*, 012512.

(44) Head-Marsden, K.; Mazziotti, D. A. Communication: Satisfying fermionic statistics in the modeling of open time-dependent quantum systems with one-electron reduced density matrices. *Journal of Chemical Physics* **2015**, *142*, 051102.

(45) Chakraborty, R.; Mazziotti, D. A. Noise-assisted energy transfer from the dilation of the set of one-electron reduced density matrices. *Journal of Chemical Physics* **2017**, *146*, 184101.

(46) Jaynes, E. T.; Cummings, F. Comparison of quantum and semiclassical radiation theories with application to the beam maser. *Proceedings of the IEEE* **1963**, *51 (1)*, 89–109.

(47) Stenhold, S. Beyond the Jaynes-Cummings model. *Journal of Physics B: Atomic, Molecular and Optical Physics* **2013**, *46 (22)*.

(48) Kraus, K., *States, Effects, and Operations: Fundamental Notions of Quantum Theory*; Springer-Verlag Berlin Heidelberg: 1983.

(49) Delves, L. M.; Mohamed, J. L., *Computational Methods for Integral Equations*; Cambridge University Press: 1985.

(50) Linz, P., *Analytical and Numerical Methods for Volterra Equations*; S.I.A.M., Philadelphia: 1985.

(51) Press, W. H.; Teukolsky, S. A.; Vetterling, W. T.; Flannery, B. P., *Numerical Recipes in C: The Art of Scientific Computing*; Cambridge University Press: 1992, pp 794–797.

(52) Shibata, F.; Takahashi, Y.; Hashitsume, N. A generalized stochastic Liouville equation. Non-Markovian versus memoryless master equations. *Journal of Statistical Physics* **1977**, *17 (4)*, 171–187.

(53) Chaturvedi, S.; Shibata, F. Time-convolutionless projection operator formalism for elimination of fast variables. Applications to Brownian motion. *Physik B* **1979**, *35*, 297.

(54) *Maple 2018*; Maplesoft, Waterloo: 2018.

(55) Gill, P. E.; Murray, W.; Saunders, M. A. SNOPT: An SQP Algorithm for Large-scale Constrained Optimization. *SIAM Journal on Optimization* **2002**, *12*, 979–1006.

# CHAPTER 7

# SATISFYING FERMIONIC STATISTICS IN THE MODELING OF NON-MARKOVIAN DYNAMICS WITH ONE-ELECTRON REDUCED DENSITY MATRICES

Parts of this chapter are reprints from a paper submitted for publication by K. Head-Marsden and D. A. Mazziotti (2019).

## 7.1 Introduction

Lindlbad derived a general equation to model environmental effects in open, time-dependent quantum systems while preserving the non-negativity of the density matrix[1–3]. However, when used in conjunction with the 1-particle reduced density matrix, or 1-RDM, fermion statistics are not inherently preserved[4–7]. Additional constraints have been derived on the Lindbladian operators to ensure that the 1-RDM obeys the Pauli exclusion principle[8]. Here, we extend these constraints to treat non-Markovian dynamics.

Despite the prevalence of non-Markovian dynamics in a variety of physical systems such as information transfer in qubits and energy transfer in photosynthetic light harvesting complexes, general and accurate treatment of such dynamics remains a challenge[9–20]. Methodologies for non-Markovian dynamics include the quantum jump methods, quantum trajectory approaches, and master equation methods[21–36]. Recently we developed an extension of Lindblad's formalism to treat non-Markovian dynamics by taking an ensemble of Lindbladian trajectories (ELT)[37]. The advantage of the ELT method is that it provides a theoretically complete description of non-Markovian dynamics without violation of the complete positivity of the density matrix [37]. With a proper choice of the Lindbladian channels it can in principle match the system density matrix obtained from the exact system-bath density matrix.

Here we extend the ELT theory for non-Markovian dynamics to treat systems with multiple fermions. We show that the constraints that we previously derived for the Lindblad equation can be applied to each Lindblad trajectory of the ELT method to maintain the fermion statistics. In particular, we use the convexity of the constrained density matrices to prove that the ensemble inherits the constraints of the individual trajectories. These constraints are critical because without them the many-fermion system can collapse into a many-boson-like system in potentially extreme violation of the Pauli exclusion principle. The ELT with fermion constraints offers a theoretically complete description of non-Markovian dynamics without violation of the Pauli principle.

After developing the theoretical extension of the ELT method in Section 7.2.3, we apply the resulting ELT method in Section 7.3. We apply the ELT method to three distinct systems of two fermions in three levels. While the electrons violate the fermion statistics without the constraints, correct fermion behavior is recovered with the constraints.

## 7.2 Theory

The constraints on the Lindbladian matrices to ensure fermionic statistics and the generalization of the Lindblad equation to the non-Markovian regime are reviewed in Sections 7.2.1 and 7.2.2, respectively. In Section 7.2.3 we generalize the ELT method to treat systems with multiple fermions. While the derivations are presented in the notation of first quantization, all of the results can also be expressed without modification in the notation of second quantization.

### *7.2.1 Fermion Conditions on Lindbladian Matrices*

The Lindblad equation for the 1-RDM is given by,

$$\frac{d^1D}{dt} = -i[^1H, ^1D] + \sum_{j=1}^{N} \mathcal{L}(^1D, ^1C), \tag{7.1}$$

where $^1H$ is the one-body Hamiltonian, $^1D$ is the 1-RDM, $L(^1D, ^1C) = {}^1C_j {}^1D {}^1C_j^\dagger - \frac{1}{2}\{{}^1C_j^\dagger {}^1C_j, {}^1D\}$ where $^1C$ are the one-body Lindbladians[1–3].

The use of the 1-RDM requires additional constraints referred to as the $N$-representability conditions: (i) Hermiticity, (ii) normalization to $N$ particles, and (iii) two linear matrix inequalities:

$$^1D \succeq 0 \tag{7.2}$$

$$^1Q \succeq 0, \tag{7.3}$$

where $^1Q$ is the 1-hole RDM[38–43]. The nonnegativity of the 1-particle and 1-hole RDMs is equivalent to the Pauli exclusion principle that the eigenvalues of the 1-RDM must lie in the interval [0,1].

In Ref. [8] we derived a constraint on the Lindbladian (bath) operators that is necessary and sufficient for the 1-RDM to obey the fermion statistics expressed in the Pauli exclusion principle. For a single dissipative channel, the Lindbladian matrix must be normal[8],

$$[C, C^\dagger] = 0, \tag{7.4}$$

or if there are multiple dissipative channels, the constraint can be written as a summation over multiple commutators. As previously shown, the simple constraint is a subset of the general constraint since if all Lindbladians are normal, then the summation is trivially

zero. However, with multiple channels the Lindbladians have greater flexibility and are not required to be normal as long as cancellation among terms causes the sum to be zero[8].

### *7.2.2 Ensemble of Lindbladian Trajectories Method*

Taking the ensemble average of Lindbladian trajectories originating from different points in the system's history produces a new density matrix,

$$D(t) = \sum_{i=1}^{N} \omega(\tau_i) e^{\mathcal{L}(\tau_i)} D(t - \tau_i), \tag{7.5}$$

where $\omega(\tau_i)$ are statistical weights, $\tau_i$ are lag times, and $e^{\mathcal{L}(\tau_i)}$ are the Lindbladian propagators[37]. Since this method takes positive trajectories from many different points in the system's history, the system memory is built into the dynamics. Through density matrices from different times in the history the system has the opportunity to regain information that was previously lost to the surroundings. As shown in previous work, this method provides a full account of the system's memory while maintaining the positivity of the density matrix[37].

### *7.2.3 Fermion Conditions in the ELT Method*

The density matrix from the ELT method is an ensemble of individual Lindbladian trajectories. Since each trajectory produces a positive semidefinite density matrix, the new density matrix will also be positive semidefinite. Due to this relationship and the convexity of the sets of both the 1-electron and 1-hole RDMs, enforcing the Pauli principle on each trajectory is equivalent to enforcing the principle for the ensemble of trajectories. For completeness a formal proof of this result is given in the next section. The constraint on the Lindbladians

is thus similar to the constraint for the multiple dissipative channels case,

$$\sum_i [C_i, C_i^\dagger] = 0. \tag{7.6}$$

It should be noted that due to the multiple trajectories in the ensemble, this constraint is analogous to the more general constraint previously derived. It is not necessary that each Lindbladian matrix be normal, only that the sum of all the commutators vanishes. For example, two Lindbladian channels could be paired so that each channel has a bath matrix that is the adjoint of the other channel's bath matrix, causing the sum in Eq. (7.6) to vanish.

### *7.2.4 Convexity of the 1-RDM Set*

The set of density matrices with eigenvalues in the interval [0,1] is convex, and hence, the ensemble average of matrices in the set produces another matrix in the set. Because this result is central to the present work, we present a proof of the set's convexity in the following theorem.

**Theorem 1.** *Let $M_i$ be matrices with eigenvalues $\{\lambda_j^{(i)}\}$ and eigenfunctions $\{\phi_j^{(i)}\}$ and $M = \sum_i \omega_i M_i$ with eigenvalues $\{\tilde{\lambda}_j\}$ and eigenfunctions $\{\tilde{\phi}_j\}$, if $\{\lambda_j^{(i)}\} \in [0,1]$, $\omega_i \geq 0$, and $\sum_i \omega_i = 1$ then $\{\tilde{\lambda}_j\} \in [0,1]$.*

*Proof.* Start by taking the expectation value of $M$ in the basis of an eigenvector $\tilde{\phi}_j$,

$$\begin{aligned} \langle \tilde{\phi}_j \mid M \mid \tilde{\phi}_j \rangle &= \langle \tilde{\phi}_j \mid \sum_i \omega_i M_i \mid \tilde{\phi}_j \rangle & (7.7) \\ &= \sum_i \omega_i \langle \tilde{\phi}_j \mid M_i \mid \tilde{\phi}_j \rangle & (7.8) \end{aligned}$$

Now consider the eigenfunctions $\phi^{(i)}_{\max}$ corresponding to the maximum eigenvalues of $M_i$,

$$\begin{aligned} \sum_i \omega_i \langle \tilde{\phi}_j \mid M_i \mid \tilde{\phi}_j \rangle &\leq \sum_i \omega_i \langle \phi^{(i)}_{\max} \mid M_i \mid \phi^{(i)}_{\max} \rangle & (7.9) \\ &\leq \sum_i \omega_i & (7.10) \\ &\leq 1 & (7.11) \end{aligned}$$

using $\{\lambda^{(i)}_j\} \in [0,1]$ with equality holding if $M_i$ and $M$ share the same eigenfunctions. An analogous argument can be made using the eigenfunctions $\phi^{(i)}_{\min}$, corresponding to the minimum eigenvalues of $M_i$,

$$\begin{aligned} \sum_i \omega_i \langle \tilde{\phi}_j \mid M_i \mid \tilde{\phi}_j \rangle &\geq \sum_i \omega_i \langle \phi^{(i)}_{\min} \mid M_i \mid \phi^{(i)}_{\min} \rangle & (7.12) \\ &\geq 0 & (7.13) \end{aligned}$$

using $\{\lambda^{(i)}_j\} \in [0,1]$ again with equality holding if $M_i$ and $M$ share the same eigenfunctions. Therefore,

$$\{\tilde{\lambda}_j\} \in [0,1]. \tag{7.14}$$

□

## 7.3 Applications

The ELT method was previously applied to the Jaynes-Cummings model, which is a two-level system interacting with the cavity field[37, 44, 45]. To verify the extended version of the ELT method to capture fermion statistics, we employ here a three-level system with two fermions[21]. There are three primary ways of arranging three different energy levels, as shown in Fig. 7.1. The ELT method with and without constraints on the Lindbladian is

employed to calculate occupation numbers of the three states for each of the three systems.

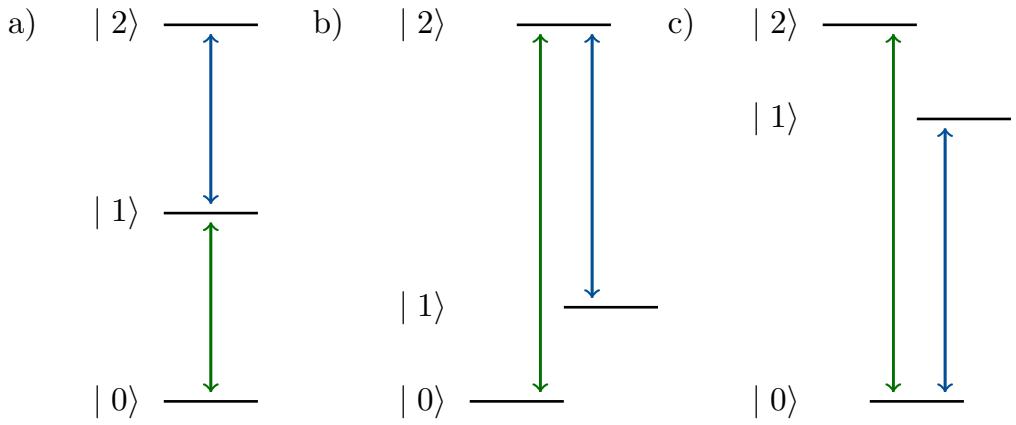


Figure 7.1: Three level systems arranged with a) ladder states, b) one higher-in-energy state connected to two lower-in-energy states ($\wedge$) and c) two higher-in-energy states connected to one lower-in-energy state ($\vee$). The interactions through $C_1$ are shown in green and the interactions through $C_2$ are shown in blue.

### *7.3.1 Computational Methodology*

For the three systems shown in Fig. 7.1 the following Lindbladian matrices are used,

$$\begin{aligned} C_{a,1} &= |0\rangle\langle 1| \\ C_{a,2} &= |1\rangle\langle 2|\,, \end{aligned} \tag{7.15}$$

$$\begin{aligned} C_{b,1} &= |0\rangle\langle 2| \\ C_{b,2} &= |1\rangle\langle 2|\,, \end{aligned} \tag{7.16}$$

and

$$\begin{aligned} C_{c,1} &= |0\rangle\langle 2| \\ C_{c,2} &= |0\rangle\langle 1|\,, \end{aligned} \tag{7.17}$$

respectively for the unconstrained calculation. For the constrained calculation, the number of trajectories is doubled to include an additional trajectory for the adjoint of each dissipative operator such that $\sum_i [C_i, C_i^\dagger] = 0$.

The Lindblad equation in Eq. (7.1) is used to propagate both the 1-particle and 1-hole density matrices from each time in the history of the ELT method. The density matrices are obtained through a fourth-fifth-order Runge-Kutta method for solving differential equations in Maple[46, 47]. For all calculations the initial conditions consist of one fermion in state $|2\rangle$, one fermion in state $|1\rangle$, and one hole in state $|0\rangle$.

To obtain a set of weights that contains non-Markovian dynamics in the 3-level system, we use weights that are optimized to reproduce the complete non-Markovian time dynamics of the two-level detuned Jaynes-Cummings model with parameters reported in Ref. [9]. The optimization of the weights is performed in Maple[46, 47] by a sequential quadratic programming algorithm [48]. To recap the parameters, $\gamma_0 = 1.091$ is inversely proportional to the timescale of system decay, $\lambda = 0.3\gamma_0$ is inversely proportional to the timescale of bath decay, and $\Delta = 2.4\gamma_0$ is the amount of detuning. For all calculations, $\frac{1}{\lambda}$ is used as the unit of time. Two sets of weights are calculated, one set for the 1-particle RDM and one set for the 1-hole RDM, as shown in Fig. 7.2.

Although these weights are obtained from numerical optimization, it is interesting to note that when accessing memory further back, for $\tau > 10$ the weights of the 1-particle RDM and 1-hole RDM trajectories alternate in their ebbs and flows. This alternation corresponds to the flow of energy into the bath (1-particle RDM) and from the bath (1-hole RDM). This intuitively makes sense as the 1-particle RDM and 1-hole RDM are complimentary entities related by the Pauli exclusion principle.

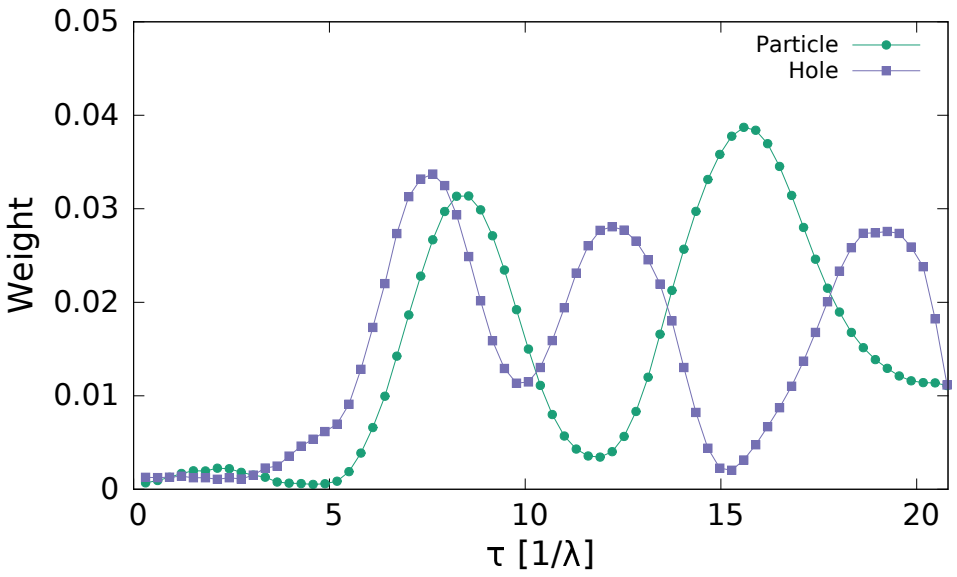


Figure 7.2: Weights as a function of lag time $\tau$ for the particle and hole (green circles and purple squares respectively) trajectories as calculated using the two-level detuned Jaynes-Cummings model, with $\gamma_0 = 1.091, \lambda = 0.3\gamma_0$, and $\Delta = 2.4\gamma_0$.

### *7.3.2 Results*

The first system is the 3-level ladder system, where the occupied state $|2\rangle$ decays to the occupied state $|1\rangle$, which in turn decays into the unoccupied state $|0\rangle$ as shown in Fig. 7.3. The second system is the 3-level $\wedge$ system where the occupied state $|2\rangle$ decays to the occupied state $|1\rangle$ and the unoccupied state $|0\rangle$, as shown in Fig. 7.4. The third system is the 3-level $\vee$ system where the two occupied states $|2\rangle$ and $|1\rangle$ decay into the unoccupied state $|0\rangle$, as shown in Fig. 7.5.

In all three configurations, it can be seen that when the Lindbladians are unconstrained, the fermions behave as bosons and pile up in a given state, violating the Pauli exclusion principle. However, when the constraint on the Lindbladian matrices is applied, the fermions obey the Pauli exclusion principle and each of the state occupations remains physically reasonable.

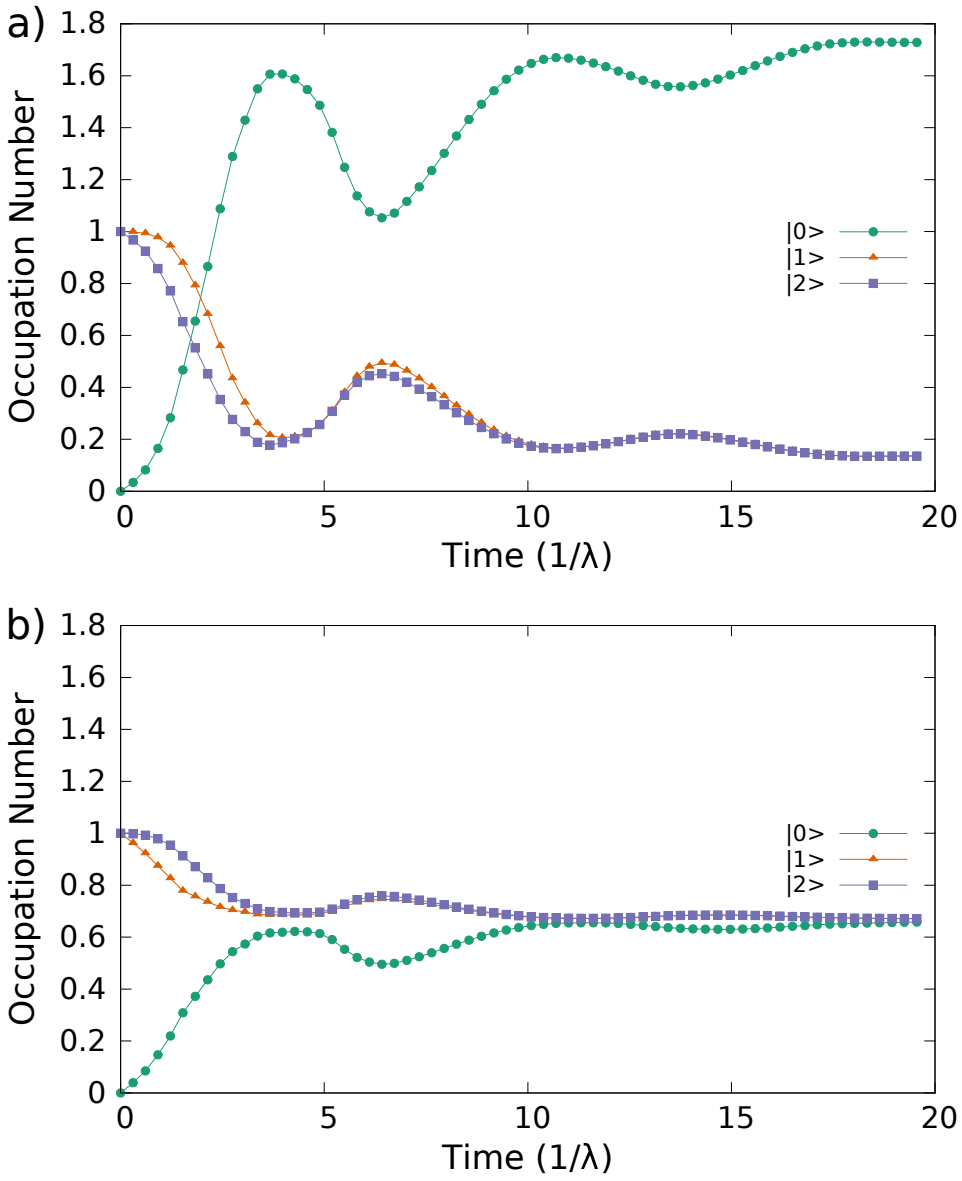


Figure 7.3: Occupation numbers for states $|0\rangle$, $|1\rangle$, and $|2\rangle$ (green circles, orange triangles, and purple squares respectively) in the ladder configuration with a) unconstrained Lindbladians and b) constrained Lindbladians such that $\sum_i [C_i, C_i^\dagger] = 0$.

## 7.4 Discussion and Conclusions

Many physical systems where non-Markovian dynamics are prevalent are also many-electron systems. For example, a method which models electron transport through a photosynthetic light harvesting complex needs to preserve fermion statistics. Moreover, if this system is

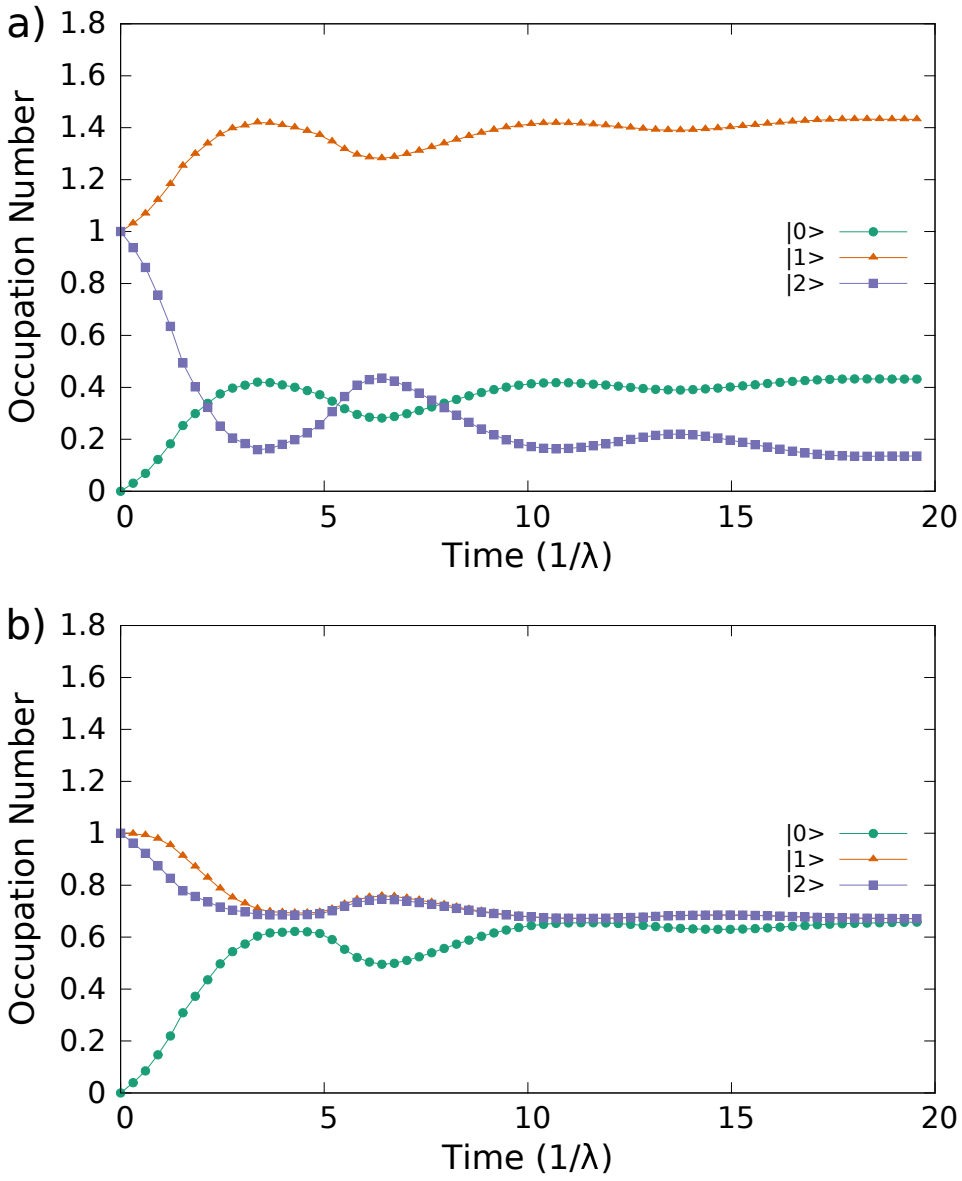


Figure 7.4: Occupation numbers for states $|0\rangle$, $|1\rangle$, and $|2\rangle$ (green circles, orange triangles, and purple squares respectively) in the $\wedge$ configuration with a) unconstrained Lindbladians and b) constrained Lindbladians such that $\sum_i [C_i, C_i^\dagger] = 0$.

embedded in a complex protein environment, it also must capture non-Markovian dynamics. Here, we generalized a non-Markovian method based on an ensemble of Lindbladian trajectories to treat systems of multiple fermions. Lindbladian operators from each time in the system's history are constrained to preserve fermion statistics. These constraints

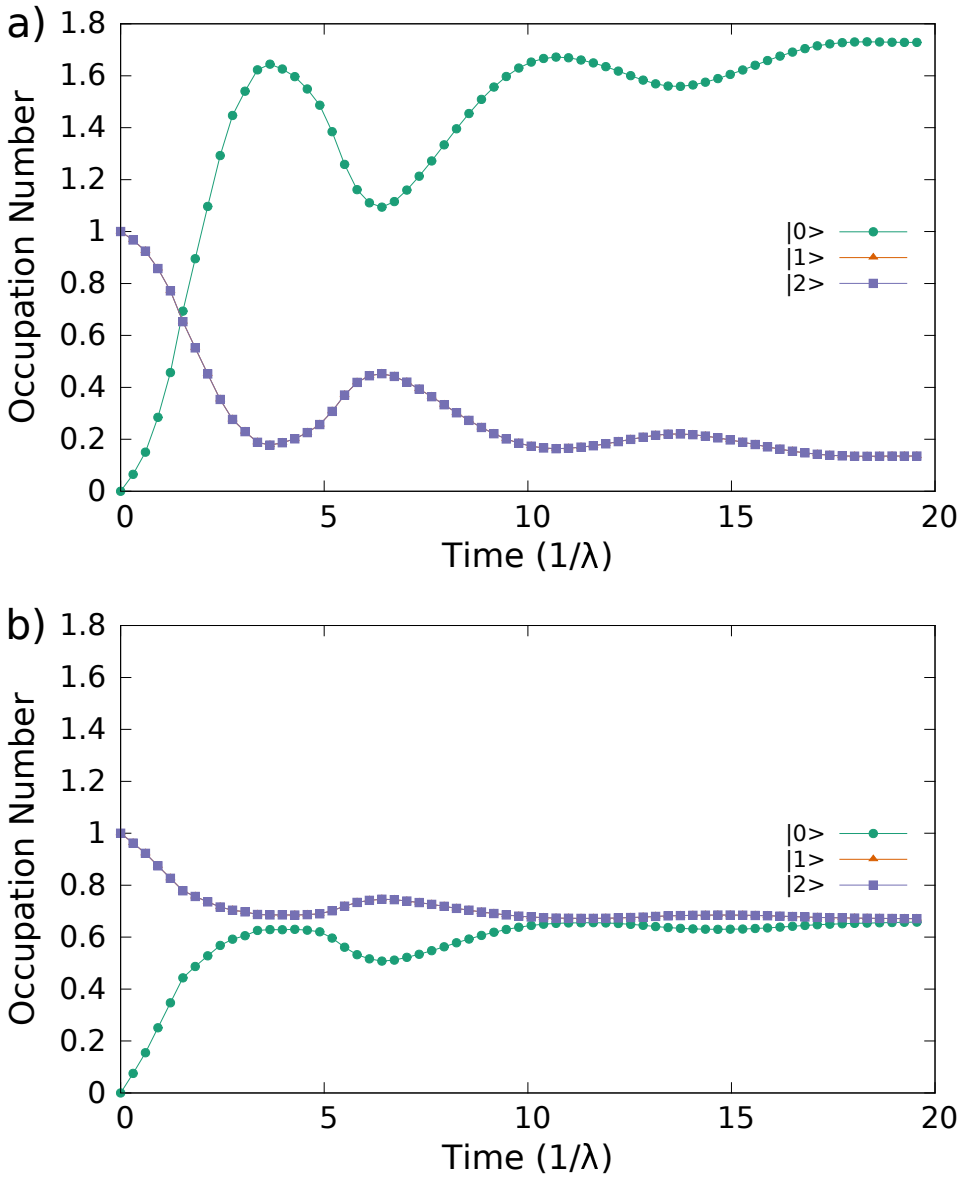


Figure 7.5: Occupation numbers for states $|0\rangle$, $|1\rangle$, and $|2\rangle$ (green circles, orange triangles, and purple squares respectively) in the $\vee$ configuration with a) unconstrained Lindbladians and b) constrained Lindbladians such that $\sum_i [C_i, C_i^\dagger] = 0$.

were verified to maintain fermion statistics through a variety of three-level systems with two electrons.

Many non-Markovian methods rely on the Lindbladian formalism, such as Monte-Carlo quantum jump methods or several master equation methods[21, 49]. The derived constraints

on the Lindbladian bath operators are potentially useful in not only the ELT method but other non-Markovian methods. The present work offers an initial but important step towards improving the treatment of non-Markovian dynamics in many-fermion quantum systems.


(1) Kossakowski, A. On quantum statistical mechanics of non-Hamiltonian systems. *Reports in Mathematical Physics* **1972**, *3*, 247.

(2) Lindblad, G. On the generators of quantum dynamical semigroups. *Communications in Mathematical Physics* **1976**, *48 (2)*, 119–130.

(3) Gorini, V.; Kossakowski, A.; Sudarshan, E. C. G. Complete positive dynamical semigroups of $N$-level systems. *Journal of Mathematical Physics* **1976**, *17 (5)*, 821–825.

(4) Pershin, Y. V.; Dubi, Y.; Di Ventra, M. Effective single-particle order-N scheme for the dynamics of open noninteracting many-body systems. *Physical Review B* **2008**, *78*, 054302.

(5) Rothman, A. E.; Mazziotti, D. A. Nonequilibrium steady-state electron transport with N-representable density matrices from the anti-Hermitian contracted Schrodinger equation. *Journal of Chemical Physics* **2010**, *132*, 104112.

(6) Rosati, R.; Iotti, R. C.; Dolcini, F.; Rossi, F. Derivation of nonlinear single-particle equations via many-body Lindblad superoperators: A density-matrix approach. *Physical Review B* **2014**, *90*, 125140.

(7) Nguyen, T. S.; Nanguneri, R.; Parkhill, J. How electronic dynamics with Pauli exclusion produces Fermi-Dirac statistics. *Journal of Chemical Physics* **2015**, *142*, 134113.

(8) Head-Marsden, K.; Mazziotti, D. A. Communication: Satisfying fermionic statistics in the modeling of open time-dependent quantum systems with one-electron reduced density matrices. *Journal of Chemical Physics* **2015**, *142*, 051102.

(9) Maniscalco, S.; Petruccione, F. Non-Markovian dynamics of a qubit. *Physical Review A* **2006**, *73*, 012111.

(10) Shen, H. Z.; Li, D. X.; Su, S.-L.; Zhou, Y. H.; Yi, X. X. Exact non-Markovian dynamics of a qubit coupled to two interacting environments. *Physical Review A* **2017**, *96*, 0133805.

(11) Bellomo, B.; Lo Franco, R.; Compagno, G. Entanglement dynamics of two independent qubits in environments with and without memory. *Physical Review A* **2008**, *77 (3)*, 032342.

(12) Fassioli, F.; Olaya-Castro, A.; Scholes, G. D. Coherent energy transfer under incoherent light conditions. *Journal of Physical Chemistry Letters* **2012**, *3 (21)*, 3136–3142.

(13) Ishizaki, A.; Calhoun, T. R.; Schlau-Cohen, G. S.; Fleming, G. R. Quantum coherence and its interplay with protein environments in photosynthetic electronic energy transfer. *Physical Chemistry Chemical Physics* **2010**, *12 (27)*, 7319–7337.

(14) Renger, T.; Marcus, R. A. On the relation of protein dynamics and exciton relaxation in pigment-protein complexes: An estimation of the spectral density and a theory for the calculation of optical spectra. *Journal of Chemical Physics* **2002**, *116 (22)*, 9997–10019.

(15) Skochdopole, N.; Mazziotti, D. A. Functional subsystems and strong correlation in photosynthetic light harvesting. *Advances in Chemical Physics* **2014**, *154*, 355–370.

(16) Skochdopole, N.; Mazziotti, D. A. Functional Subsystems and Quantum Redundancy in Photosynthetic Light Harvesting. *Physical Chemistry Letters* **2011**, *2*, 2989.

(17) Chakraborty, R.; Mazziotti, D. A. Noise-assisted energy transfer from the dilation of the set of one-electron reduced density matrices. *Journal of Chemical Physics* **2017**, *146*, 184101.

(18) Mazziotti, D. A. Two-Electron Reduced Density Matrix as the Basic Variable in Many-Electron Quantum Chemistry and Physics. *Chemical Reviews* **2012**, *112*, 244–262.

(19) Foley IV, J. J.; Mazziotti, D. A. Measurement-driven reconstruction of many-particle quantum processes by semidefinite programming with application to photosynthetic light harvesting. *Physical Review A* **2012**, *86*, 012512.

(20) Mazziotti, D. A. Effect of strong electron correlation on the efficiency of photosynthetic light harvesting. *Journal of Chemical Physics* **2012**, *137*, 074117.

(21) Piilo, J.; Harkonen, K.; Maniscalco, S.; Suominen, K. A. Open system dynamics with non-Markovian quantum jumps. *Physical Review A* **2009**, *79 (6)*, 062112.

(22) Barchielli, A.; Pellegrini, C.; Petruccione, F. Quantum Trajectories: Memory and continuous observation. *Physical Review A* **2012**, *86 (6)*, 063814.

(23) Berklebach, T. C.; Reichman, D. R.; Markland, T. E. Reduced density matrix hybrid approach: An efficient and accurate method for adiabatic and non-adiabatic quantum dynamics. *Journal of Chemical Physics* **2012**, *136*, 034113.

(24) Berklebach, T. C.; Markland, T. E.; Reichman, D. R. Reduced density matrix hybrid approach: Application to electronic energy transfer. *Journal of Chemical Physics* **2012**, *136*, 084104.

(25) Breuer, H. P.; Kappler, B.; Petruccione, F. Stochastic wave-function method for non-Markovian quantum master equations. *Physical Review A* **1999**, *59 (2)*, 1633–1643.

(26) Ferialdi, L. Exact closed master equation for Gaussian non-Markovian dynamics. *Physical Review Letters* **2016**, *116*, 120402.

(27) Fetherolf, J. H.; Berkelbach, T. C. Linear and nonlinear spectroscopy from quantum master equations. *Journal of Chemical Physics* **2017**, *147*, 244109.

(28) Moix, J. M.; Cao, J. A hybrid stochastic hierarchy equations of motion approach to treat the low temperature dynamics of non-Markovian open quantum systems. *Journal of Chemical Physics* **2013**, *139*, 134106.

(29) Montoya-Castillo, A.; Berklebach, T. C.; Reichman, D. R. Extending the applicability of Redfield theories into highly non-Markovian regimes. *Journal of Chemical Physics* **2015**, *143*, 194108.

(30) Vacchini, B. Non-Markovian master equations from piecewise dynamics. *Physical Review A* **2013**, *87 (3)*, 030101.

(31) Wismann, S.; Karlsson, A.; Laine, E.; Piilo, J.; Breuer, H. P. Optimal state pairs for non-Markovian quantum dynamics. *Physical Review A* **2012**, *86*, 062108.

(32) Shibata, F.; Takahashi, Y.; Hashitsume, N. A generalized stochastic Liouville equation. Non-Markovian versus memoryless master equations. *Journal of Statistical Physics* **1977**, *17 (4)*, 171–187.

(33) Shabani, A.; Lidar, D. A. Completely positive post-Markovian master equation via a measurement approach. *Physical Review A* **2005**, *71*, 020101(R).

(34) Budini, A. A. Post-Markovian quantum master equations from classical environment fluctuations. *Physical Review E* **2014**, *89 (1)*, 012147.

(35) Breuer, H. P. Genuine quantum trajctories for non-Markovian processes. *Physical Review A* **2004**, *70 (1)*, 012106.

(36) Yu, T.; Diósi, L.; Gisin, N.; Strunz, W. T. Post-Markov master equation for the dynamics of open quantum systems. *Physical Review A* **2004**, *70 (1)*, 012106.

(37) Head-Marsden, K.; Mazziotti, D. A. Ensemble of Lindblad's trajectories for non-Markovian dynamics. *Physical Review A* **2019**, *99 (2)*, 022109.

(38) Coleman, A. J. Structure of Fermion Density Matrices. *Reviews of Modern Physics* **1963**, *35*, 668.

(39) Garrod, C.; Percus, J. K. Reduction of the N-Particle Varational Problem. *Journal of Mathematical Physics* **1964**, *5*, 1756.

(40) Coleman, A. J.; Yukalov, V. I., *Reduced Density Matrices: Coulson's Challenge, Chapter 4*; Springer: 2000.

(41) Mazziotti, D. A. Structure of Fermionic Density Matrices: Complete N-Representability Conditions. *Physical Review Letters* **2012**, *108*, 263002.

(42) Piris, M. Global Method for Electron Correlation. *Physical Review Letters* **2017**, *119*, 063002.

(43) Schilling, C. Communication: Relating the pure and ensemble density matrix functional. *Journal of Chemical Physics* **2018**, *149*, 231102.

(44) Jaynes, E. T.; Cummings, F. Comparison of quantum and semiclassical radiation theories with application to the beam maser. *Proceedings of the IEEE* **1963**, *51 (1)*, 89–109.

(45) Breuer, H. P.; Petruccione, F., *The Theory of Open Quantum Systems*; Oxford University Press: 2002.

(46) *Maple 2018*; Maplesoft, Waterloo: 2018.

(47) Hairer, E.; Nørsett, S.; Wanner, G., *Solving Ordinary Differential Equations I: Nonstiff Problems, 2nd ed.* Springer-Verlag, Berlin: 1993.

(48) Gill, P. E.; Murray, W.; Saunders, M. A. SNOPT: An SQP Algorithm for Large-scale Constrained Optimization. *SIAM Journal on Optimization* **2002**, *12*, 979–1006.

(49) Stefanescu, E.; Scheid, W.; Sandulescu, A. Non-Markovian master equation for a system of Fermions interacting with an electromagnetic field. *Annals of Physics* **2008**, *323*, 1168–1190.